Biomechanics and energetics of swimming☆

Olivia H. Hawkins[a], Valentina Di Santo[b], and Eric. D. Tytell[a,*,1]
[a]*Tufts University, Medford, MA, United States,* [b]*University of California, San Diego, CA, United States*
[*]*Corresponding author. e-mail address: eric.tytell@tufts.edu*

Chapter outline

1 Introduction 3
2 A brief history of studying fish swimming 5
3 Steady locomotion 7
3.1 Traditional kinematic parameters 7
3.2 Traditional parameters and swimming performance 9
3.3 Swimming modes 13
3.4 Dimensionless swimming parameters 15
3.5 Computing kinematic parameters 19
4 Forces 27
4.1 Gravity and buoyancy 27
4.2 Drag 29
4.3 Local drag forces 31
5 Musculoskeletal dynamics 32
5.1 Body-caudal fin swimming 32
6 The contribution of fins to steady swimming 34
6.1 Fin types 34
6.2 Fin rays 35
6.3 Fins as stabilizers 38
6.4 Fins as propulsors: Pectoral fin swimming 39
6.5 Fins as propulsors II: Dorsal, anal, and pelvic fins 42
6.6 Fins as sensory structures during swimming 44
7 Unsteady locomotiont 45
7.1 Turning 45
7.2 Vertical maneuvering 50
8 Fish swimming energetics 51
9 Swimming performance under climate change 54
References 58

☆ Topics: Emphasize new results and approaches to understand fish moving in unsteady flows; energetics; ontogeny, musculoskeletal dynamics, new techniques, and approaches (covered in other chapters: feeding, terrestrial locomotion, tissues, sensory systems, robotics, ecomechanics, collective behaviors, evolution)

[1] Senior author

Fish Physiology. https://doi.org/10.1016/bs.fp.2025.06.003

Abstract
In this chapter, we outline the fundamental biomechanics of fish swimming. We introduce steady locomotion and the key parameters used to quantify it, detailing methods for estimating these parameters with a focus on body and caudal fin swimming. We also discuss the forces a fish encounters while moving through water and how its swimming motion counteracts these forces. Following this, we examine fin structure and function, highlighting their roles in stability, propulsion, and maneuverability, with particular importance for turning and vertical movements. Although unsteady behaviors are less understood, we summarize current insights and promising techniques for their quantification. Finally, we address the energetics of swimming and explore how biomechanical and physiological characteristics might be affected by climate change.

Abbreviated terms

2A	Maximum excursion, peak to peak amplitude.
f	frequency, tail beat frequency.
T	Period.
fps	frames per second.
λ or *k*	Wavelength.
V	wave speed.
ϕ	phase.
s	arc length.
M*, *m	mass.
M_i	fraction of total mass in a segment of a fish.
W_i	horizontal width of a segment of a fish.
H_i	dorso-ventral height of a segment of a fish.
com	center of mass.
κ	2D curva θ ture.
θ_i	angle of curvature of a segment of a fish.
SVD	singular value decomposition.
â(t)	unit vector pointing along the primary axis of a swimming body.
κ_s	traveling wave of curvature.
A(s)	wave amplitude.
t	time.
H	Hilbert transform.
$\hat{V}$	body wave speed.
L, BL	body length.
BL s^{-1}	body lengths per second.
U	swimming speed of a fish.
Re	Reynolds number.
μ	dynamic viscosity.
St	Strouhal number.
Sw	swimming number.
v	kinematic viscosity.

λ*, or SW	specific wavelength.
BCF	body and caudal fin locomotion.
F	inertial force.
C_a	accelerated fluid.
ρ	density.
AR	aspect ratio.
R_{turn}	turn radius or path curvature.
U*(t)*	instantaneous linear speed.
A_c	centripetal acceleration.
g	gravitational acceleration.
C_g	coefficient of normal acceleration.
MO_2	rate of change in oxygen in a respirometry chamber relative to a fish's mass.
b	allometric coefficient.
2D	two-dimensional.
3D	three-dimensional.

1 Introduction

Fishes make up half of the vertebrate diversity on the planet and have a wide variety of different body and fin shapes (Nelson et al., 2016). Such diversity in morphology is also coupled with differences in swimming kinematics, performance, and neuromuscular control. In this chapter, we aim to (1) reference some of the foundational work in the field while providing updates from the last 20 years of fish swimming research, (2) describe a standardized approach to calculating commonly used kinematic variables, (3) briefly link hydrodynamics, sensory biology, and comparative anatomy of fin and body structures to our current understanding of fish swimming, (4) summarize recent findings in fish energetics, and (5) reflect on future directions for studies of fish locomotion, particularly in the context of climate change.

We start with an introduction to the history of studying fish swimming to provide context before we address where the field is at now and where it is going. This section is not a full review of the field's history, but rather an introduction or reminder of the lines of thinking that have guided the last century of fish swimming research.

This section is followed by a summary (Section 3) of commonly quantified dimensional and dimensionless swimming parameters and what they mean in the context of swimming performance. We then discuss swimming modes, which were originally classified by Breder (1926), but have since been reclassified as a continuum of locomotor behavior (Di Santo et al., 2021). Following our description of these parameters, we present methods for how to calculate them using the package *fishmechr*, an open source package for R (Tytell, 2025). Classification of locomotor behavior is an important area for future research as we move away from trying to force fishes into one of the

original swimming mode categories towards a more realistic and comprehensive analysis of the diversity and occasional convergence of fish swimming kinematics, particularly when accounting for 3D movements. This section is written entirely within the context of steady swimming, and unsteady swimming will be discussed later in Section 7.

The next section of the chapter (Section 4) briefly addresses forces that a fish experiences during swimming, which are binned into three groups: vertical forces (buoyancy and gravity), forward-backward forces (thrust and drag), and side-to-side or lateral forces. We also discuss viscous forces and how they affect larval fishes specifically. We then move on in Section 5 to discuss musculoskeletal dynamics during body-caudal fin swimming (axial locomotion) in the context of muscle activation patterns. For more detail, see Chapter 4 for a review on the structure and mechanics of fish tissues (Clark and Amarnadh, 2025).

Next, we pivot in Section 4 to a discussion of the contribution of the fins during steady swimming. This section is divided into small reviews of fin anatomy and function during steady swimming, including their roles as stabilizers, primary propulsors, and sensory structures. In the last decade, it has become clear that fins are important not only because they produce forces, but also are used for mechanoreception. We consider this an important new addition to the chapter, but also see the review on how vision and the lateral line impact swimming in Chapter 5 (McHenry and Peterson, 2025).

We next provide a short description of some recent work on unsteady swimming (Section 7). We first summarize some of the classic and recent work regarding routine turning, which has historically received much less attention than fast-start or startle responses which are generally on the maximal side of turning performance. Fast start mechanics were extensively reviewed in a previous edition of this series (Wakeling, 2006). We also discuss vertical swimming, which has received little attention even though many fishes swim up and down in the water column routinely.

At several points throughout the chapter, we mention possible energetic costs in the context of both steady and unsteady swimming. In Section 8, we cover the basics of fish energetics, a field aimed at understanding how much oxygen fishes are using to perform daily tasks, in the context of swimming and station holding. Previous reviews provide additional species specific trends in energetics (Di Santo and Goerig, 2025; Lauder and Di Santo, 2015).

We end the chapter with ideas for future directions of fish swimming biomechanics and energetics research. Primarily, we suggest that future research should consider the effects of climate change on the morphology, biomechanics, and metabolism of fishes, all of which could have effects on persistence of currently threatened species. We provide examples of studies that have already began this pursuit, and ultimately advocate for a new integrative field called EcoPhysioMechanics (Di Santo, 2022).

2 A brief history of studying fish swimming

Humans have been observing and noting behaviors of fishes for thousands of years, with some of the earliest documented accounts tracing back to India around 2500 years ago (Webb, 1984). Much later, in the 4th century, Aristotle detailed his ideas on how fishes swim and observations of fish fins a series of texts: *The History of Animals, Movement of Animals,* and *Progression of Animals* (translations published as Aristotle, 1937a, 1937b, 1910). In the Renaissance, Rondelet expanded upon Aristotle's ideas by considering the use of the body, fins, and swim bladder of fishes during swimming (Alexander, 1983; Drucker and Summers, 2008; Rondelet, 1554). Borelli followed up on the work of Aristotle and Rondelet in the 17th century, hypothesizing that the paired pectoral fins of fishes are used for stability and maneuverability (Borelli, 1680). However, Borelli assumed that these fins did not have any role in powering forward swimming, an idea in which many later studies have proved incorrect (Drucker and Summers, 2008). For more detailed information on the early history of studying fish swimming see Alexander (1983), and for similar information from the perspective of studying the contributions of the fins to swimming see Drucker and Summers (2008).

Later in the 19th century, the study of fish swimming captured the attention of more scholars. Pettigrew (1874) hypothesized that when fishes swim using body bending, the body waves are not propagated—rather they are standing waves characterized by specific 's' bends. Soon afterward, however, new camera technology was used to show the opposite—waves of undulation do travel down the body and fins. By this time, methods and techniques for recording fast movements were improving, allowing for easier descriptions and quantitative analyses of fish swimming (Webb, 1984). See McHenry and Hedrick (2023) for a review of the many technological advancements that improved our ability to make kinematic measurements. Marey was the first to capture fish swimming through sequential photographs of rays, seahorses, and eels (Marey, 1894, 1890). Further development of cine-photography allowed François-Franck (1906) to observe the fluid flow around a fish by imaging India ink moving through the gills of a carp. Even though the ability to record fish and fluid movement for the first time was an exceptional step forward for understanding fish biomechanics, quantitative data was still lacking.

Early attempts at measuring quantitative parameters of fish mechanics began with Houssay in the early 1900s, who tried to estimate power during swimming by tethering fishes to a weighted apparatus and prompting them to swim forward to lift various weights (reviewed by Alexander, 1983). In the 1920s and '30s, Sir James Gray began developing the first mathematical models of swimming fish, in which he treated the body as a series of segments, each with a measurable normal and tangential force, which are referred to in Section 4 as "resistive forces". At the same time, he quantified some of the traditional kinematic parameters, such as the speed of the body wave and

forward swimming speed, from sequential photographs of fishes swimming through still water (Gray, 1933). He also made some of the earliest attempts to understand the neuromechanics of swimming through spinal cord transections in eels (Gray, 1935). This work not only provided evidence for new hypotheses on undulatory swimming, but also laid the foundation for early work investigating how body waves are modulated in fishes. Other researchers, particularly Breder (1926) were beginning to make more detailed accounts of the diversity of fish swimming styles, making the first record in English of different swimming modes and gait transitions in fishes. These original classifications and their limitations are discussed in detail in Section 3 of this chapter.

Following the heightened interest in the mechanics and forces related to fish swimming, many new models and lines of inquiry emerged. Bainbridge developed a "fish wheel", an early flume, to examine how swimming kinematics and tail motion depend on fish size (Bainbridge, 1963, 1958), Sir James Lighthill developed a theory of swimming forces that focused on the reaction of the fluid to the side-to-side acceleration of the body, now called elongated body theory or a "reactive" model (Lighthill, 1970, 1969, 1960), and T. Yao-Tsu Wu developed a different approach that allowed him to investigate how fins and body shape influence force balance of swimming fishes (Wu, 1971a, 1971b, 1971c, 1971d). Robert Blake expanded these hydrodynamic models of propulsion to oscillating and undulating fins based on kinematics of diverse groups of fishes from mandarins to knifefishes (Blake, 2004, 1983a, 1981; Blake et al., 2009). For a comprehensive analysis on Blake's work on the mechanics of median and paired fins, see Blake (2004) and his chapter from the original *Fish Biomechanics* text (Blake, 1983b). He also authored a book which focused entirely on summarizing the knowledge of the mechanics and hydrodynamics of fish swimming at the time (Blake, 1983c).

With growing advancements in technology and many new important contributions to the field of fish biomechanics, researchers could begin to look for patterns to test and connect those patterns to the ecology and evolution of fishes more broadly. One of the foundational publications that spearheaded this line of thinking was Paul Webb's (1975) monograph on hydrodynamics and energetics of fish swimming, later summarized for a general audience in *Form and Function in Fish Swimming* (Webb, 1984). In the review, Webb suggested that the design of fish bodies and fins (form) could be mapped to swimming functional traits, and that fishes could be specialists in cruising, maneuvering, or acceleration, or be generalists of all three. Webb worked with Daniel Weihs to review the performance costs associated with different forms and kinematics (Weihs and Webb, 1983). Webb published numerous reviews on the fins of fishes and their role in stability as well as steady and unsteady swimming maneuvers (e.g., Webb, 2006; Webb and Weihs, 2015).

Our chapter also covers the contribution of the fins to steady swimming and unsteady maneuvers, although in less detail than previous reviews. For exceptional reviews of the evolutionary history of the caudal fin of fishes and

changes in anatomy over time, see Giammona (2021) and Lauder (2000, 1989). For more recent discussion of the anatomy of paired fins as well as their activation patterns and hydrodynamics, see Drucker and Lauder's reviews (Drucker et al., 2006; Lauder and Drucker, 2004). For understanding how fishes manipulate flow passively (no muscular input) and actively (using fine motor control) with their bodies and fins, see Fish and Lauder (2017, 2006). Despite all of these reviews, the function and control of fins is still less well understood than that of the body. In particular, there is still room for more analyses regarding activation patterns in fin muscles, the evolution of fin structure as it relates to fin use across understudied groups of fishes, and the sensory role of the fins during swimming (see Aiello et al., 2018; Hale et al., 2022; Williams et al., 2013 for discussions of the sensory role of the fins).

Our chapter is meant to review the current ideas and questions related to the biomechanics of fish swimming and energetics, and particularly, to serve as a guide for new biomechanists entering the field. Notable additions to this edition include the introduction of *fishmechr* (Tytell, 2025), an open-source R-based workflow designed to standardize and demystify the analysis of 2D swimming kinematics, and a new section on the sensory functions of fins, complementing Chapter 5's focus on the lateral line system (McHenry and Peterson, 2025). In response to pressing environmental challenges such as climate change and habitat degradation, we conclude our chapter by advocating for greater integration between biomechanists, conservationists, local stake holders, and policy makers. We describe *EcoPhysioMechanics* (Di Santo, 2022)—a new integrative framework that emphasizes the collaboration between these groups and increased focus on the physiological effects of climate change—to understand how populations of fishes will respond to a changing world given the advantages or limitations of their swimming mechanics.

3 Steady locomotion

3.1 Traditional kinematic parameters

Most fishes swim by generating undulating waves along their bodies or fins, a motion that can be precisely analyzed through parameters commonly used to describe waves. Therefore, most of the parameters used to quantify swimming kinematics are also parameters of waves, including amplitude, frequency, wavelength, and wave speed (Fig. 1). The maximal displacement of a wave is called the *amplitude* (*A*). Although amplitude can be measured all along the body, the tail beat amplitude (often just called the "amplitude") is typically measured at the tip of the tail (Fig. 1A). Amplitudes measured at other body or fin points are sometimes referred to as *excursion* (Fig. 1C). Amplitude is the distance from a central axis to the maximum excursion on left or right. The peak-to-peak distance, from maximum excursion on one side to maximum on

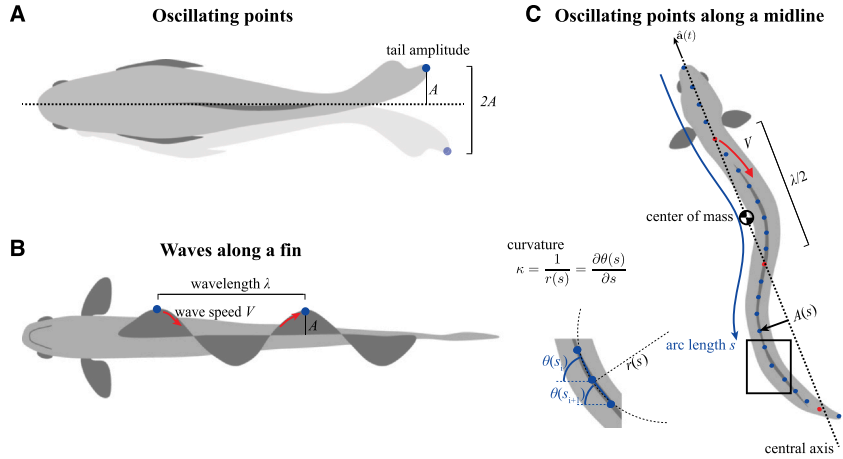

FIG. 1 Waves on a fish. (A) Motion of a fish tail, seen from above. (B) Motion of a ribbon fin, seen from below. (C) Midline of a fish, seen from below. The inset shows variables associated with calculating body curvature. Red dots indicate nodes of the body wave and the red arrow shows the movement of the propagating body wave, or wave along a fin, which is used to indicate wave speed. While amplitude (A(s)) is shown at the tail in panel A, it calculated for points along the body as well, as shown in C.

the other, is 2*A*, but is also occasionally referred to as amplitude. The other key parameter is the *frequency* (*f*), or the number of times the fin or body completes a cycle, which is the inverse of the *period* (*T*), or the time it takes for the point to complete one cycle, so that $f = 1/T$ (see Fig. 5B, in Section 3.5. for an illustration). A cycle for oscillating points, for example, the tip of a fish's tail, would be the movement of the tail from the location of its most extreme displacement across the midline to the opposite location of extreme displacement and back. The tail tip of fishes is often thin compared to the body, and fins are often fairly transparent, thus making accurate tracking difficult. Paying special attention to the contrast of the tail when setting up cameras or using an off-axis camera viewing the fish from below may help resolve this during subsequent processing (see Section 3.5.1). When working with video data, the time component of the frequency will be represented by the number of frames it took for the point to complete a full cycle divided by the frame rate at which the behavior is filmed. For any point that is tracked on a fish, the frequency of oscillation can be calculated as

$$f = \frac{Number\ of\ cycles}{Number\ of\ frames\ analyzed/frame\ rate}$$

where *f* is frequency in Hertz (Hz) and the frame rate is the filming speed (e.g., 200 fps).

Amplitude and frequency define the behavior of a single oscillating point along the body or a fin, but two additional parameters are required to understand the traveling components of the wave: *wavelength* (λ) and *wave speed* (V). Wavelength is the distance between two adjacent crests or troughs of a wave (Fig. 1B), or in the case of a fish's body, the distance between the peaks or midpoint crossings of the body undulation (see the red points on Fig. 1C). The wave speed V is the speed the wave moves along the body or fin, and is generally approximated as

$$V = \lambda f.$$

Wave speed, wavelength, and frequency share a fairly consistent relationship when assuming the parameter of interest is held constant. However, in fishes, the assumption of a strictly constant behavior is often violated; therefore the expected relationships among wave speed, wavelength, and frequency are not always observed when regressed against the swimming speed of the fish.

Frequency, wavelength, and wave speed are all related to the *phase* ϕ of the wave, or the fraction of the cycle. Phase starts at zero at the beginning of a cycle and increases to a maximum value (usually 1, 2π, or 360°) at the end of the cycle and then wraps back around to zero. The point at which phase is zero is arbitrary; often it is the point at which the excursion increases across zero, but sometimes it is at a peak in the cycle. Similarly, the maximum value, termed the *modulus*, of the phase, is a choice; here, we use phase mod 1, which corresponds to using phase values that cycle from 0 to 1. Phase is also commonly expressed mod 2π or mod 360, for 2π radians or 360° in a circle, respectively. Estimating the phase of the kinematic cycle can be challenging (e.g., see Revzen and Guckenheimer, 2008), but we outline a procedure in Section 3.5.

3.2 Traditional parameters and swimming performance

Each wave parameter—amplitude, frequency, wavelength, and wave speed—plays a role in determining the efficiency, speed, and maneuverability of fish swimming. For instance, a larger amplitude at the tail tip typically results in greater thrust, enhancing forward propulsion (particularly during acceleration, e.g., Akanyeti et al., 2017; Schwalbe et al., 2019). Higher frequency, or the rate at which these waves are produced, can increase swimming speed but may require more energy, affecting endurance. Wavelength and wave speed influence how efficiently the fish can move through water (Anastasiadis et al., 2023; Nangia et al., 2017); a longer wavelength can reduce drag, while faster wave speeds allow rapid adjustments in direction and speed, critical for agile maneuvers. Together, these parameters interact to define a fish's overall swimming performance and its ability to navigate complex environments (Fig. 2).

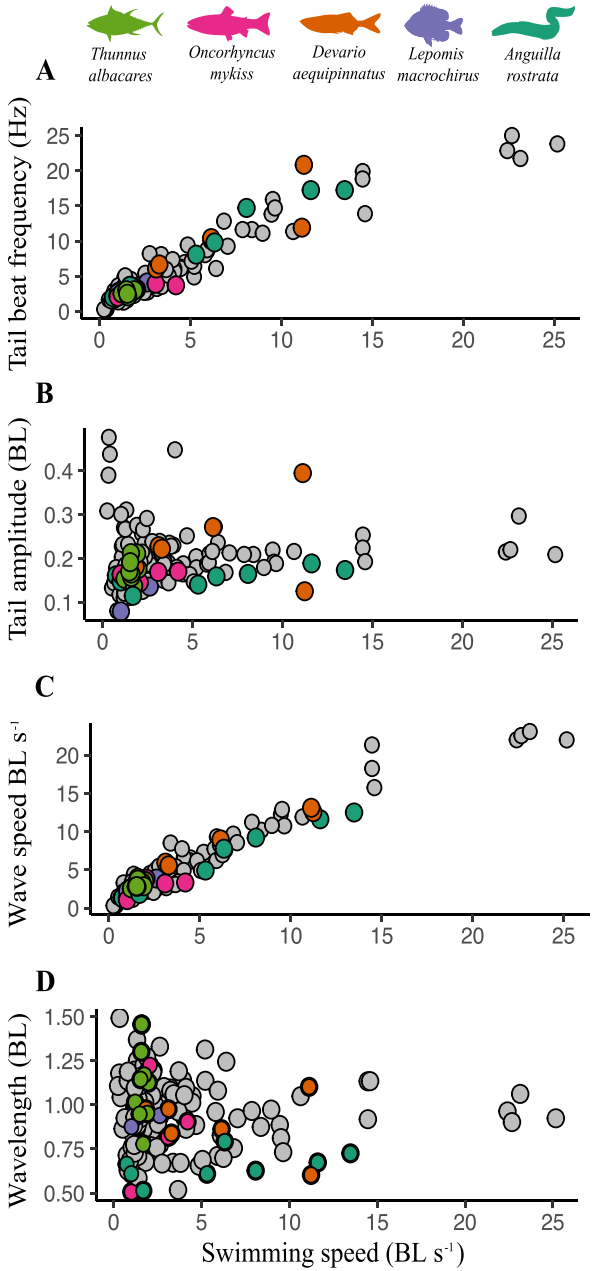

FIG. 2 Swimming kinematics from a diversity of fish species. Colored points show five selected species, shown with silhouettes at the top with other species in gray points. The selected species represent diverse body shapes of fishes and are used to illustrate species differences in common metrics of swimming kinematics. (A) Tail beat frequency. (B) Tail amplitude. (C) Body wave speed. (D) Body wavelength. BL refers to body length. *Modified from Di Santo et al. (2021).*

One of the simplest measures of performance is swimming speed, often measured in body lengths traveled per second (BL s^{-1}). Using body lengths instead of a standard unit of measurement such as meters allows for performance comparisons across body sizes and species. Body size, along with shape, kinematics, and internal mechanisms such as body stiffness, may account for differences in the effect of changing wave parameters on swimming speed (Bainbridge, 1963, 1958; Hoover and Tytell, 2020; Hunter and Zweifel, 1971; Sánchez-Rodríguez et al., 2023; van Weerden et al., 2014). In most cases, swimming speeds recorded for most fishes are not free-swimming speeds but rather speeds set using flow tunnels. Therefore, swimming speed is often treated as a predictor of wave parameters and shown on the x axis, rather than an outcome of the swimming movements (van Weerden et al., 2014; Webb et al., 1984).

Fishes that swim by undulating their bodies and caudal fins tend to increase swimming speed by increasing tail beat frequency, rather than adjusting other parameters such as amplitude, which can reduce the cost of transport during steady swimming (Bainbridge, 1963; Di Santo et al., 2021; Hunter and Zweifel, 1971; Li et al., 2021; Sánchez-Rodríguez et al., 2023) (Fig. 2A). Similarly, for fishes that use fins rather than body undulations to swim, increased fin beat frequency typically results in increased swimming speeds (Drucker et al., 2006; Drucker and Jensen, 1996; George and Westneat, 2019; Webb, 1973).

The range of frequencies that fishes use for steady swimming also depends on body size. In general, smaller fishes use higher frequencies. For adult fishes below about 0.5 m in body length (not including larval fishes), maximum tail beat frequency is limited by the maximum contraction speed of the muscles, and tends to peak at around 20 Hz (Sánchez-Rodríguez et al., 2023). At larger body sizes, the maximum frequency decreases inversely as body size increases (Sánchez-Rodríguez et al., 2023).

Similar to frequency, the speed at which a propulsive wave travels along the body is proportional to the swimming speed (Gray, 1933; Tytell et al., 2010; Wardle et al., 1995), but propulsive wave speed is faster than the swimming speed of the fish (van Weerden et al., 2014) (Fig. 2C).

Shark locomotion is similar to that of bony fishes that use their body and caudal fin to swim, but with several key differences (Lauder and Di Santo, 2015). Like bony fishes, most species swim using body undulations, where waves of lateral bending travel down the body to generate thrust (Webb and Keyes, 1982). Median and paired fins actively contribute to control, helping to balance pitch, roll, and yaw, with pectoral fins reoriented during maneuvers to generate torques and dorsal fins assisting in stabilization. Unlike most bony fishes, a defining feature of shark propulsion is their heterocercal tail, which produces a downward-inclined momentum jet that induces a pitching torque around the center of mass, counteracted by lift forces from the body and head to maintain a stable trajectory (Wilga and Lauder, 2002). Additionally, shark

skin is covered in dermal denticles that modify boundary layer flow; experimental work suggests these structures reduce drag and may enhance thrust on oscillating surfaces (Oeffner and Lauder, 2012).

Many researchers have attempted to quantify the efficiency of swimming, particularly as a way to compare fish or fish-like robots to man-made devices with propellers. For a propeller, efficiency is often measured as a Froude efficiency, or the ratio of "useful power" (typically the thrust force multiplied by the speed) to the total power. A propeller can be tested separately from a hull, which allows a clear definition and measurement of thrust separately from drag, but the same is not true of a fish. One cannot separate a fin and measure the thrust it produces separately from the drag on the body, which makes both the definition and measurement of thrust challenging for fishes. See Schultz and Webb (2002) and Tytell (2007) for detailed discussions of these challenges.

However, there are commonly used metrics that are related to the efficiency of swimming. In the context of wave speed, efficiency should increase as the propulsive wave speed gets closer to the swimming speed. To quantify this effect, researchers use a dimensionless metric called the *slip ratio,* defined as

$$\textit{Slip ratio} = \frac{U}{V}$$

where U is the swimming speed of the fish and V is the propulsive wave speed (Lighthill, 1970). Slip ratios that are closer to 1 indicate more efficient swimming as the propulsive wave speed matches or is close to the forward swimming speed of the fish, suggesting that input power is not lost to the wake. However, simulations show that higher slip ratios also may limit a fish from making efficient maneuvers out of a steady swimming bout (Yu et al., 2013, 2012). The average slip ratio is $\sim$0.7, but it can vary substantially depending on the species and behavior (Videler, 1993). To further complicate this idea, the propulsive wave speed is not always consistent along the length of a fish. For example, Di Santo et al. (2021) found that for thunniform fishes, wave speed decreased along the body, resulting in lower speeds at the tail tip. In other species such as eels, stiffening of the caudal region increases the wave speed, which is thought to then increase swimming speed or decrease the energetic costs of body bending from head to tail at a particular speed (Long, 1998). To better understand the importance of changing wave speed along the body, more work investigating hydrodynamic advantages, body stiffness, and other internal mechanisms of propulsive wave modulation is necessary.

In contrast to frequency or wave speed, the tail beat amplitude and body wavelength typically do not correlate well with steady swimming speed (Fig. 2B and D). Tail beat amplitude is often lower at the lowest swimming speeds, but at higher speeds, it tends to remain fairly constant (Bainbridge, 1963; Di Santo et al., 2021; Videler, 1993; Webb and Weihs, 1986). Computational work by Li et al. (2021) suggested that increasing swimming speed

by modulating frequency alone may be more energetically efficient than also altering body amplitude. In general, amplitude tends to change along the body in a 'U' shaped pattern, with the highest amplitude at the tail, a lower amplitude at the head, and the minimum amplitude somewhere in the anterior two thirds of the body (Di Santo et al., 2021). There may be species-specific differences in this pattern: for example, hagfishes have generally higher body and head amplitudes than similarly shaped eels (Akanyeti et al., 2017; Di Santo et al., 2021; Gillis, 1998; Jayne and Lauder, 1995a; Lim and Winegard, 2015). Additionally, different species of hagfishes show different relationships with tail beat amplitude while increasing swimming speed—*Myxine glutinosa*, a burrowing specialist, increases amplitude at the tail tip while *Eptatretus stoutii*, a more free swimming hagfish, decreases tail beat amplitude (Lim and Winegard, 2015). Head amplitude also appears to differ across many species although it does not seem to impact swimming speed (Di Santo et al., 2021). In contrast to fishes that swim mainly with their bodies, for some species that swim with undulatory fins, fin amplitude is closely correlated with swimming speed (Li et al., 2005; Ruiz-Torres et al., 2013; Youngerman et al., 2014).

Similarly, body wavelength does not correlate well with swimming speed in many species. It was originally thought to vary primarily with body shape, with elongate fishes tending to use a shorter wavelength than other species. For example, eels and other elongate fishes use shorter wavelengths than tuna (typically $\sim$0.75 BL and $>$1.1 BL, respectively), and some species seem to have more variability in wavelength than others (Di Santo et al., 2021; Long and Nipper, 1996). Moreover, shallow-bodied species tend to have shorter wavelengths than deeper bodied species (van Weerden et al., 2014). These differences were often categorized into "swimming modes," which we discuss later in the chapter. Recently, however, more careful examination indicates that body wavelength may correlate more strongly with swimming speed than previously recognized (Anastasiadis et al., 2023; Stin et al., 2024). In elongate fishes, body wavelength tends to increase with increasing swimming speed (Stin et al., 2024). Some species (such as African aba, *Gymnarchus niloticus*) that undulate a long ribbon fin to power swimming, also increase wavelength as swimming speed increases (Li et al., 2005).

3.3 Swimming modes

The diversity of body and caudal-fin (BCF) locomotion has traditionally been categorized into discrete swimming modes, each defined by specific kinematic and morphological characteristics. The major categories—anguilliform, subcarangiform, carangiform, and thunniform modes—were first introduced by Breder (1926) and later expanded upon by Lighthill (1969), who provided a theoretical framework for understanding these modes in terms of hydrodynamics. For example, anguilliform swimmers, such as eels, are characterized by their ability to undulate nearly the entire length of their body, whereas

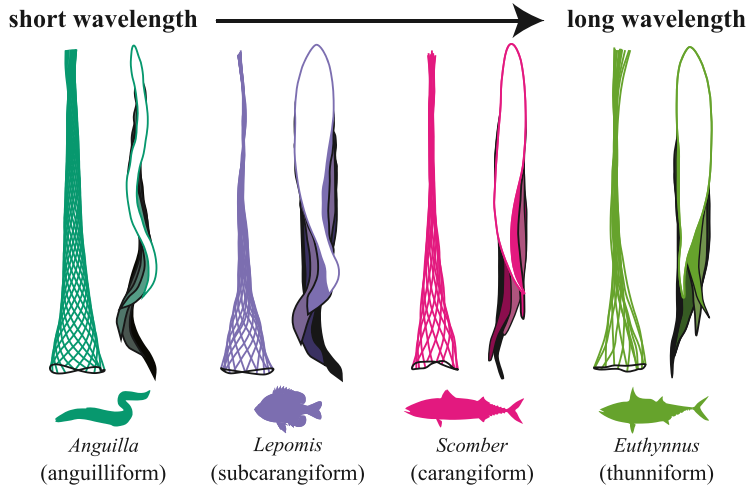

FIG. 3 Continuum of swimming modes, increasing from short to long body wavelengths. Traced outlines of swimming fishes representing the four categories of undulatory swimming and their corresponding midline traces from experimental data. The fish outlines are shown swimming forward with each shaded outline showing progression over time. The midlines represent the body of the fish tracked from snout to tail over a tail beat cycle with different color lines indicating time. Fishes swam between 1.6 body lengths per second (BL/s) and were comparable lengths (20–25 cm total length). The four genera and their general body shapes representing the four classical modes are *Anguilla* (eel, anguilliform), *Lepomis* (sunfish, subcarangiform), *Scomber* (mackerel, carangiform), and *Euthynnus* (tuna, thunniform). *This figure is adapted and modified from Lauder and Tytell (2006). Midline and kinematics outlines are based on data from Tytell and Lauder (2004), Tytell (unpublished), and Donley and Dickinson (2000).*

thunniform swimmers, like tuna, are believed to generate thrust primarily through movements of the caudal fin, with minimal oscillation of the body. This classification has been widely accepted and used to describe and predict the swimming behaviors of a wide range of fish species (Lauder and Tytell, 2006; Sfakiotakis et al., 1999; Webb, 1984).

However, recent studies, including a comprehensive analysis of 43 fish species (Di Santo et al., 2021), challenged the validity of these discrete categories. The findings reveal that the kinematics of undulatory swimming do not conform to these traditional modes. Instead, the swimming behaviors of fishes represent a continuum with wide overlap of locomotor strategies, rather than distinct and separate categories. Fig. 3 shows the classic divisions in swimming modes, but note how similar the kinematics are, particularly for the subcarangiform through thunniform modes. This continuum is evident when examining key kinematic parameters, such as body wavelength, oscillation amplitude, and head-to-tail amplitude ratios. Contrary to the expected decrease in head-to-tail amplitude from anguilliform to thunniform modes, the data show significant overlap in these parameters across species with varying

morphologies. For example, both eels (anguilliform) and tuna (thunniform) do not differ significantly in head-to-tail amplitude ratios during steady swimming, a finding that contradicts the long-held assumption of distinct locomotor modes (Di Santo et al., 2021).

The concept of a continuum in fish swimming modes is further supported by the variability observed within species traditionally classified into the same category. Analysis showed that species classified as subcarangiform or carangiform displayed a wide range of kinematic behaviors that often overlapped with those of anguilliform and thunniform swimmers. For instance, species like the Atlantic salmon (*Salmo salar*), typically classified as subcarangiform, have swimming kinematics more similar to anguilliform species, with a shorter propulsive wavelength and higher head amplitude than expected. This variability underscores the limitations of using rigid categories to describe fish locomotion and highlights the need for a more nuanced understanding of swimming mechanics that considers the full spectrum of locomotor strategies (Akanyeti et al., 2022, 2017; Di Santo et al., 2021).

In fact, Di Santo et al. (2021) found that the amplitude of the undulating wave in 92 % of tested individuals was well described by a second order polynomial curve. In a robotic model, using a similar increasing amplitude wave required substantially less energy to swim at the same speed as a robot that used a constant amplitude along the body (Anastasiadis et al., 2024). This approach not only identifies common locomotor strategies across species, but it also clarifies how fishes achieve propulsion efficiency by optimizing body wave patterns to minimize drag and maximize thrust during swimming. By capturing the nuances of amplitude variation along the body, the model reveals how different species, regardless of their morphology, fine-tune their body movements to maintain energy-efficient propulsion, adjusting their swimming mechanics to varying environmental conditions (Di Santo and Goerig, 2025).

While the traditional classification of fish swimming modes has been instrumental in advancing the understanding of fish biomechanics, it is increasingly clear that this framework is too simplistic to capture the complexity of fish locomotion. The findings advocate for a shift towards recognizing the continuum of swimming strategies employed by fishes, which better reflects the diversity and adaptability of these animals in their aquatic environments. This continuum perspective not only enhances the understanding of fish biomechanics but also has practical implications for fields such as fisheries management, conservation, and the design of biomimetic robots, where accurate representations of fish locomotion are critical (Castro-Santos et al., 2022; Lauder, 2022).

3.4 Dimensionless swimming parameters

Dimensionless parameters are a very important way to compare the relative importance of certain effects. They are ratios of parameters in the same units

(also called "dimensions"), structured so that the units cancel out, and the final parameter has no units (hence, it is called "dimensionless"). Dimensionless parameters are therefore independent of the original units of measurement. See Barenblatt (2003) for an introduction to dimensionless parameters and dimensional analysis.

A crucial dimensionless parameter for understanding swimming fish is the Reynolds number, a ratio of inertial and viscous forces in a fluid. It characterizes the physical interaction fishes have with the fluid. Water is a dense, incompressible fluid and the size and speed of the fish moving through that fluid greatly impacts the way fluid moves around a fish. The Reynolds number (*Re*) is defined as

$$\mathrm{Re} = \frac{\rho U L}{\mu}$$

where ρ is the density of the fluid at a given temperature and salinity ($kg{\cdot}m^{-3}$), U is the flow speed ($m{\cdot}s^{-1}$), L is a characteristic length (typically the length or width of the fish or the diameter of an object; in m), and μ is the dynamic viscosity of the fluid at a given temperature and salinity ($N{\cdot}s{\cdot}m^{-2}$). High Re means that inertial forces are stronger than viscous forces, and also indicates whether the flow around the fish is laminar or turbulent (Fig. 4A). If the Reynolds number is less than about 1, viscous forces predominate. For fishes with a *Re* in this range, it likely feels like swimming in honey and flow around the fish will remain laminar. For a Reynolds number that is about 1000 or greater, inertial forces dominate. In this case, the flow around a fish will continue to move freely until it is disturbed, causing turbulent flow. In the middle of the two extremes ($1 < Re < 1000$) there is a range of transient flow that is neither strictly laminar or turbulent. In general, a small and slow swimmer will experience viscous forces while a large and fast swimmer will experience inertial forces (Videler, 1993). Despite the differences in types of forces, from mostly viscous forces while in larval form, to inertial forces later in development, undulatory movements of the body allow fishes to produce thrust (McHenry and Jed, 2003; Müller et al., 2008; Taylor, 1952; Videler, 1993). See more on the Reynolds number in Vogel (1994).

The Reynolds number also predicts whether the wake, or flow behind a fish, will be laminar or turbulent. For a cylinder with *Re* greater than 1, the wake normally takes the form of a von Kármán street, which consists of pairs of counter-rotating pockets of water called vortices (Fig. 4B). For fishes, however, the wake produced is a reverse von Kármán street, with the direction of circulation opposite that of the traditional von Kármán street (Fig. 4B). To understand how vortex shedding impacts fish swimming performance, and classify the behavior of the wake, another dimensionless parameter is used: the Strouhal number (*St*).

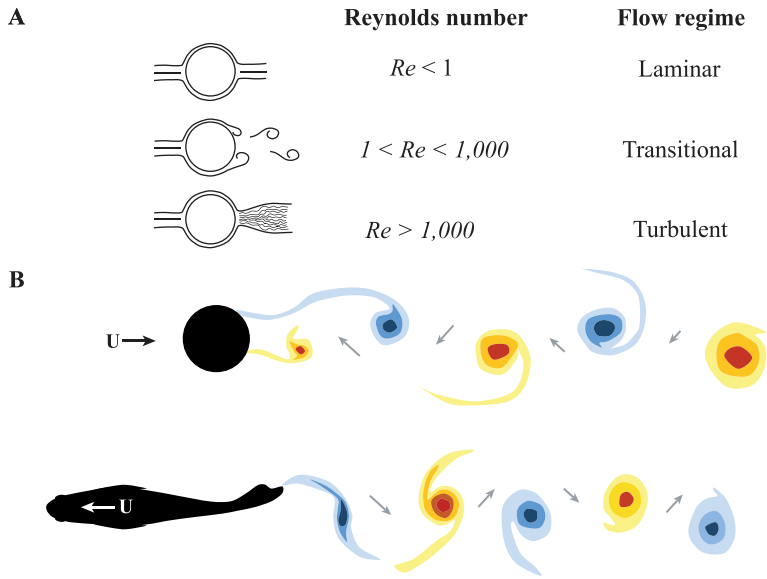

FIG. 4 Reynolds number and von Karman wakes. (A) Schematic of flow in laminar, intermediate, and high Reynolds number ranges. (B) von Karman wave from a bluff body and a reverse von Karman wake from a swimming fish where blue and orange regions indicate clockwise and counterclockwise vorticity, respectively.

The Strouhal number was originally developed to quantify how stationary bodies in a flow shed vortices (like the cylinder in Fig. 4B) (Triantafyllou et al., 1993, 2000, 1991). The Strouhal number is defined as

$$St = \frac{2fA}{U}$$

where f is the tail beat frequency (in Hz or s^{-1}), A is the tail beat amplitude (in m; Fig. 1A), and U is the average swimming speed of the fish (in m s^{-1}). It is defined relative to the total width of the wake, approximated by the peak-to-peak amplitude of the tail, which is $2A$. Triantafyllou et al. (1993) and later Taylor et al. (2003) suggested that the swimming efficiency would be highest when a fish uses a Strouhal number near 0.3. The shape and kinematics of the trailing edge, either in the case of a caudal fin of a fish or a flapping hydrofoil, impacts the timing and shape of shedding vortices (Lauder, 2000; Nauen and Lauder, 2002; Wang et al., 2022). Furthermore, the swimming speed of the fish, wave properties of the body, and median paired and unpaired fin wakes also change patterns of the wake behind the fish (Müller et al., 2001, 1997; Nauen and Lauder, 2002; Tack et al., 2024; Tytell, 2006; Tytell et al., 2008; Tytell and Lauder, 2004). The wake around a fish greatly impacts its propulsive efficiency as the wake may impart higher drag, amplify jets to produce thrust, or in some cases produce lift (Godoy-Diana and Thiria, 2018; Lauder,

2000; Lucas et al., 2020; Tack et al., 2024; Wilga and Lauder, 2002). Within a narrow range of *St* between 0.2 and 0.4, the reverse von Kármán street generated by the flapping tail acts as to amplify hydrodynamic instabilities in the unsteady wake, producing more thrust with less motion, and leading to higher performance (Moored et al., 2012; Triantafyllou et al., 1993). The measured range of *St* associated with peak efficiency for fishes, marine mammals, and even fliers is between 0.2 and 0.4, with most large fishes swimming at a *St* around 0.3 (Eloy, 2012; Rohr and Fish, 2004; Saadat et al., 2017; Taylor et al., 2003; Triantafyllou et al., 1993, 2000, 1991).

Although many researchers calculate Strouhal number based on body movement, in its original use, it is related to vortex shedding, which is a high Reynolds number effect. For small fishes at lower *Re*, we can calculate *St*, but its influence on swimming seems to be less clear. Indeed, the relationship between St and the Reynolds number is weak in the laminar regime ($\mathrm{Re} < 1$), $St \propto \mathrm{Re}^{-1/4}$ meaning that *St* tends to become larger for smaller or slower animals (Gazzola et al., 2014).

The Strouhal number is related to swimming efficiency as it combines "input" parameters (such as frequency and amplitude of tail oscillations) with an "output" parameter (swimming speed). This relationship provides insight into the effectiveness of energy transfer from body movement to propulsion. Gazzola et al. (2014) attempted to isolate purely "input" parameters with a dimensionless parameter they called the swimming number *Sw* defined as

$$Sw = \frac{2fAL}{v}$$

where *f* is tail beat frequency, *A* is tail beat amplitude, *L* is the length of the fish, and *v* is the kinematic viscosity (Gazzola et al., 2014). The swimming number is essentially a transverse *Re*, or the Reynolds number of the side-to-side motion of the tail, and for high Reynolds number swimmers, $\mathrm{Re} \propto Sw$ (Gazzola et al., 2014). *Sw* allows for the connection of undulatory motions of a swimmer (the "input") to the measured swimming speed through the traditional Reynolds number (the "output"). For swimmers in the laminar regime, $\mathrm{Re} \propto Sw^{4/3}$ (Gazzola et al., 2014).

Strouhal number and swimming number are related to the motion of the tail. To characterize the body motion or waves on a fin, some researchers have developed dimensionless parameters related to the wavelength. For instance, Bale et al. (2015) and Nangia et al. (Nangia et al., 2017) estimated the specific wavelength λ*, defined as

$$\lambda^* = \frac{\lambda}{\tilde{a}}$$

where λ is the wavelength on the f, and $\tilde{a}$ is the average amplitude of waves across the body or fin. They referred to the specific wavelength as SW, but to avoid confusion with the swimming number *Sw*, we suggest λ*. Similar to

Strouhal number, swimmers tend to use specific wavelengths that fall within a relatively narrow range that seem to be related to propulsive thrust or efficiency. For species that swim using a traveling wave on their body, λ^* is typically close to 10 (Nangia et al., 2017), while for those that use their fins to swim, λ^* of the fins tends to be close to 20 (Bale et al., 2015). Bale et al. and Nangia et al. collected data from a wide range of species and sizes, and they suggest that these values of λ^* are optimal for thrust production.

3.5 Computing kinematic parameters

To estimate the kinematic parameters, researchers generally take high speed video of fish swimming and then digitize points along the midline of the body (e.g., the blue points in Fig. 1C).

3.5.1 Take good videos

To estimate kinematics accurately, one must have clear video that shows the movement of interest. Roche et al. (2023) provided detailed guidelines for estimating kinematics for fast starts, much of which is relevant here. We briefly summarize these guidelines. First, decide if you need 2D or 3D data. For 2D data, we recommend a single camera placed either above or below the tank, perpendicular to the swimming direction. If you take video from above, you may want to place a sheet of clear plastic on the surface of the water to minimize wave distortions. For 3D data, you will need two or more synchronized views, ideally separated by angles of approximately 90°. To estimate the 3D location of a point, you will need to be able to identify that point unambiguously in at least two camera views. Points like the eye or the tip of a specific fin ray are good; points like the "the middle of the peduncle" are not as good. Hedrick (2008) describes a method and a software package that aids in identifying corresponding points in multiple views and then triangulates the 3D location.

Next, set your camera parameters. This process is usually a compromise between high enough frame rates and exposure speeds, lighting, focus, and the camera aperture (also called F-stop). Start by selecting a frame rate and exposure duration (sometimes called the "shutter speed"). Around 100 frames per second and 2–5 ms exposure duration is appropriate for many fish and behaviors. Higher frame rates and lower exposure durations will be typically be necessary for smaller fish or faster behaviors. Be careful to choose a exposure duration that will avoid motion blur for the fastest movements. Next, choose an aperture (also called F-stop). Larger apertures (corresponding to lower F-stop numbers) let in more light, but also have a narrower depth of focus. Things that are too close or too far from the camera will be out of focus. Smaller apertures (higher F-stops) let in less light but will be easier to maintain focus. You can alleviate some of these challenges by making sure you have bright enough illumination. Many scientific cameras are sensitive to infrared light that fish cannot see, which means that you can use very bright infrared lights without affecting fish behavior.

3.5.2 Digitize points on the body

Once you have clear videos, you must digitize points along the body. This can be done manually, using programs like DLTdv (Hedrick, 2008), or semi-automatically using computer vision techniques (e.g., DeepLabCut: Mathis et al., 2018; Mathis and Mathis, 2020; SLEAP: Pereira et al., 2022). Sometimes the outline of the body is easiest to see, and then you can digitize the left and right sides and then estimate the midline (e.g., Jayne and Lauder, 1995b); in other cases, there are clear features along the midline that can be digitized directly.

The number of points that need to be digitized depends on the kinematic parameters to be estimated. To estimate frequency, you only need one point at the tip of the tail or any posterior location. To estimate tail beat amplitude, you need a minimum of three points: the snout, a point near the center of mass, and the tail tip. With these three points, you will be able to estimate a central location and a central axis, as detailed below. Finally, to estimate the body wavelength, you need a minimum of about four points per wavelength. For eels or anguilliform swimmers that tend to have slightly more than one wave along their bodies, that means that you probably need at least six points along the body. For carangiform swimmers that have a longer wavelength, you may be able to use fewer points.

Once you have digitized midlines, there are a number of important steps to estimate the kinematics accurately based on midlines. Many researchers have developed their own procedures and code. To streamline future work, we have developed an R package (fishmechr: Tytell, 2025) that performs all of the calculations described below. Our suggested workflow is detailed below.

1. Compute the arc length along the curve of the body.
2. If the points are not consistently at the same arc length, interpolate the points so that each one is at a consistent point on the body. It is often useful to do some smoothing as part of this step.
3. Compute a center location. Ideally this is the center of mass, but it could be approximated in a variety of ways.
4. Compute the body curvature or excursion relative to a central axis.
5. Estimate the phase of the oscillation at each point. You can either detect peaks and zero crossings or use a mathematical technique called the Hilbert transform.
6. Use temporal and spatial derivatives of the phase to estimate the oscillation frequency, body wavelength, and body wave speed.
7. Based on the phase, identify individual undulation cycles. Within each cycle, you can identify the range of body excursion or curvature to compute the amplitude.

This workflow differs from some previous approaches in two main ways. First, it does not assume that the fish is swimming along the horizontal or vertical axis in the video. It can work with videos of freely swimming fishes, including ones in which the fish swims along a curved path, as well as videos

taken in a flow tunnel. Second, it estimates the phase for each point along the body, which allows a straightforward estimation of cycle-by-cycle kinematic parameters (such as amplitude) or merging with other data sets, like electromyographic data, that may contain information that is related to the cycle. We suggest estimating phase using the Hilbert transform, a Fourier-based technique that incorporates information about the entire waveform, rather than just detecting features like peaks. Using peaks or other features of the waveform to estimate phase, frequency, or amplitude is prone to error, because any erroneous peak detected leads to large errors in frequency or amplitude. See Revzen and Guckenheimer (2008) for a detailed discussion of phase and procedures for its estimation.

3.5.2.1 Compute arc length

Most kinematic variables are best specified in terms of arc length s (Fig. 1C), the distance along the curve of the body from the head to a particular point i:

$$s_i = \sum_{j=2}^{i} \left[(x_j - x_{j-1})^2 + (y_j - y_{j-1})^2 \right]$$

where (x_i, y_i) is the location of point i. Using arc length is better than something like the x coordinate for two reasons. First, a fish does not often swim precisely along an axis, which means that the points would need to be rotated. Second, many fish swim with relatively large amplitude motions, which means that the distance along the curve is significantly larger than the distance along the swimming direction, particularly near the tail where amplitudes are higher.

3.5.2.2 Interpolate points for a consistent position

Ideally, we want each point to represent a consistent location on the fish's body. Particularly with fishes that do not have clear landmarks along the body, we may be able to mark the middle of the body easily, but at points that may slide along the fish's length. We can use a spline to interpolate points at a consistent location. Additionally, digitized points often have some error. As part of the interpolation process, we can use a smoothing spline to smooth out some of that error. See examples in the *fishmechr* package (Tytell, 2025).

3.5.2.3 Estimate a center location

The center location is a weighted average location and may not be located exactly on the fish's body (Fig. 1C). During undulatory swimming, all points on a fish's body move laterally as well as forward, meaning that you may introduce errors if you use a specific anatomical point as a reference for the kinematics or the swimming speed. Instead, we suggest using one of the metrics below. For a midline defined by x and y coordinates, there are four main ways to identify the center location, also referred to as the center of mass (COM).

1. If m_i is the mass of segment located between (x_i, y_i) and (x_{i+1}, y_{i+1}), then

$$x_{com} = \frac{1}{2M} \sum_{i=1}^{n-1} m_i (x_{i+1} + x_i)$$

$$y_{com} = \frac{1}{2M} \sum_{i=1}^{n-1} m_i (y_{i+1} + y_i)$$

   where M is the total mass of the fish. If you know the mass distribution but not the true masses of segments, you could also let M be 1 and then m_i would be the fraction of the total mass in segment i.
2. If you do not know the mass distribution, then you can approximate m_i in several ways. The best is to use the width and height of the body. If the body, without the fins, has an elliptical cross section, where w_i is the horizontal width and h_i is the dorso-ventral height at point i, then the volume of the segment from (x_i, y_i) and (x_{i+1}, y_{i+1}) is

$$V_i = \pi \Delta s_i (w_i h_i + 1/2 \Delta w_i h_i + 1/2 \Delta h_i w_i + 1/3 \Delta w_i \Delta h_i)$$

   where $\Delta s_i = s_{i+1} - s_i$, $\Delta w_i = w_{i+1} - w_i$, and $\Delta h_i = h_{i+1} - h_i$. Then we approximate $m_i \approx \rho V_i$, where ρ is the density of the fish, which we assume here to be constant, so that

$$x_{com} = \frac{\sum_{i=1}^{n-1} [V_i (x_{i+1} + x_i)]}{2 \sum_{i=1}^{n-1} V_i}$$

$$y_{com} = \frac{\sum_{i=1}^{n-1} \left[V_i (y_{i+1} + y_i) \right]}{2 \sum_{i=1}^{n-1} V_i}$$

3. Often the width is visible from a camera from above or below, but the height is not known. If the height does not vary greatly, a reasonable approximation is that $m_i \propto w_i$, so that

$$x_{com} = \frac{\sum_{i=1}^{n} w_i x_i}{\sum_{i=1}^{n} w_i}$$

$$y_{com} = \frac{\sum_{i=1}^{n} w_i y_i}{\sum_{i=1}^{n} w_i}$$

4. Choose one point along the body to use as the center. This could be the snout or a point close to the center of mass. This has been called the "stretched-straight center of mass", but tends to give inaccurate estimates of velocity or acceleration (Roche et al., 2023).

3.5.2.4 Estimate curvature or lateral excursion

Curvature: The 2D curvature κ of the midline in the horizontal plane is often a useful variable to compute. It can be thought of in two different ways. First, it is the inverse of the radius of curvature: the radius of a circle drawn through three successive points (Fig. 1C, inset). The smaller the radius of curvature, the sharper the body bend, and the larger the value of k. This estimate for curvature is defined as

$$k = \left[\frac{\partial x}{\partial s}\frac{\partial^2 y}{\partial s^2} - \frac{\partial y}{\partial s}\frac{\partial^2 x}{\partial s^2}\right]\left[\left(\frac{\partial x}{\partial s}\right)^2 + \left(\frac{\partial y}{\partial s}\right)^2\right]^{-3/2}$$

Second, it is the spatial derivative of the angle of each segment (Fig. 1C, inset). If a segment at arc length s has an angle θ (in radians) to the horizontal axis, then the curvature is

$$k = \frac{\partial \theta}{\partial s}$$

The angle for segment i is $\theta_i = \tan^{-1}(y_{i+1} - y_i, x_{i+1} - x_i)$.

Although both formulas are mathematically equivalent, they have slightly different properties depending on the measurement error on the x and y positions.

Lateral excursion: One can also estimate the body phase, and then the wavelength and wave speed, based on the excursion of the body relative to a primary axis, or the direction the fish is swimming. We suggest using the singular value decomposition (SVD) to estimate the primary axis, then using a low-pass filter to remove any oscillations at the tail beat frequency or higher. Start with a matrix $\mathbf{X}$ of x and y coordinates of points along the body at a specific time:

$$\mathbf{X}_{n\times 2} = \begin{pmatrix} x_1 & y_1 \\ x_2 & y_2 \\ \vdots & \vdots \\ x_n & y_n \end{pmatrix}$$

where the subscript indicates the size of the matrix (n points along the body by 2 coordinates).

First, center each axis by subtracting the location of the center of mass or the mean of each column, to produce a matrix, $\mathbf{X^C}$ centered around 0. Then the singular value decomposition allows you to write the matrix in the form

$$\mathbf{X}^C_{n\times 2} = \mathbf{U}_{n\times n}\mathbf{\Sigma}_{n\times 2}\mathbf{V}^T_{2\times 2}$$

The matrix $\mathbf{V}_{2\times 2}$ then represents the principal axes of the body in that frame, one parallel to the main body axis and one perpendicular. The matrix can be estimated at each time point, to produce a time-varying matrix $\mathbf{V}(t)$.

Assuming the amplitude is relatively small, the first column of $\mathbf{V}$ represents a unit vector pointing along the primary axis of the body (which we call $\hat{\mathbf{a}}(t)$; Fig. 1C) and the second column is a unit vector normal to the primary axis.

We suggest using a low pass filter with a cutoff frequency below the tail beat frequency to smooth the components of the $\hat{\mathbf{a}}(t)$ vector, making sure to normalize it after smoothing. See implementation details below.

3.5.2.5 Estimate phase

To estimate the undulation frequency, body wavelength, and wave speed, consider a simple equation for the midline. Fish swim using a traveling wave of curvature κ_s or lateral excursion defined at an arc length s along the body as

$$\kappa(s, t) = A(s)\cos\left(2\pi\left[\frac{s}{\lambda} - ft\right]\right) \tag{1}$$

where $A(s)$ is the wave amplitude, λ is the wavelength, f is the oscillation frequency, and t is time. In this case, the phase of the oscillation $\phi(s, t)$, or the fraction of a cycle completed at a particular point along the body and time is approximately equal to the argument of the cosine, $\phi(s, t) = 2\pi[s/\lambda - ft]$. If the amplitude A varies over quickly over time or space, this approximation may not be exactly correct.

If we can estimate the phase accurately, then we can use a spatial derivative (i.e., with respect to s) to estimate λ, the body wavelength, and a temporal derivative (i.e., with respect to t) to estimate f, the undulation frequency. Therefore, estimating phase of the points along the body, specifically at the tail, provides better temporal resolution compared to counting tailbeats across a set number of frames. Estimating phase also makes it easier to compare the timing of movement across points of interest on the body and fins. See Fig. 5 for an illustration of the phase and its derivatives.

Below, we describe two methods for estimating phase.

3.5.2.6 Use the Hilbert transform

One convenient and relatively robust way to estimate the phase of each body point involves the use of the Hilbert transform $\mathcal{H}$, a procedure that uses the Fourier transform to estimate a periodic signal that is 90° shifted relative to another. In essence, given a cosine signal, the Hilbert transform returns the sine with the same amplitude and frequency. The utility of this operation is that it lets us estimate the "analytic signal", a complex-valued signal where the magnitude of the complex number is the amplitude of the wave, and the phase angle of the complex number is the phase of the signal. For example, the analytic signal of the curvature κ would be

$$\kappa^*(s, t) = \kappa(s, t) + i\mathcal{H}\{\kappa(s, t)\}$$

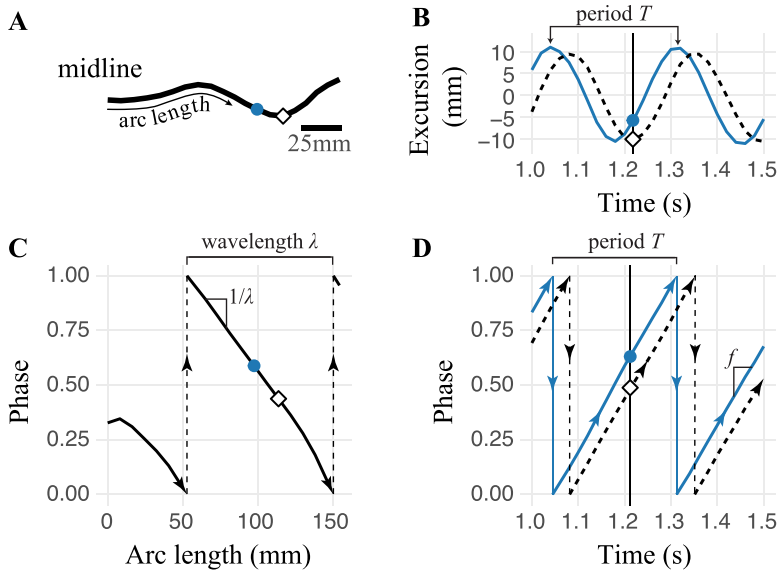

FIG. 5 Phase along the body of a swimming fish. (A) Midline of the fish, seen from above, highlighting two points (blue circle and open black diamond). (B) Side-to-side excursion of the two points, showing the cycle period T. The vertical line indicates the time of the midline in panel A. (C) Phase of the points along the body relative to arc length, showing the body wavelength. Decreasing phase along the body indicates that the wave is traveling backward. The slope of the line is equal to $1/\lambda$. (D) Phase of the two points relative to time, showing the cycle period and the frequency f (the slope of the lines). While phase ranges from 0 to 1 here (denoting a cycle), note that the bounds could also be 0° to 360°, or 0 to 2π.

where i is the imaginary number. (Note that the hilbert function in R and Python returns the full analytic signal, not just the imaginary component as written above). For a complex number $C = a + ib$, the magnitude is denoted by $\|C\| = [a^2 + b^2]^{1/2}$ and the phase angle is denoted by $\angle C = \tan^{-1}(b/a)$.

One can also estimate the analytic signal using the Hilbert transform for the lateral excursion of the body $z(s, t)$, where z is the lateral position of a point on the body, relative to the central axis of the body, as described above.

The analytic signal thus provides an estimate of the phase can be estimated as a continuous function of both time and position along the body. Other techniques for estimating phase require identifying particular features in the signal (such as peaks or zero crossings) and therefore do not estimate phase as a continuous signal. The estimated phase $\hat{\phi}$ is thus

$$\hat{\phi}(s, t) = \angle\kappa^*(s, t).$$

For a traveling wave, this phase, as estimated here, is equal to the argument of the cosine function from the traveling wave Eq. (1), $\hat{\phi}(s, t) = 2\pi[s/\lambda - ft]$.

The Hilbert transform only works well for this analysis with signals that are centered around zero and consist of many relatively smooth tailbeats. To use the Hilbert transform on a lateral position, it is important to subtract a baseline value or use a high pass filter to ensure that the signal is centered around zero.

Similarly, if the signal is noisy, the phase $\hat{\phi}$ will not increase steadily and the derivatives used to estimate $\hat{f}$ and $\hat{\lambda}$ will not be meaningful. It is best to filter the input signal using low pass filter (which removes high frequency noise) or a bandpass filter (which removes both slow fluctuations that are not related to the tail beat and high frequency noise) so that the oscillations are smooth.

The complex phase angle, as defined above, typically increases from -π to π (or from 0 to 1, as shown in Fig. 5C and D) and then jumps back to $-\pi$ (or 0). To estimate frequency or wavelength, before performing the derivatives, one should estimate a smoothly increasing phase (which we will refer to as $\hat{\phi}_c(t)$) using the function unwrap (a standard function in modern programming languages), which searches for jumps and removes them.

3.5.2.7 Detect peaks and zero crossings

We can also estimate phase by detecting specific features in the oscillation, such as peaks or zero crossings, and then interpolating a continuous value for the phase using a spline curve. For a cosine function, as above, a positive peak has phase $\hat{\phi} = 0$, a downward zero crossing has phase $\pi/2$, a negative peak (i.e., a trough) has phase π, and an upward zero crossing has phase $3\pi/2$. By identifying these features and their corresponding phases (e.g., marked at "period" in Fig. 5B), one can then interpolate a continuous phase.

Using this method requires careful error checking. Peaks can be identified erroneously, particularly if there is noise in the signal. We recommend using a strong smoothing filter on the curvature or lateral excursion before estimating phase. See examples and numerical details in the R package *fishmechr* (Tytell, 2025).

3.5.2.8 Use the phase to estimate frequency and wavelength

We can then use the estimated phase to compute the frequency and wavelength by taking derivatives in time or space (Fig. 5C and D), respectively,

$$\hat{f}(t) = \frac{1}{2\pi}\frac{\partial}{\partial t}\hat{\phi}_c(s,\, t) \text{ and } \hat{\lambda}_s(t) = 2\pi\left(\frac{\partial}{\partial s}\hat{\phi}_c(s,\, t)\right)^{-1}$$

where $\hat{\phi}_c(t) = \text{unwrap}[\hat{\phi}(t)]$. Estimated this way, frequency should be the same at every point along the body. Therefore, you can average $\hat{f}$ across the body or choose a single point along the body (usually the tail) to use as the estimate of frequency. The body wave speed $\hat{V}$ is the product of the two:

$$\hat{V}(t) = \hat{\lambda}(s,\, t)\hat{f}(t)$$

3.5.2.9 Quantify swimming parameters on a cycle-by-cycle basis

Once you have estimated a good undulation phase, it is straightforward to quantify other parameters that vary every cycle. Usually, we need to define an overall phase of the entire body oscillation. It's best to choose the most reliable phase estimate, which is usually the phase of the tail tip or a point near the tail (e.g., $\hat{\phi}(L, t)$, where L is the body length).

As phase increases past 2π, it will jump back to 0. Most programming languages have a functioned called unwrap that looks for those jumps and removes them, producing a steadily increasing phase, $\hat{\phi}_c(t)$. Then the cycle number is

$$C(t) = \lfloor \hat{\Phi}_c(t)/(2\pi) \rfloor$$

where the L brackets denote the floor operation (a standard function in modern programming languages) that rounds down to the next lowest integer value.

For example, to find the body amplitude, search within each cycle to find the range of motion for each body point and divide by two. See details in the R package *fishmechr*.

4 Forces

For movement through water, fishes are subject to five main classes of forces: gravity, buoyancy, thrust, drag, and lateral forces. The overall force on the body is often separated conceptually into the three orthogonal axes relative to the body orientation or swimming direction (Fig. 6): forward-back forces, often separated again into the forward force thrust and the backward force drag; side-to-side or lateral forces; and vertical forces. These body forces act at the center of mass, but represent the sum of all the forces acting on different sections of the body and fins.

4.1 Gravity and buoyancy

Most fishes are nearly neutrally buoyant, meaning their average density is close, but not identical, to that of water. Importantly, their density distribution is uneven throughout the body (Aleyev, 1977; Fath et al., 2023; Webb and Weihs, 1994). Skeletal elements are significantly denser than water, while buoyancy-regulating structures, most commonly gas-filled swim bladders, are markedly less dense. This internal disparity allows fishes to fine-tune their buoyancy, maintaining equilibrium in the water column (Alexander, 1982; Steen, 1970). Swim bladder morphology varies across fish groups. In physoclistous fishes, the swim bladder is sealed and gas exchange is mediated by a specialized gas gland. By contrast, physostomous fishes retain a pneumatic duct connecting the swim bladder to the digestive tract, enabling them to regulate buoyancy by gulping or releasing air (Steen, 1970). Sharks and other

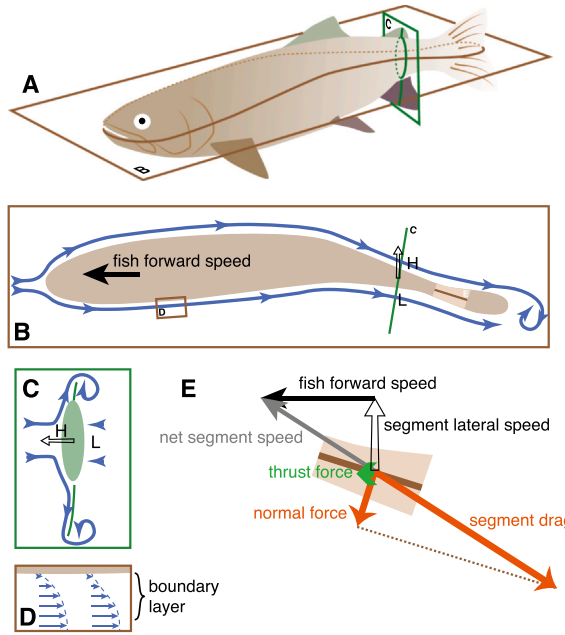

FIG. 6 Flow and forces on a swimming fish. (A) Horizontal and vertical transverse planes around a swimming trout. (B) Flow around the fish in the horizontal plane, shown as blue streamlines. The solid arrow represents the fish's forward speed, and the open arrow indicates the lateral movement of a segment. H, L; high and low pressure, respectively. (C) Flow around a segment in the transverse vertical plane, shown as blue streamlines. (D) Flow close to the body at two points along the fish, showing the thickening of the boundary layer via the changing magnitudes of the black arrows. (E) Movement (black and gray arrows) and forces (orange and green arrows) on a segment of the body, indicating how the thrust force is produced.

elasmobranchs do not have swim bladders, but instead have evolved lipid-rich livers that reduce their overall density (Bone and Roberts, 1969; Gleiss et al., 2017).

Even in a state of near-neutral buoyancy, fishes must counteract gravitational torque. Gravity acts at the center of mass (COM), a point influenced by the spatial distribution of dense tissues. In contrast, the buoyant force resulting from hydrostatic pressure acts upward at the center of buoyancy (COB), which corresponds to the centroid of the fish's displaced volume (Smits, 2000). These two centers are rarely exactly at the same point. Their separation generates a torque that induces rotations in pitch and roll, compromising postural stability (Fath et al., 2023; Webb and Weihs, 1994). Although the magnitude and direction of COM-COB separation have been measured in only a few species, available data show consistent anterior-posterior displacement, with the potential to produce nose-up or nose-down pitching torques (Fath et al., 2023; Webb and Weihs, 1994). Recent work suggests that the swim bladder

(in bluegill sunfish) is mobile in the body cavity, which could change the location of the center of mass (Fath et al., 2023). Other species have swim bladders with multiple compartments that might allow them to actively control this hydrostatic instability (Aleyev, 1977).

To counteract these destabilizing torques, many fishes generate hydrodynamic lift. This is achieved either through body morphology or fin-based propulsion. Elasmobranchs, for example, possess dorsoventrally asymmetric bodies that function similarly to aerofoils, producing lift during forward motion (Alexander, 1990). Similarly, other fishes use the lift force from their pectoral fins to provide an upward force to counteract gravity (e.g., sturgeon: Wilga and Lauder, 1999).

Historically, hovering in near-neutrally buoyant fishes was assumed to incur negligible energetic cost. However, recent findings challenge this view. Di Santo et al. (2025) demonstrated that hovering demands continuous, fine-tuned fin adjustments to maintain stability, effectively doubling metabolic rates compared to resting. The energetic costs scale with morphological features and stabilizing behavior: species with greater COM-COB separation and increased caudal fin activity exhibit higher costs. Conversely, fishes with posteriorly located pectoral fins and streamlined bodies display enhanced stability and reduced energetic expenditure. These findings underscore that hydrostatic equilibrium is inherently unstable in most near-neutrally buoyant fishes, and that maintaining it is metabolically expensive (Di Santo et al., 2025). Dynamic stabilization, therefore, exerts a strong selective pressure on fish morphology, with implications for both evolutionary biology and bioinspired design.

4.2 Drag

Drag on a body in a fluid is parallel to the overall flow direction and comes from three different physical effects: viscosity, pressure differences, and acceleration.

4.2.1 Viscous drag

Viscous drag, or skin friction, is a consequence of the viscosity of the water. For a fish swimming in still water, very to the body, the water moves at the same speed as the body; far away from the body, the water is stationary; in between, there is a gradient in flow speed (Fig. 6D). Due to viscosity, this gradient causes a force on the body.

Viscous forces are particularly important for larval fishes, which swim at low and intermediate Reynolds numbers (less than about 100). At the larval stage, fishes have not fully formed their fins and most muscles are not differentiated (Downie et al., 2020). In larval zebrafish, for which the effects of viscous forces have received great attention, circulation of vortices decreases during swimming (Müller et al., 2000), escape responses are less successful (Danos and Lauder, 2012), and generating enough flow for suction feeding is

difficult (China and Holzman, 2014; Holzman et al., 2015; Yavno and Holzman, 2018). As one way to "escape" the effects of viscous forces, larvae may invest more energy in body growth as increasing body size (L) is one way to increase Reynolds number rapidly (Müller and Videler, 1996; Yavno and Holzman, 2018).

4.2.2 Pressure drag and separation

Pressure drag is due to the shape of the body or segment. Consider the flow around a fish's body in the horizontal plane (Fig. 6B). As the fish moves through the water, then water parts around its anterior body, causing a high pressure zone. As the water flows around the curve of the body, it flows back together, causing low pressure on the sides, and another high pressure zone behind the fish (Fig. 6C). The anterior high pressure is always higher than the posterior high pressure zone, resulting in a net backward force of drag (Faber, 1995). The reason the posterior high pressure is lower than the anterior high pressure is that the inertia of the fluid prevents it from completely converging around the back of the body. Thus at high Reynolds numbers (over about 100), when inertia is more important than viscosity, the pressure drag becomes a much larger force than viscous drag.

Separation is a high Reynolds number effect. When the fluid curves around the leading surface of a body, its inertia will tend to cause it to continue diverging, while viscosity will tend to cause it to adhere to the surface and converge. If the inertial force is sufficiently high, the fluid will not converge fully (see e.g., Fig. 4A in the transitional and turbulent regimes). Close to the body, this effect means that the flow will stagnate or even reverse direction. This region of separated flow causes much lower pressure on the trailing surface, and a much larger pressure drag than if the flow had not separated.

For swimming fish, however, flow in a horizontal plane either does not separate or separates only in a very small region that would not cause substantial changes in drag (Anderson et al., 2001; Fish and Lauder, 2006; Yanase and Saarenrinne, 2015). The lack of separation may be because of the undulatory movement itself, particularly because the traveling body wave moves backwards faster than the forward swimming speed (Akbarzadeh and Borazjani, 2019; Lu and Yin, 2005), or because of flow interactions with scales (Vandenberg et al., 2024) or denticles, an effect particularly well described for shark denticles (Afroz et al., 2016; Domel et al., 2018; Lang et al., 2011; Oeffner and Lauder, 2012).

4.2.3 Acceleration reaction, added mass

When a body accelerates through a fluid, it faces the usual Newtonian inertial force, $F = ma$, where the force is proportional to its mass and the acceleration. However, because fluid surrounds the body, it must also accelerate some of the

fluid around it. This accelerated fluid is, in essence, "added mass". Thus, for a body accelerating through a fluid, it is often appropriate to write

$$F = (1 + C_A)ma \text{ or } F = (m + C_A\rho V)a$$

where C_A is an added mass coefficient, representing the additional fluid that is accelerated when the body itself accelerates (Denny, 1993). For a fish accelerating forward, it is difficult to calculate an added mass coefficient, but fluid dynamic measurements suggest that the body and caudal fin movements increase the added mass coefficient substantially above what would be expected for a similarly shaped rigid body (Tytell, 2004; Wise et al., 2018).

4.3 Local drag forces

Above, we considered the force on a fish's body as a whole. But to understand the fluid dynamic mechanisms important for swimming, it is often simplest to think of many small segments of the body and imagine them as stationary, with the water moving around them (Fig. 6E). This allows us to think about the forces individually on each segment, which then add up to get the force on the fish's entire body. When the water flows over a segment of a fish's body, it exerts a drag force that is parallel to the instantaneous direction of the flow over that segment.

For a small segment of the body, we often think of the segment as stationary and the water flow moving past it. Local drag is parallel to the local flow, but because of the segment's local velocity and the resulting flow over it, the local drag on a segment may be in a different direction than the body drag on the whole fish, even though (confusingly) we call them both "drag".

In fact, because fishes bend their bodies for propulsion, some segments of the body are moving backwards relative to the center of mass and the swimming direction. This means that local drag on these segments includes a component of thrust relative to the whole body. While the primary motion of the body segment is side-to-side, the traveling wave on the body moves backwards faster than the fish moves forward, leading to a net backward motion of some segments on the body and thus a thrust force.

Flow over a body segment is also affected by separation differently than the entire body. As described above, flow in the horizontal plane does not separate around the body as a whole, probably due to the undulatory motion. But fluid also moves vertically around segments of the body and then separates over the dorsal and ventral surfaces. This vertical separated flow is made stronger by the presence of sharp edges, such as the median fins (Godoy-Diana and Thiria, 2018). The vertical flow separation can lead to streamwise vortices shed off the median fins (Flammang et al., 2011; Tytell, 2006; Tytell et al., 2008) or the dorsal and ventral surfaces. The strength of this streamwise vortex shedding was underappreciated for a long time, but may actually represent an important

component of the total drag and thrust on the body (Godoy-Diana and Thiria, 2018; Tytell, 2006).

Because the swimming movement involves moving the body from side to side, individual body segments are constantly accelerating and decelerating. Through the acceleration reaction, these accelerations of local segments also accelerate the flow near the body, resulting in added mass forces on each segment.

4.3.1 Resistive and reactive forces

The pressure and viscous forces together are termed resistive forces, and are related to the velocity of the segment. Specifically, viscous drag is proportional to the component of the local velocity parallel to the surface of the body, called the tangential component, and pressure drag is proportional to the square of the component of velocity perpendicular to the surface, called the normal component. Summing up the normal and tangential forces on the segments is termed a resistive model of forces on the body (Piñeirua et al., 2015; Taylor, 1952). An graphical example of this resistive force calculation is shown in Fig. 6E. Note that the thrust forces (small green arrow in Fig. 6E) depend on the angle of the segment, and can often be quite small relative to the lateral forces (see discussion in Bale et al., 2014).

The forces due to the acceleration reaction are termed reactive forces, and are related to the acceleration of a segment in the backward direction. Ultimately, the reactive forces are reflected in the strength of the vertical vortices shed off the trailing edges of the caudal fin or the median fins. Note that the reactive component of the thrust force is not shown in Fig. 6E.

The importance of resistive and reactive forces depends on the shape of the body and the undulatory motion. Resistive models for swimming, initially developed in the 1950s (Taylor, 1952), were eclipsed by reactive models and later by computational fluid dynamics, but more recent work is suggesting that resistive forces play an important role in swimming, particularly for elongate fishes (Gemmell et al., 2015; Godoy-Diana and Thiria, 2018; Piñeirua et al., 2015; Stin et al., 2024). In general, more anguilliform swimmers that have larger amplitude motions on the anterior body have more thrust due to resistive forces, while fishes with more thunniform or carangiform swimming, with less anterior body motion, tend to have more thrust due to reactive forces. Combined resistive and reactive models (Piñeirua et al., 2015) can do a good job of accounting for the total force on the body.

5 Musculoskeletal dynamics

5.1 Body-caudal fin swimming

For routine body and caudal fin swimming, fishes use myotomal muscle, the nesting segments along the body called myomeres. Such muscle is divided anatomically as well as functionally. At slower speeds, fishes mainly use slow-twitch

red muscle, which produces relatively low forces and never really fatigues because it uses aerobic metabolism (Syme, 2006). In most fish species, these muscle fibers are located in a thin superficial band on the lateral edges of the body, and the fibers are largely parallel to the body. Some species have an intermediate aerobic fiber type, called pink muscle, that produces higher forces and is additionally recruited at higher speeds (Coughlin and Rome, 1996). Red and pink muscle typically have close to a 1:1 gear ratio, in which shortening of the muscle directly corresponds to body curvature (Coughlin, 2002; Jimenez and Camp, 2023).

At the highest speeds, fishes use fish-twitch white muscle fibers (Jayne and Lauder, 1994), which can make up 75 % to nearly 100 % of the cross-sectional area of the skeletal muscles (Greek-Walker and Pull, 1975; Jimenez and Brainerd, 2021). White muscle fibers are not parallel to the vertebral column, and typically have a steeper angle for fibers located closer to the vertebrae (Gemballa and Vogel, 2002). This leads to gear ratios typically much higher than 1 for white fibers, where a given amount of shortening in white muscle fibers produces much more body curvature than for red fibers (Wakeling and Johnston, 1999). These white muscle fiber orientations have been hypothesized to allow a consistent amount of shortening in all white muscle fibers, regardless of their medio-lateral position (Alexander, 1969; van Leeuwen, 1999), but evidence to support this hypothesis is mixed (see discussion in Jimenez et al., 2021). In general, as speed increases, white muscle activity increases, but red and pink muscles also continue to be at least partially active (Jayne and Lauder, 1994), even though they may not be able to contract fast enough to produce useful power.

Along with the functional progression from red to white muscle, myotomal muscles are also recruited in a spatial pattern, from posterior to anterior for red and pink muscle, and possibly from ventral to dorsal for white muscle. At low swimming speeds, posterior red muscle is active and anterior muscle may be only weakly active or completely silent, with anterior muscle becoming active at higher speeds (Coughlin and Rome, 1999; Gillis, 1998; Jayne and Lauder, 1995a; McGlinchey et al., 2001) or during acceleration (Schwalbe et al., 2019). For white muscle, recent work has suggested that there may be a progression from ventral to dorsal activation in some species (Jimenez and Brainerd, 2021), although other studies suggest that white muscle is active at similar levels across the dorso-ventral axis (Jayne and Lauder, 1995c), and the patterns may differ across species and behaviors (Jimenez and Brainerd, 2021).

Despite this work characterizing muscle activity, the mechanisms of force transmission from the muscles to the skeleton of fishes remains unclear (Gemballa and Vogel, 2002; Syme, 2006; Westneat and Wainwright, 2001). The skin, collagenous layers, tendons, muscles, and bone all interact during swimming, meaning that the transmission of force is likely complex (Videler, 1993; Wainwright, 1983). Some myomeres may insert onto various tendons, but others may have their myosepta attaching to the ends of other myosepta (Shadwick and Gemballa, 2006; Wainwright, 1983). Myomeres can also span multiple vertebrae without directly attaching to them, while others have

tendinous attachments to parts of the skeleton such as the neural and hemal processes of the vertebrae (Shadwick and Gemballa, 2006). Furthermore, the horizontal septum, which is a collection of collagen in crossed-fiber arrays, is suggested to be important for force transmission towards the backbone in scombrid fishes and may be helpful for other groups as well (Westneat et al., 1993). White muscle can also attach to the vertical septum or other myosepta and myoseptal tendons, and the angle of attachment changes along the body (Gemballa and Vogel, 2002; Shadwick and Gemballa, 2006). For a recent review of what is known about the transmission of forces within a fish, see Shadwick (2024). Chapters from previous editions of this series and chapters from Videler (1993) also go into detail about muscle and tendon architecture as they relate to fish swimming (Shadwick and Gemballa, 2006; Summers and Long, 2006; Videler, 1993; Wainwright, 1983).

5.1.1 *Timing of activity*

Red muscles alternate activity on the left and right sides, progressing along the body from rostral to caudal (Blight, 1977), and the white muscle displays a similar pattern once it becomes active (Jayne and Lauder, 1995c, 1994; Jimenez and Brainerd, 2021). For most fishes, rostral muscles are active for a longer fraction of the cycle than caudal muscles. Overall, the duty cycle (the fraction of the bending cycle when muscle is active) is often around 30 % (Videler, 1993). In bluegill sunfish, for example, it varies from about 35 % rostrally to about 28 % caudally during steady swimming and increases by 5 or 10 % at all sites during acceleration (Schwalbe et al., 2019).

Similar to the wave of body bending (Eq. 1), there is therefore a traveling wave of muscle activity. The activity wave has the same frequency as the bending wave, but typically a longer wavelength (McMillen et al., 2008; Wardle et al., 1995; Williams et al., 1989), a difference that results in a lag at any location on the body between the onset of neural activity and body bending. This neuromechanical phase lag tends to get larger closer to the tail. For example, near the rostral end of the body, red muscle on the left side generally becomes active just as the body begins to bend to the left, and stays active nearly until the body is fully bent to the left. Closer to the tail, however, red muscle on the left side tends to become active when the body is bending toward the right, stretching the left muscle, and stays active only the very beginning of the bending to the left side (Schwalbe et al., 2019; Wardle et al., 1995).

6 The contribution of fins to steady swimming

6.1 Fin types

Beyond the diversity of body shapes, fishes also differ substantially in both the shape and structure of their fins. In general, most fishes have five different types of fins: dorsal, anal, pelvic, pectoral, and caudal fins (Fig. 7). The

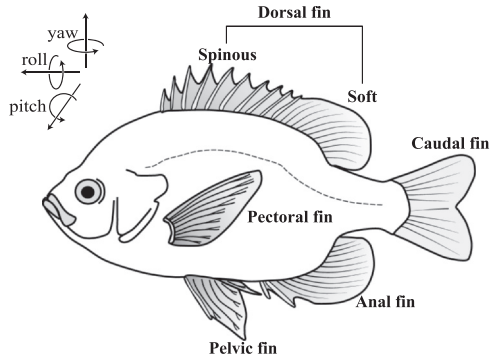

FIG. 7 Schematic of a typical percomorph, based on a bluegill sunfish. The fins and cardinal rotational axes are indicated.

pectoral and pelvic fins are paired, on the left and right sides, while the dorsal, anal, and caudal fin are unpaired and are called median fins, since they run along the middle of the body. All of the fins have muscles at their bases that can move them actively to produce thrust for swimming or for fine scale maneuvering and stability (Fish and Lauder, 2017; Webb, 2006).

The external shape of a fin is often quantified using aspect ratio, $AR = span^2/area$, where the span is some measure of the length of the fin. High aspect ratio fins, or those that are relatively long and narrow, tend to be more efficient at producing lifting forces; these might include the pectoral fins of some wrasses and the caudal fin of tuna. Low aspect ratio fins may therefore be more important for producing drag forces for rowing or maneuvering.

6.2 Fin rays

The musculoskeletal anatomy of median paired and unpaired fish fins is generally similar across all bony fishes. Each fin contains fin rays, which are long rod-like elements, called lepidotrichia. The rods are then attached to a series of basal cartilages which articulate with supports connecting the fin to the skeleton. The rays are made of bone and are segmented (Fig. 8A), and they are split along their length into pairs of ray elements called hemitrichia (Fig. 8B and C). The proximal parts of the fin ray are generally unsegmented and unbranched, but towards the end of the fin ray it becomes segmented and eventually branched (Fig. 8B). Some fin rays in the median fins have fused lepidotrichia called spines, which may protrude on their own, or be covered in a membrane to make a spinous fin. In the center of paired hemitrichia lies a collagen core, and at the tips of the hemitrichia there are branched keratinous elements called actinotrichia (Arita, 1971; Becerra et al., 1983; Chadwell and Ashley-Ross, 2012; Flammang et al., 2013). Cartilaginous fishes (sharks, skates, rays, and chimaeras; Elasmobranchii and Holocephali) have similar

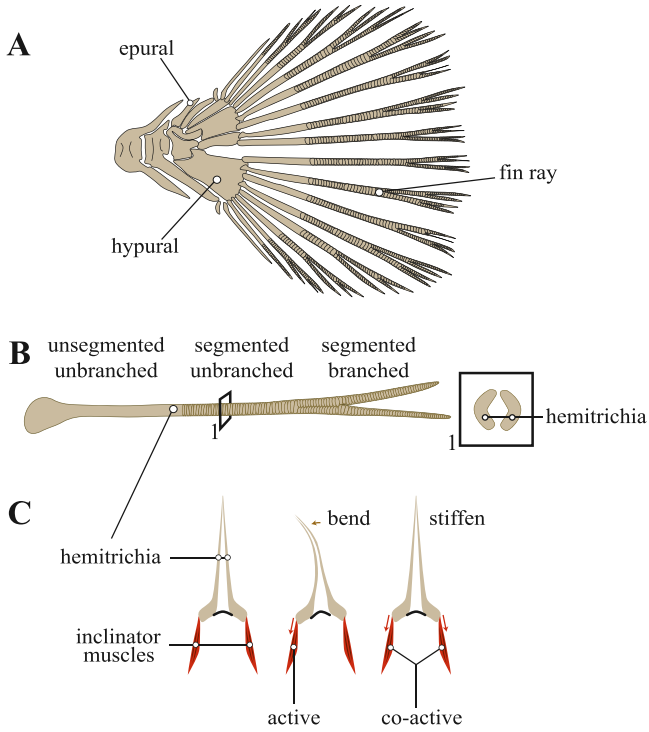

FIG. 8 Fin ray anatomy. (A) Diagram of the rays in a typical ray-finned fish caudal fin. (B) An individual fin ray, showing the main regions. The cross Section 1 shows the two halves, called hemitrichia. (C) Longitudinal cross section of fin ray from the soft dorsal fin, showing the two hemitrichia and the mechanisms of bending or stiffening of the fin.

rod-like elements in their fins: the rods are called ceratotrichia and are made of keratinized collagen, and they are attached to radial and basal cartilages (Kemp, 1977).

6.2.1 *Musculoskeletal anatomy of the caudal fin*

The musculoskeletal anatomy of fish caudal fins (Fig. 8A), like the paired and unpaired fins, also differs among fishes based on ecology and evolutionary history (Giammona, 2021; Lauder, 1989). For many basal fishes, including most sharks and basal actinopterygians (ray-finned fishes), the tail is called heterocercal, because it is asymmetric, with a larger dorsal lobe. More derived bony fishes generally have an externally symmetric fin, termed a homocercal fin. Internally, even for many fishes with externally symmetric fins, the last caudal vertebrae fuse upwards into the dorsal lobe of the caudal fin, causing an internal dorso-ventral asymmetry (Ferrón et al., 2017; Giammona, 2021; Lauder, 1989). In some lampreys (Petromyzontiformes) and lobed finned fishes (Sarcopterygii), this asymmetry extends even further, with the notochord

or vertebral column extending dorsally to the dorsal tip of the caudal fin (Chang et al., 2006; Giammona, 2021). In contrast, the notochord or vertebrae from other basal groups such as hagfishes (Myxiniformes) and extinct anaspids, thelodonts, and heterostracans extend into the ventral lobe of the caudal fin (Giammona, 2021).

For an extensive review of the major evolutionary changes in caudal fin intrinsic musculature over time, see Lauder (2000, 1989). Most of what is known about extant ray-finned fish intrinsic caudal fin musculature comes from a series of studies on sunfish in which the descriptive anatomy and function are characterized (Flammang and Lauder, 2009, 2008; Lauder, 2000). In short, the groups of muscles share broad functional roles such as lateral flexion of the fin, fin abduction or pinching, and rotation of the caudal peduncle and fin (Flammang and Lauder, 2008). Intrinsic muscles in sunfish are typically recruited above swimming speeds of 0.5 body lengths per second, and change fin shape and stiffness during steady swimming as well as aid in fine maneuvers and acceleration performance (Flammang and Lauder, 2009, 2008). The presence and absence of certain muscle groups and their corresponding function have not been reported for most groups of fishes. Analysis of intrinsic fin muscles across multiple ecologically and evolutionarily diverse groups of fishes will provide additional context for observed patterns of fish swimming and maneuvering performance.

6.2.2 *Musculoskeletal anatomy of other fins*

The musculoskeletal anatomy of median paired and unpaired fish fins is generally similar across all fishes. Similar to the basal elements in the caudal fin, the rays in the dorsal and anal fins attach to bony elements called pterygiophores that are located between the neural and haemal arches of the vertebrae respectively. Different from the caudal fin, however, some fin rays in the median fins have fused lepidotrichia called spines, which may protrude on their own, or be covered in a membrane to make a spinous fin (Fig. 7). The pectoral fins can also differ substantially. Specifically, for lobe-finned fishes (Sarcopterygii, the lineage from which land animals descend), the rods articulate with basal elements that protrude on to the fin rather than elements held within the body (Romer and Parsons, 1986). For ray-finned fishes (Actinopterygii, the lineage that includes most extant bony fishes), the supports for fin rays in the pectoral fins make up a pectoral girdle that sits intramuscularly in the fish.

The median fins in ray finned fishes are controlled by paired inclinator, depressor, and elevator muscles (Winterbottom, 1973). In particular, to control lateral movements, bending, and stiffening of the fin rays, fishes use paired inclinators, which originate in the fascia and insert onto the lateral heads of each hemitrich (Chadwell and Ashley-Ross, 2012; Flammang and Lauder, 2009, 2008). The hemitrichia can slide past each other, except at the tip. This means that fin inclinator muscles at the base of the fin (Fig. 8C) can actively

bend the ray or stiffen it (Alben et al., 2006; Fish and Lauder, 2017; Lauder and Drucker, 2004). For instance, to bend a ray, one inclinator shortens while the other maintains length. To stiffen a fin ray, the two inclinators can be active at the same time (Fig. 8C). The fin erector and depressor muscles originate on the pterygiophores (bony supports) and insert onto the anterolateral and posterolateral processes of the fin ray head (Chadwell and Ashley-Ross, 2012; Eaton, 1945). The erectors and depressors allow for changes in surface area of the fins which can aid in stabilizing the fish or maneuverability (Jayne et al., 1996).

The paired fins of fishes (pectoral and pelvic fins) are controlled by sets of muscles that vary in attachment and size depending on how they are used during locomotion, and the evolutionary history of the fish (Siomava and Diogo, 2018). In general, the major groups of muscles in these fins are arrectors, abductors, adductors, elevators, depressors, retractors, and protractors (Eaton, 1945; Winterbottom, 1973). In ray-finned fishes, arrector muscles control the spread and angle of the fin rays, thus the changing area and angle of attack of the fin (Drucker et al., 2006; Fish and Lauder, 2017; Lauder and Drucker, 2004). To move the fin forwards and backwards and up and down, fishes use protractor, retractor, elevator, and depressor muscles, respectively (Drucker et al., 2006; Eaton, 1945). The abductor and adductor muscles are sometimes present in discrete bundles which attach to the base of fin rays, or in sharks, attach to the ceratotrichia (Lauder and Drucker, 2004). The abductor muscle moves the fin away from the body while the adductor brings the fin closer to the body (Drucker et al., 2006; Lauder and Drucker, 2004). Changes in muscle attachment, size, and activation patterns, coupled with the mechanical properties of the paired fin skeletal architecture and external shape can all affect locomotor performance in fishes– these ideas will be explored by Chapter 4 (Vol 41: Clark and Amarnadh, 2025) and Chapter 8 (Vol 41: Higham et al., 2025).

6.3 Fins as stabilizers

During steady swimming, fins can generate hydrodynamic forces to stabilize the fish. The ability to stabilize is critical as most fish are passively unstable (Fath et al., 2023; Hoover and Tytell, 2020; Webb, 2006) and because a fish commonly encounters flow perturbations that would cause it to lose its swimming trajectory (Weihs, 1993). Forces that are not related to buoyancy control mechanisms can be divided into two main types: trimming and corrective (Webb, 2024, 2006). Trimming forces are generated by the flow around the fins when they are held relatively still in a particular orientation as the body moves forward, similar to the way a flaps or ailerons might be used to control flight on an airplane. Fishes can then modulate the trimming forces by actively controlling the orientation, shape, or stiffness of the fins (Fish and Lauder, 2017; Webb, 2006; Wilga and Lauder, 2000, 1999). Corrective forces, in contrast, are produced when the fins moves actively and rapidly to direct force

(Drucker et al., 2006; Fish and Lauder, 2017). Trimming forces are therefore either active or passive, while corrective forces are active.

Different fishes may have different abilities to correct for perturbations due to the placement of their fins relative to their center of mass. For instance, the paired fins that are behind a fish's center of mass, such as pelvic fins, often produce a downward force that can stabilize the body in the event of a disturbance that causes the body to pitch upwards (Webb, 2006). In contrast, upward forces from the pectoral fins, which are sometimes anterior to the center of mass, would increase upward pitch. Since most fishes have both pelvic and pectoral fins, stabilization can occur due to the arrangement of both pairs of fins along the body. Other fins, such as the dorsal, anal, and pelvic fins, also contribute to stabilizing the fish. For instance, in the spiny dogfish, the first dorsal fin tends to be more important for stability while the second dorsal fin can generate thrust, with the first dorsal fin undergoing bilateral muscular activation to stiffen the fin (Maia and Wilga, 2016). In bluegill and yellow perch, the dorsal fin also helps stabilize the fish through the generation of lateral force (Drucker and Lauder, 2001; Tytell et al., 2008). In brook trout, dorsal and anal fins both produce lateral forces that may keep the body from rolling during steady swimming (Drucker and Lauder, 2005; Standen and Lauder, 2007). For dorso-ventrally compressed fishes such as cownose rays, stability during wave action can be achieved by holding the pectoral fins angled upwards (termed a "positive dihedral angle"), which tends to passively correct roll perturbations (Fish and Hoffman, 2015; Weihs, 1993).

6.4 Fins as propulsors: Pectoral fin swimming

While considerable attention is given to fishes that use body-caudal fin undulation to swim, there are also many fishes that rely primarily on their pectoral fins for steady swimming, or use their pectoral fins at low swimming speeds. In particular, a large group of cartilaginous fishes, the stingrays, electric rays, sawfishes, guitarfishes, and skates, together called batoids (Compagno, 1999), are dorsoventrally flattened with very large pectoral fins and reduced caudal fins, and most only swim with the pectoral fins. Some groups of bony fishes also specialize in pectoral fin swimming, but are not as morphologically specialized as batoids.

6.4.1 Pectoral fin swimming in batoids

Pectoral fin swimming in batoids involves flapping the fins up and down in a wavelike pattern. In some species, particularly the pelagic stingrays, this motion is called oscillatory. In other species, particularly skates and most stingrays, the motion results in a traveling wave that passes along the fin, called undulatory swimming, but there is a continuum of swimming patterns from oscillatory to undulatory.

For batoids that use undulatory locomotion, there is often more than one wave present on the fins at the same time (Webb, 1984). These fishes are generally benthic, and undulations of the pectoral fins are assumed to be more efficient than the oscillatory flapping of more pelagic batoids (Di Santo and Kenaley, 2016). The relationships between swimming speed and wave kinematics in batoids using undulatory locomotion and fishes that use propulsive waves along their body are fairly similar. For example, for the blue-spot stingray (*Taeniura lymma*), increased swimming speed is correlated with increased fin beat frequency and wave speed while the number of waves decreased and amplitude stayed constant (Rosenberger and Westneat, 1999), but there may be subtle differences across species (Rosenberger, 2001). Some species, such as the little skate (*Leucoraja erinacea*), modify their undulatory kinematics at high swimming speeds by active stiffening and curvature control to cup their fins into flow (Di Santo et al., 2017a), but this results in high energetic costs (Di Santo et al., 2017b).

For batoids that use oscillatory locomotion, the pectoral fins actively flap, mainly along the leading edge, and passive undulation along the chord and span of the fins (Breder, 1926; Fish et al., 2017; Rosenberger, 2001). Unlike the round fins of undulatory batoids, species that use oscillatory locomotion generally have fins that are triangular—potentially reducing drag while providing a high surface area for lift (Fish et al., 2017; Rosenberger, 2001). The cross section of the pectoral fins of oscillatory swimmers is essentially an airfoil, and the flexibility of their fins increases towards the fin tip (Fish et al., 2017; Heine, 1992; Klausewitz, 1964; Rosenberger, 2001). These fishes often use a flapping motion that is asymmetric in time, with a faster downstroke and a slower upstroke and glide period (Fish et al., 2017). Different species also have spatial asymmetry: large pelagic batoids such as mobulid rays tend to flap their fins further downward, below the body axis, than semi-benthic species such as cownose rays (*Rhinopterus bonoasus*). These semi-benthic rays flap their fins upward more, and the downstroke rarely ends below the body axis, possibly due to its proximity to the benthos during feeding (Fish et al., 2017; Klausewitz, 1964; Rosenberger, 2001). For most species in which flapping kinematics are documented, the flapping amplitude of the pectoral fins remained similar across swimming speeds while the frequency increased with an increase in swimming speed, similar to fish that swim with their caudal fins (Fish et al., 2017; Heine, 1992). For batoids, oscillatory flapping is usually assumed to be less efficient than undulatory fin motion, but flapping generates sufficient thrust for high-speed cruising and falls withing the optimal range of Strouhal numbers (Fish et al., 2017, 2016). At low swimming speeds the Strouhal number is high, possibly indicating less efficient swimming (Fish et al., 2017).

6.4.2 Pectoral fin swimming in non-batoid fishes

Many groups of fishes, including sunfishes (Centrarchidae), wrasses and parrotfishes (Labridae), surfperches (Embiotocidae), sticklebacks (Gasterostidae),

ratfishes (Chimaeridae), and poachers (Agonidae), use pectoral fin swimming at low speeds before transitioning to body-caudal fin swimming at higher speeds depending on the species (Drucker et al., 2006). The kinematics and resulting hydrodynamics of the pectoral fins at low speeds differs across species and is broadly classified into flapping and rowing, but many fishes use intermediate behaviors between the two extremes (Drucker et al., 2006; Walker and Westneat, 2002).

Overall, pectoral fin flapping is considered to generate thrust mainly by lift-based mechanisms, which can lead to substantial thrust on both the up and downstroke (Webb, 1973). Pectoral fin rowing relies mainly on drag-based mechanisms that generate thrust on the backstroke (Blake, 1981), with a feathered recovery stroke that produces little or no thrust (but see Lauder et al., 2006).

The flapping motion is a mainly up and down movement of the fin, with little to no recovery stroke (Drucker et al., 2006; Walker and Westneat, 2002). One species that uses flapping based pectoral fin locomotion is the spotted ratfish, *Hydrolagus colliei* (Combes and Daniel, 2001; Foster and Higham, 2010). Unlike body-caudal fin undulation or pectoral fin swimming in most batoids, the spotted ratfish increases its stroke amplitude as swimming speed increases, with the highest fin velocity observed during the downstroke (Foster and Higham, 2010). During a flapping cycle, the wing tip makes an oval shape, while in other pectoral fin flappers such as labrids (specifically *Gomphosus*, *Cirrhilabrus*, *Tautoga,* and *Scarus)* a figure eight shape is made—possibly due to different demands for thrust and lift (Aiello et al., 2020; Drucker et al., 2006; Foster and Higham, 2010; Walker and Westneat, 2002; Westneat and Walker, 1997). For *G. varius* and other labrids that almost exclusively use pectoral fin flapping to power swimming, flapping can power swimming at high speeds (up to 6 body lengths per second; Westneat and Walker, 1997). In other groups such as Embiotocidae (surfperches) and Centrarchidae (sunfishes), both flapping frequency and flapping amplitude increase with swimming speed with amplitude reaching a plateau at speeds when the fish tend to transition to using caudal fin swimming (Drucker and Jensen, 1996; Drucker and Lauder, 2000; Mussi et al., 2002; Webb, 1973).

The rowing motion is more common in many species at low swimming speeds. Several species of rowing wrasses (such as *Halichoeres bivittatus* and *Paracheilinus octotaenia*) decrease the stroke plane angle as swimming speed increases, thus increasing their ability to generate thrust via rowing before switching to axial undulation (Walker and Westneat, 2002). In bluegill sunfish, pectoral fin swimming is sustained only up to speeds of around 1 body length per second (Drucker and Lauder, 1999; Gibb et al., 1994). At low swimming speeds, one laterally oriented vortex ring is shed while at higher speeds that approach the maximum speed before the transition to axial undulation a pair of vortex rings are formed (Drucker and Lauder, 1999). The flexibility of the fins helps to increase thrust (Drucker and Lauder, 2000; Lauder et al., 2006).

During the outstroke, the fins make a cupped shape while during fin retraction, there is a slight deformation in the upper edge of the fin, possibly to stabilize the leading-edge vortex (Drucker and Lauder, 2000, 1999; Lauder and Madden, 2007). In addition to fin flexibility, the orientation and precise movements of the pectoral fins during rowing can minimize drag during fin retraction (Walker, 2004). Some fish species such as icefish and poachers keep the pectoral fins extended to glide in between power strokes (Archer and Johnston, 1989; Nowroozi et al., 2009).

Many studies of pectoral fin and caudal fin swimming separate the two as a discrete transition from purely pectoral fin swimming at low speeds to purely body and caudal fin swimming at higher speeds. But many fish species pair pectoral fin swimming with body caudal fin swimming at speeds beyond the gait transition. For example, silver mojarra (*Eucinostomus argenteus*) produce medially oriented vortices that are recaptured by the caudal fin after a tail beat cycle (Tack et al., 2024). Additionally, mojarra observed by Tack et al. (2024) in the field all used a combination of pectoral fin and caudal fin swimming at many speeds and not just during gait transitions.

Other fishes coordinate the median fins with the pectoral fins to power swimming. This coordination has been observed in pufferfishes (Tetraodontiformes), pipefishes and seahorses (Syngnathiformes), boxfishes (Ostraciiformes), and triggerfishes and filefishes (Balistiformes) (Breder, 1926; Breder et al., 1942; Drucker et al., 2006; Hove et al., 2001; Korsmeyer et al., 2002). The pectoral fin movements are either undulatory in nature, as observed in seahorses and some pufferfish, or within the flapping to rowing continuum as observed in triggerfishes and boxfishes (Breder, 1926; Hove et al., 2001; Korsmeyer et al., 2002).

Overall, pectoral fin swimming, and particularly its coordination with the dorsal, anal, and caudal fins, seems to have substantial behavioral flexibility, and likely more than body-caudal fin swimming. For example, pectoral fin rowers can beat their fins at the same time or alternate them, and it is unclear why they shift between synchronous and alternating gaits. Moreover, the coordination in fins is complex and flexible, as observed by Tack et al. (2024).

6.5 Fins as propulsors II: Dorsal, anal, and pelvic fins

The use of the dorsal, anal, and pelvic fins as propulsors during steady swimming is less well understood compared to the pectoral fins and the caudal fin. The dorsal fin of fishes was originally thought to be something like a passive keel, but studies over the last 20 years have shown that its motion and stiffness are actively controlled to produce lateral and thrust forces during swimming. For example, in the bluegill sunfish, the inclinator muscles for the soft dorsal fin are active during swimming (Jayne et al., 1996; Lauder and Drucker, 2004). The dorsal fin produces vortices of similar strength to those shed by the caudal fin, and the caudal fin is likely able to harness the incoming

vortices to enhance thrust (Tytell, 2006; Tytell et al., 2008). Similarly, in several sharks (the spiny dogfish *Squalus acanthias* and the bamboo shark *Chiloscyllium plagiosum*), the dorsal fins actively produce thrust forces (Maia et al., 2017; Maia and Wilga, 2016, 2013).

For bluegill swimming at speeds above 1 body length per second, the dorsal and anal fins oscillate in phase with each other and increase lateral displacement as swimming speed increases (Standen and Lauder, 2005). The anal fin, like the dorsal fin, produces thrust, and the summation of dorsal and anal fin forces are approximately equal to the force produced by the caudal fin (Tytell, 2006; Tytell et al., 2008). Some fishes such as triggerfishes have taken this to an extreme, and power swimming primarily by flapping the dorsal and anal fin (George and Westneat, 2019; Korsmeyer et al., 2002; Wright, 2000). Boxfishes also use their dorsal and anal fins to produce thrust (Hove et al., 2001). At speeds greater than 1 body length per second, the flapping frequency of all three fins increases linearly with swimming speed while amplitude becomes constant (Hove et al., 2001). In seahorses and pipefishes, the dorsal fin undulates together with the pectoral fins to produce downwards and posteriorly directed force during steady swimming (Breder et al., 1942). In *Hippocampus* seahorses and *Syngnathus* pipefish, dorsal fin undulation at high frequencies (>30 Hz for the seahorse and around 20 Hz for the pipefish) is controlled by individual inclinator muscles which produce positive work (force and displacement in same direction) at higher frequencies observed in fin muscles of other fishes (Ashley-Ross, 2002).

Several groups of species have evolved elongated dorsal or anal fins, called "ribbon fins", and swim by passing undulatory waves down the fins while keeping the body relatively still and straight (Jagnandan and Sanford, 2013; Ruiz-Torres et al., 2013; Sefati et al., 2013). Many of these species produce and sense electrical fields with receptors in their bodies, and it is hypothesized that ribbon fin locomotion helps electrosensory perception because it allows them to move while keeping the body straight to better sense the electrical field (Snyder et al., 2007). For example, the weakly electric aba (*Gymnarchus niloticus*) tend to increase the wavelength, wave speed, and amplitude of the dorsal fin as swimming speed increases, but decrease the frequency (Li et al., 2005). Bowfin (*Amia calva*), which do not have electrosensation, mostly increase the frequency of undulation to move forwards at speeds up to 1 body length per second and tend to transition to body and caudal fin swimming at high speeds (Jagnandan and Sanford, 2013).

The propulsive role of the pelvic fins of fishes has received considerably less attention as their primary function is assumed to be for stabilizing the body during swimming (Harris, 1938). However, studies investigating the role of the pectoral fins during steady swimming find that in addition to stabilization, the pelvic fins of trout can produce lateral forces that may aid in forward swimming through muscle-powered oscillations at low speeds (Standen, 2010, 2008). There remains a large gap in our understanding of the role of pelvic fins

for propulsion and given the importance of the pelvic fins for locomotion on land and along the benthos in some fishes, there are likely patterns of diverse pelvic fin function that are currently unknown.

6.6 Fins as sensory structures during swimming

Fins have been long recognized as propulsive structures, but more studies are indicating that they are also important sensory structures. The role of mechanosensation in fins has not been studied extensively, but there is evidence of sensory function of fins in catsharks (Lowenstein, 1956), rays (Ridge, 1977), catfish (Aiello et al., 2016), trout (Buckland-Nicks, 2016; Buckland-Nicks et al., 2011), lanternfish (Buckland-Nicks and Reimchen, 2022), bluegill (Flammang and Lauder, 2013; Williams et al., 2013; Williams and Hale, 2015), blind cavefish (Marketaki et al., 2025), and wrasses (Aiello et al., 2020, 2017).

Mechanosensation is best understood in the pectoral fins, primarily from studies of bluegill sunfish. To sense deformation and bending of the fin rays, the pectoral fins of bluegill contain 4 nerves that start at the base of the fin, running through some of the musculature and distal fin rays (Williams et al., 2013). The nerves branch and innervate the core between the hemitrichs, branching again as the fin rays branch, with additional branches innervating the fin membrane (Williams et al., 2013). The nerves respond to bending in the fin rays (Williams et al., 2013). When fin ray nerves were transected, fin kinematics changed during hovering to include more bouts of small, high frequency fin beats (Williams and Hale, 2015). Additionally, in the absence of vision and lateral line senses, bluegill used their pectoral fins to touch obstacles to help them traverse a peg obstacle course (Flammang and Lauder, 2013). In parrotfish, transection of the pectoral fin afferent nerves resulted in higher flapping frequencies, more inclined stroke plane angle, higher angular velocity of the fin stroke, and a transition to axial swimming at lower speeds (Aiello et al., 2020). Antagonistic muscle groups in the pectoral fins tended to be active simultaneously more often after nerve transection, potentially stiffening the fin to compensate for a lack of sensory information (Fig. 9) (Aiello et al., 2020). Furthermore, in another labrid group (wrasses), species with stiffer fin rays had pectoral fin ray afferents with increased sensitivity at lower bending amplitudes, indicating mechanosensory feedback may be a hidden link in the evolution of fin properties and thus swimming behavior (Aiello et al., 2017).

The sensory role of the other fins during swimming is less clear than that of the pectoral fins. For trout, catfish, and lanternfish, an accessory fin on their dorsal surface called an adipose fin is heavily innervated (Aiello et al., 2016; Buckland-Nicks and Reimchen, 2022; Buckland-Nicks, 2016; Buckland-Nicks et al., 2011). The adipose fin can sense its own magnitude of displacement, acting as a flow sensor prior to flow reaching the caudal fin (Aiello et al., 2016; Buckland-Nicks and Reimchen, 2022; Buckland-Nicks, 2016; Reimchen and Temple, 2004). The increased ability to sense flow would be important in high

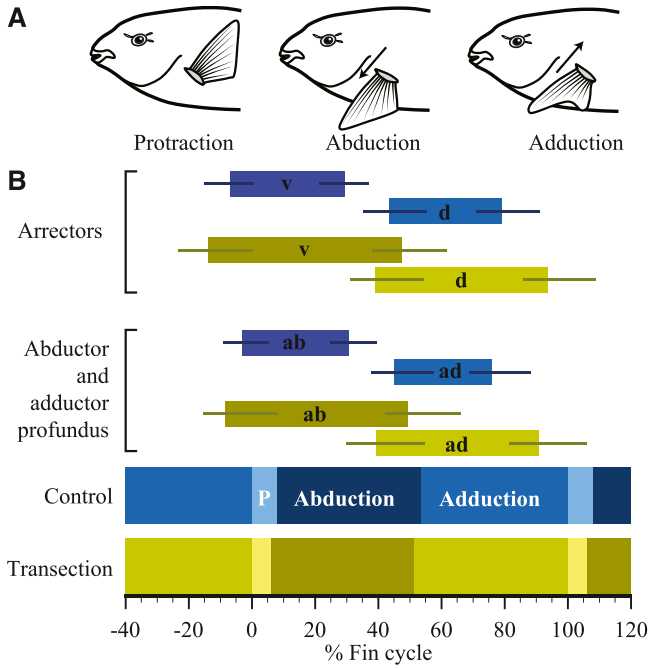

FIG. 9 Mechanosensation affects pectoral fin coordination in parrotfish. (A) Primary motions of the fin. (B) Muscle activity before (blue colors) and after (yellow colors) transection of the sensory nerve. The arrectors ventralis (v) and dorsalis (d) are important for spreading the fin rays and the abductor and adductor profundus control abduction (ab) and adduction (ad). Note the overlap between antagonist muscles after transection (yellow bars). The bottom bars show the overall pattern of protraction, abduction and adduction. *Modified from Aiello et al. (2020).*

flow habitats such as streams or rivers, and it has been observed that in catfish species living in these types of habitats are more likely to have adipose fins than species that live in slow moving or stagnant waters (Temple and Reimchen, 2008). However, in the deep sea where there are generally not high flows, lanternfish retain an innervated adipose fin, potentially due to increased microturbulence as they make their vertical migrations to follow prey (Buckland-Nicks and Reimchen, 2022). Currently, it is presumed that the dorsal, anal, pelvic, and caudal fins of fishes have sensory capabilities and likely impact stability and fine corrective movements during steady swimming, but there are few studies being conducted in this area (Aiello et al., 2018).

7 Unsteady locomotiont

7.1 Turning

Turning is an incredibly common and important locomotor behavior in fishes as it is used for prey capture, mating, predator avoidance, and the navigation of

hydrodynamically and structurally complex habitats. Many fishes spend more of their time turning or accelerating than they do swimming steadily (Coughlin et al., 2024; Webb, 1991). Researchers have devoted more effort to studying escape responses than routine maneuvering. However, like fast starts, routine turns retain distinct kinematic phases. For example, in both fast starts and routine turns, the maneuver is initiated by a change in heading (Howe and Astley, 2020). The rest of the turn is completed through a series of passive and active movements of the body and fins depending on the species.

Characterizing turning is much more complicated than steady swimming. Overall performance can be quantified with a variety of parameters, including the minimum turn radius (or the maximum path curvature) and the maximum turning rate. Turn radius r_{turn} or path curvature can be computed in the same was as body curvature (Fig. 1C) but applied to the location of the center of mass over time, and is best expressed relative to body length. Turning rate is typically estimated based on the angular velocity (deg/s) of the head segment. Researchers also quantify linear and angular momentum and acceleration through the turn. Overall, there tends to be a tradeoff between high linear momentum, high angular velocity, and low turn radius (Fish et al., 2018; Webb, 2006). Measures of turn angle or curvature are sometimes called "maneuverability", while measures of speed or angular acceleration are sometimes called "agility" (Howe and Astley, 2020).

Like with steady swimming, it is best to characterize turning performance with nondimensional parameters. A variety of metrics have been proposed, though none have become common. One relatively simple metric is the centripetal acceleration, which can be estimated directly as the component of the acceleration vector that is perpendicular to the velocity (Howe and Astley, 2020), or more simply as

$$a_c(t) = \frac{U(t)^2}{r_{turn}(t)}$$

where $U(t)$ is the instantaneous linear speed and $r_{turn}(t)$ is the turn radius at that time. Webb (2006) and Bandyopadhyay proposed nondimensionalizing a_c by dividing by gravitational acceleration g to produce a coefficient of normal acceleration $C_g = \max a_c/g$ that makes it easier to compare animals to underwater vehicles (Bandyopadhyay, 2002). In coral reef fishes and boxfishes that primarily use the pectoral fins to swim, r_{turn} is typically low, but the linear speed U through the turn is also quite low, meaning that the centripetal acceleration is also low (Gerstner, 1999; Walker, 2000). Other fishes that use their bodies to turn typically have higher turning radii, but also maintain a higher velocity through the turn, resulting in higher centripetal acceleration. For example, giant danio *Devario aequipinnatus* perform routine turns with centripetal accelerations of more than 2 g and minimum radii of about 0.1 BL, while maintaining speeds up to 9 BL s^{-1} (Howe and Astley, 2020). Turning bluefin tuna are more extreme. They can turn with radii as small as 0.2 BL

while maintaining swimming speeds near 10 BL s^{-1}, resulting in centripetal accelerations greater than 10 g (Downs et al., 2023).

Routine turning, by its nature, tends to be variable and challenging to study in a controlled way. Despite this challenge, many researchers have explored how fishes that use different locomotor modes complete routine turns. Most of the work on turning in fishes focuses on body-caudal fin swimmers such as bluegill and trout. In bluegill, asymmetric forces due to asymmetric pectoral fin use provides an inertial force that contributes to torque, causing yaw (Drucker and Lauder, 2002, 2001; Lauder and Drucker, 2004). The pectoral fin on the side opposite to the direction of the turn is pulled towards the body, thus generating a lateral vortex ring with a central jet more powerful than jets produced while swimming steadily (Drucker and Lauder, 2001). When the opposite pectoral fin pulls closer to the body, it generates a vortex ring that moves posterior to the fish, again with a much stronger jet than produced during steady swimming (Drucker and Lauder, 2001). With one laterally oriented jet that causes yaw, and one posteriorly oriented jet that generates thrust, the net movement of the fish consists of both rotation and translation. The dorsal and anal fins also contribute to yaw turns in bluegill, likely due to jet formation on the side opposite of the trajectory causing torque (Drucker and Lauder, 2001; Standen and Lauder, 2005; Webb, 2006). In bluegill, the dorsal and anal fins are both located on the posterior body near the caudal fin, but in trout, the dorsal fin is more anterior while the anal fin remains closer to the tail. For trout, the anal fin contributes a higher force during maneuvers than the dorsal fin, likely due to its proximity to the caudal fin and its square-like shape (Standen and Lauder, 2007). Additionally, the pelvic fins of trout, while not used for thrust or torque production during a turn, are thought to provide stabilization after turning (Standen, 2008). For both bluegill and trout, the body and the caudal fins produce large normal forces in addition to the jets from asynchronous fin use, increasing momentum at the center of mass to power turns (Drucker and Lauder, 2002, 2001; Lauder and Drucker, 2004; Weihs, 1993).

For other body-caudal fin swimmers that are more specialized for high-speed cruising such as tuna, the dorsal, anal, and caudal fins contribute to turning (Downs et al., 2023; Li, 2021; Pavlov et al., 2017). Pacific bluefin tuna, make turns that can be classified into three types: gliding turns, powered turns, and ratchet turns, each of which use the caudal fin differently (Downs et al., 2023). During gliding, the tuna uses its tail as a rudder, while during powered and ratchet turns, the tail makes symmetrical and asymmetrical motions respectively (Downs et al., 2023). The dorsal and anal fins of tuna can also be actively stiffened via musculo-vascular control of their lymphatic system and undergo changes in area and shape that likely contribute to maneuvers (Pavlov et al., 2017).

Batoids have very stiff bodies, and turn using their pectoral fins. Nevertheless, they still manage to achieve similar performance space to other

rigid bodied animals (Fish, 1999; Parson et al., 2011). However, oscillatory swimming batoids and undulatory swimming batoids turn differently, with oscillating species making use of both powered turns and gliding turns and undulatory species using asymmetrical undulations of their pectoral fins (Parson et al., 2011).

Tunas, batoids, and other species with very stiff bodies have relatively high yaw moment of inertia (Fish, 1999; Schaefer and Summers, 2005). Other fishes can bend their bodies to reduce the moment of inertia, much as a figure skater can pull their arms in to speed up rotation. For example, zebrafish flick their tails to one side to produce initial torque for a turn, then bend their bodies to reduce moment of inertia and accelerate through the turn (Dabiri et al., 2020). Similarly, several species of sharks use high body curvature during turns (Porter et al., 2009; Shadwick and Goldbogen, 2012), and the maximal curvature is predicted by the body morphology, including the shape of the body cross-section, properties of the vertebral column (Porter et al., 2009), and lateral white muscle activation patterns (Shadwick and Goldbogen, 2012). The black ghost knifefish, a species that normally holds its body rigid and powers swimming using an undulating ribbon fin, nevertheless turns by bending its body and modulating its ribbon fin kinematics (Hawkins et al., 2022). During wider turns, it increases ribbon fin frequency, wavelength, and wave speed, while using its pectoral fins more synchronously, perhaps for stabilization throughout the turn (Hawkins et al., 2022). In extremely rigid fishes, such as boxfish, the pectoral fins are main drivers of turning as the only body bending that can physically occur is near the tail (Walker, 2004, 2000).

A promising set of techniques for quantifying mechanics of unsteady maneuvers like turns is to estimate the pressure field around the animal, which allows researchers to estimate the forces on the body with high temporal and spatial resolution (Dabiri et al., 2014; Lucas et al., 2017; Oudheusden, 2013). These techniques use standard particle image velocimetry (PIV) measurements, but with an additional requirement that there cannot be any shadows. Researchers usually use two or more lasers to prevent shadows. Once a complete flow field is estimated around the fish, the Navier Stokes equations can be integrated along contours that run from the boundary of the field of view, where pressure should be ambient, to the body of the fish (Dabiri et al., 2014), or other more complex techniques can be used to estimate the pressure. Pressure is force distributed over an area, which means the force on a fish's body can be estimated based on the estimated pressure and the body's surface area. These force estimates then allow precise quantification of torque and power produced, even during unsteady and relatively unpredictable behaviors like turning.

Fig. 10 shows an example of such a pressure-based calculation. Thandiackal and Lauder (2020) asked what parts of the body are actively transferring power to the fluid (positive power), and what parts are moving passively due to fluid forces (negative power). They measured the flow field around a swimming zebrafish using standard PIV (yellow arrows in Fig. 10A).

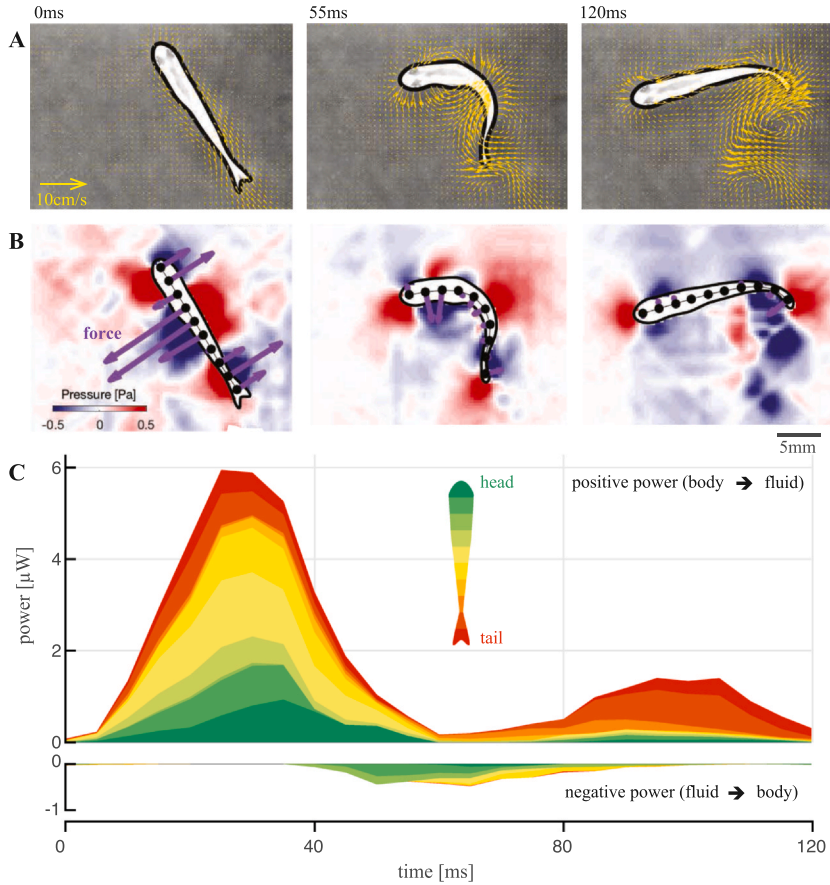

FIG. 10 Using pressure fields to quantify mechanics of turning. (A) Flow around a zebrafish during a turn at three points in time, where yellow arrows represent flow velocity. (B) Pressure field (blue and red background) and forces (purple arrows) on the fish during the same times. (C) Positive and negative power on ten segments along the body (green to red) during the turn. *Modified from Thandiackal and Lauder (2020).*

They then estimated the pressure field (blue and red background in Fig. 10B) using Dabiri's (2014) algorithm, which allowed them to estimate the pressure on the surface of the fish's body. Multiplying the pressure by the surface area of each segment of the body gave them an estimate of the force on the left and right sides of the body, which they then summed to get the net force (purple arrows in Fig. 10B). The power produced or absorbed by each segment is then the product of the net force and the segment velocity (Fig. 10C, where color from green to red indicates the segment from head to tail). Thandiackal and Lauder (2020) hypothesized that the anterior body moves actively to power the turn, and the posterior body and tail may move more passively (producing

negative power). Instead, they found relatively little negative power overall, and more centered on the midbody and head (Thandiackal and Lauder, 2020). Dabiri et al. (2020) used the same type of techniques to estimate pressure during turning in zebrafish and jellyfish and found that both animals used similar strategies: first producing torque with the tail or bell margin, then bending to reduce the moment of inertia.

Similar pressure-based techniques have also been effective for quantifying details of steady swimming performance (Gemmell et al., 2015; Lucas et al., 2020; Tack et al., 2024, 2021), and show promise for providing a more mechanistic understanding of complex swimming behaviors overall.

7.2 Vertical maneuvering

Many of the above studies have focused on movement in the horizontal plane, such as steady swimming, forward acceleration, or horizontal plane turns. However, fish live in a 3D world and regularly move vertically in the water column. They may swim upwards to catch prey at the water's surface, make quick upward and downward darts to escape predators, or even embark on diel migrations. Even the thoroughly studied fast-start escape response, often thought of as a horizontal plane movement, often involves substantial vertical movement (Domenici and Hale, 2019; Fleuren et al., 2018). Vertical movements are exhibited by fishes in both fresh and marine habitats regardless of depth, but the way in which fishes maneuver vertically in the water column has received considerably less attention than horizontal maneuvers and steady swimming depth (Coffey et al., 2020; Mehner, 2012; Neilson and Perry, 1990; Sims et al., 2005).

The interplay between active and passive control of rising and sinking in the water column has been studied in leopard sharks and sturgeon (Ferry and Lauder, 1996; Liao and Lauder, 2000; Wilga and Lauder, 2002, 2000, 1999). While the pectoral fins of both leopard sharks and sturgeon do not generate lift during steady swimming, active modulation of the pectoral fin's trailing edge generates vortices that cause reorientation of the body (Wilga and Lauder, 2000, 1999). However, the cause of destabilization to allow for vertical maneuvering occurs in slightly different ways for the shark and the sturgeon due to different forces caused by their tails. In leopard sharks, the tail generates both torque and lift, so when swimming upwards, the pectoral fins greatly decrease the negative dihedral angle (−35°) and increase their body angle to the flow (Ferry and Lauder, 1996; Wilga and Lauder, 2002, 2000). When swimming downwards, to counteract the lift from the tail, the negative dihedral angle is much smaller (−5°) and the body angle is slightly decreased (Wilga and Lauder, 2000). In sturgeon, however, the tail does not produce lift, but instead rotates, therefore changing the orientation of reaction forces (Liao and Lauder, 2000). When ascending, the tail rotates ventrally and the trailing edge of the pectoral fins curve downwards with the reaction force ventral to the

center of mass (Liao and Lauder, 2000). When descending, the tail rotates dorsally and the trailing edge of the fins flips upwards, directing the reaction force dorsal to the center of mass (Liao and Lauder, 2000).

While leopard sharks and sturgeon use a combination of passive and active movements of the body and fins that slightly deviate from steady swimming behaviors, other fishes maintain typical swimming with slight adjustments. For instance, some tuna dive in order to follow food but adjust their kinematics based on whether they are diving or ascending (Gleiss et al., 2019). When diving, they glide passively downward, reducing active swimming to 30–40 % of normal swimming activity (Gleiss et al., 2019). When ascending, they swim more or less normally, but at an upward angle (Gleiss et al., 2019). Additionally, for elongate swimmers that use whole body undulations to power swimming, similar wave patterns are used for vertical swimming. Gunnels swim vertically within nearshore habitats and to approach nightlights (Kells et al., 2016; Lamb and Edgell, 2010). Different gunnel species also twist their bodies along the long axis (referred to as "wobble"), which is hypothesized to produce upward forces as the body and tail are angled relative to the side-to-side movement (Donatelli et al., 2017). For swimmers such as oarfishes and knifefishes that use undulations of elongate fins, ribbon fin undulation is used to swim upwards and hold station in the water column as well as power the descent tail first (Benfield et al., 2013; Youngerman et al., 2014).

8 Fish swimming energetics

The majority of our knowledge regarding the energetics of fish swimming has been obtained through controlled laboratory experiments, where fishes swim against a flow of water at a set velocity (Brett, 1967, 1962; Dewar and Graham, 1994; Priede and Holliday, 1980; van Ginneken et al., 2005). Flow induces rheotaxis in fishes, leading them to orient and swim against the current. This behavior allows researchers to measure the costs of locomotion at various speeds indirectly through oxygen consumption (MO_2, the rate of change in oxygen in the chamber, relative to the fish's mass), which is calculated by monitoring the decrease in oxygen concentration within a chamber over time as the fish swims. The oxygen consumption rate is typically expressed as

$$M0_2 = \frac{\Delta 0_2 V}{M^b \Delta t}$$

where ΔO_2 is the change in oxygen concentration (usually in mg O_2 per liter), V is the volume of the respirometer chamber (in liters), Δt is the time interval over which oxygen concentration is measured (in hours), M is the body mass of the fish (in kilograms), and b is the allometric coefficient, typically ranging from 0.67 to 0.9, depending on the species or group of fish.

The coefficient b accounts for the fact that the relationship between MO_2 and body mass is not isometric; fishes do not consume oxygen at a rate directly

proportional to their size. Instead, metabolic rate scales with body mass according to this exponent, reflecting the non-linear nature of metabolic demands across different sizes and species (Schmidt-Nielsen, 1984, 1970; White and Kearney, 2014). The value of b varies among fish groups; it is important to use the correct value to ensure that the energy costs of swimming can be adjusted and compared across species.

Oxygen consumption measurements in fish are often conducted using Brett-type or Blazka swim tunnels, which track oxygen decline as fish swim against a flow. During steady swimming, oxygen consumption either increases exponentially or by following a nonlinear J- or U-shaped relationship with velocity (Di Santo et al., 2017b; Di Santo and Goerig, 2025; Zhang and Lauder, 2024). While most classic studies have shown a linear relationship between speed and metabolic rates, it has recently emerged that MO_2 at very low speeds may be significantly higher than those at intermediate speeds that are optimal for cruising. This might explain why fishes may opt to swim at intermediate rather than very low speeds, and by doing so, save energy. At high speeds, the hydrodynamic power needed to overcome body drag increases as the cube of velocity, and thus increases energetic costs of swimming exponentially. At low speeds, the power to overcome drag is small, but fishes may struggle with postural instability, which would also increase the costs of locomotion.

Oxygen consumption is the standard proxy for estimating the energetic cost of swimming, but accurate interpretation of metabolic data requires nuance. Traditionally, fish energetics have been quantified using respirometry in swim tunnels, where individuals swim against a current and oxygen consumption (MO_2) is measured over time. However, the assumption that steady-state oxygen consumption reflects the total cost of locomotion is increasingly challenged. Studies now show that excess post-exercise oxygen consumption (EPOC) must be included to avoid underestimating metabolic costs—particularly at low and high swimming speeds (Di Santo et al., 2017b; Di Santo and Goerig, 2025).

Recent empirical work has revealed that fishes may accumulate an oxygen debt even during routine swimming, suggesting that anaerobic metabolism contributes to energetic demand well below maximum speeds. For example, in clearnose skate (*Raja eglanteria*), anaerobic metabolism was evident at all speeds tested, and including the recovery oxygen cost increased total energetic expenditure by approximately 50 % (Di Santo et al., 2017b). This indicates that fish may use fast-twitch glycolytic muscle fibers intermittently even during steady swimming, contradicting the long-held assumption that low-speed locomotion is exclusively fueled by aerobic red muscle (Di Santo et al., 2017b; Svendsen et al., 2010). Moreover, these findings emphasize the shortcomings of widely used protocols like the critical swimming speed (U_{crit}) test, which incrementally increases flow speed until exhaustion. While this method offers a convenient metric of performance, it cannot differentiate aerobic from anaerobic contributions nor detect carryover effects of metabolic debt. As

demonstrated in both skates and trout, fatigue can occur at submaximal speeds when anaerobic metabolites accumulate, distorting estimates of maximal sustainable speeds and oxygen consumption (Di Santo et al., 2017b; Svendsen et al., 2012, 2010; Weber, 1991).

In addition to protocol design, methodological constraints of flow-through swim tunnels also introduce potential errors. Small chambers, in particular, may amplify wall effects, confinement stress, and spontaneous activity, artificially inflating MO_2 readings (Di Santo and Goerig, 2025; Steffensen, 1989). These conditions suppress natural swimming behavior and compromise the ecological relevance of metabolic measurements. Consequently, energy costs derived under such settings may misrepresent actual locomotor expenditure in the wild. Altogether, these insights reveal that to accurately quantify the cost of swimming in fishes, one must consider postural and stabilization costs, integrate aerobic and anaerobic metabolism, account for excess post-exercise oxygen consumption, and critically assess the limitations of laboratory protocols. Only then can we approach a comprehensive understanding of the energetic landscape underlying fish locomotion (Webb, 2006, 1984).

Measurements at low speeds are particularly challenging, since many fishes with a swim bladder are inherently unstable at low speed. For decades, researchers have reported that fishes at low speeds swim erratically, and show "restlessness". From a biomechanical perspective, this restlessness can be explained by the necessity to stabilize body posture at very low speeds which come to a cost. At lower swimming speeds, fishes encounter greater challenges in maintaining stability and equilibrium, akin to the difficulties faced by a cyclist moving slowly. Indeed, Webb (2002) estimated that postural costs constitute about 10 % of the total cost of steady swimming and should increase at lowest speeds. At higher speeds, fishes can use more subtle, and less energy intensive, adjustments of their fins and body orientation to correct deviations from their intended path. The forward momentum at these speeds also provides a stabilizing force, enhancing the fish's ability to resist perturbations such as currents, turbulence, and torques (Webb, 2002; Webb and Weihs, 2015). However, as swimming speed decreases, this forward momentum diminishes, reducing the stabilizing effect and making it more difficult for a fish to counteract any perturbations. The reduced hydrodynamic forces at low speeds also result in effectively lower inertia, meaning that even minor imbalances or external disturbances can cause significant deviations from a steady trajectory. To maintain stability, a fish must exert greater effort to make corrective adjustments, but the slower speed limits the effectiveness of these responses. As a result, swimming at low speeds can be more energetically demanding, as fishes must work harder to sustain balance and control (Di Santo et al., 2025).

Even while stationary, most fishes are inherently unstable because the center of mass (the force of gravity as it acts on the relatively dense skeleton and muscles) is separated by the center of buoyancy (the net effect of the water pressure on the body, influenced by the less dense viscera and swim bladder)

(Fath et al., 2023; Webb and Weihs, 1994). Separation of the center of mass and center of buoyancy along the anterior-posterior axis causes a pitching torque, and along the dorso-ventral axis causes a rolling torque. Despite the common anecdote that dead fish roll belly up, most fish species have a larger anterior-posterior separation, resulting primarily in pitch instability rather than roll (Aleyev, 1977; Fath et al., 2023; Webb, 2006). Fishes adjust body position to respond to these destabilizing forces by moving their fins and adjusting their body angle. As a consequence, fishes swimming slowly may show erratic, unsteady behaviors that correspond to relatively high metabolic rates when compared to intermediate cruising speeds. These costs might be even higher in negatively buoyant fishes, as they need to swim to create hydrodynamic lift, causing the speed -metabolic relationship to assume a U shape instead (Di Santo et al., 2017b).

Not all studies on swimming energetics do not show this pattern at low speeds (Korsmeyer et al., 2002; Svendsen et al., 2010). Some classic studies on fish locomotion reported high energetic costs of swimming slowly, but were attributed to what they termed "restlessness" (Brett, 1967; Sepulveda et al., 2003). Most others do not even report an increase in metabolic rates at low speeds. More studies are needed to match physiological and biomechanical measurements to assess the costs of swimming across a wide range of speeds.

9 Swimming performance under climate change

As climate change intensifies, the field of fish biomechanics must advance to systematically address the complex, interrelated effects of environmental stressors—such as temperature variability, ocean acidification, hypoxia, and habitat degradation—on fish locomotion, survival, and ecological function. We advocate a new focus on ecological physiology within the context of biomechanics, a framework termed "EcoPhysioMechanics" (Di Santo, 2022). This integrative framework combines principles of biomechanics, energetics, and ecology to provide a comprehensive approach for understanding fish adaptability, resilience, and vulnerability in rapidly changing conditions (Claireaux and Chabot, 2016; Pörtner and Knust, 2007). As climate-driven changes interact with habitat degradation, biomechanics research must pivot towards developing predictive, forward-thinking models to anticipate how fish populations, and animal populations more broadly, might respond to these unprecedented shifts by exploiting their locomotor capacities (Di Santo and Goerig, 2025). A promising direction for this field involves integrating empirical data, technological advancements, and simulation models to better understand and predict migration patterns and movement, ultimately contributing to conservation frameworks that protect species and ecosystems (Di Santo, 2024; Lubitz et al., 2024). Some additional suggestions for integrating these ideas into our proposed framework of EcoPhysioMechanics are discussed in Chapter 8 (Vol 41: Higham et al., 2025).

In particular, ocean acidification introduces significant physiological disruptions that cascade into biomechanical consequences, severely compromising the sensory, motor, and cognitive functions that underlie effective locomotion (Allan et al., 2014; Chung et al., 2014; Hamilton et al., 2014; Wang et al., 2017). In fact, acidification impacts neurotransmitter function, especially GABA receptors, which play a crucial role in behaviors like predator evasion, orientation, and spatial navigation (Munday et al., 2009; Nilsson et al., 2012). In reef fish like clownfish and damselfish, these neurological disruptions manifest as erratic swimming patterns and impaired foraging behaviors, ultimately reducing survival rates (Allan et al., 2014). Acidification also affects otolith development, compromising sensory input crucial for balance and orientation, which directly impacts locomotor control in species that rely on precise movements for habitat interaction and predator avoidance (Checkley et al., 2009; Kwan and Tresguerres, 2022). These neurological and sensory impacts call for future research that links EcoPhysioMechanics with neurobiology, exploring how acidification-induced changes in sensory processing alter fish biomechanics and locomotor behavior. As ocean acidification hotspots—regions with especially high CO_2 concentrations—emerge globally, eco-mechanics studies may prioritize species in these areas, aiming to quantify the cumulative effects of acidification on neural and sensory systems across life stages and habitats. For a review on sensory systems that may be impacted by increased acidification in aquatic systems, see Chapter 5 (Vol 41: McHenry and Peterson, 2025).

As fishes face the mounting impacts of ocean acidification, the additional stress of rising temperatures further intensifies these challenges, exerting profound effects on locomotor energetics, metabolic scope, and kinematic efficiency (Di Santo, 2016; Todgham and Stillman, 2013). While warmer waters can potentially enhance muscle contractility and burst-swimming, temperature increases quickly surpass species-specific thermal optima, leading to increases in metabolic demands (Clark et al., 2013; Pörtner and Knust, 2007). This condition elevates oxygen requirements within muscle tissue, often resulting in severe fatigue, reduced endurance, and impaired agility, which are essential for species that migrate, evade predators, or engage in high-energy behaviors (Brett, 1967). Temperature-induced stress during embryonic development is a recognized teratogenic factor in fishes, leading to skeletal deformities (Pimentel et al., 2016; Takle et al., 2005; Vilmar and Di Santo, 2022). Rising temperatures increase the occurrence of severe axial malformations, with a higher incidence of enlarged, fused, and deformed vertebrae as thermal conditions intensify (Fraser et al., 2015; Sassi et al., 2010; Takle et al., 2005; Ytteborg et al., 2010). In elasmobranchs, warming affects cartilage mineralization, possibly reducing the biomechanical stiffness of fins of species that rely on pectoral fin undulation (Di Santo, 2019). Without adequate skeletal support, these fishes may expend more energy on basic movements and experience heightened vulnerability in dynamic, high-flow environments, where fin stiffness and shape play a pivotal

role in swimming performance. To address these impacts, biomechanics research may quantify how structural and metabolic thresholds shift under elevated temperatures, particularly using 3D imaging and kinematic tracking to monitor minute biomechanical changes in real-time and pair those with energetics measurements (Vilmar and Di Santo, 2022). Such studies will be key to developing predictive models that can assess the combined impacts of acidification and temperature on biomechanical performance.

Additionally, hypoxia, which is increasingly prevalent in coastal zones and some oceanic regions, restricts aerobic capacity, limiting fish's ability to sustain high-energy activities like migration, schooling, and predator evasion (Claireaux and Chabot, 2016; Larsson, 2012; McBryan et al., 2013). Fishes in hypoxic conditions often reduce their swimming speed and adopt more conservative movement patterns to reduce costs of locomotion, a response that can delay or prevent important behaviors like foraging or mate-seeking (Claireaux and Chabot, 2016). As hypoxic zones often coincide with warming waters, fishes face compounded challenges: elevated temperatures increase metabolic demands, further exacerbating oxygen limitations. Migratory species like cod and salmon, which rely heavily on aerobic scope for their long migrations, are particularly vulnerable under these combined stressors (Claireaux and Chabot, 2016; Mandic and Regan, 2018; McBryan et al., 2013). Future research should prioritize physiological and kinematic models that simulate interactions among multiple stressors, particularly how warming and hypoxia jointly reduce aerobic scope in migratory fish. Developing predictive frameworks that consider seasonal hypoxic events, especially in estuarine and coastal nursery habitats, could significantly improve targeted conservation efforts.

All of these environmental stressors may disproportionately affect larvae and juvenile fishes. Therefore, research on developmental biomechanics is increasingly essential (Mayerl et al., 2023). Juveniles, with their high metabolic demands and still-developing systems, show greater sensitivity to acidification, hypoxia, and warming than adults, often displaying altered kinematic patterns during swimming such as changes in tail beat frequency and reduced endurance (Berio et al., 2023; Di Santo et al., 2016; Lin et al., 2019), or changes in the escape response (Ottervall, 2025). Shoaling and schooling behavior, which are critical for energy conservation and predator evasion, can deteriorate in warmer waters as cohesion weakens, leading to increased predation risk and reduced foraging efficienc (Berio et al., 2023). Understanding how developmental plasticity might buffer or exacerbate these vulnerabilities across generations will be central to assessing long term effects of stressors on locomotor performance (Donelson et al., 2012; Ryu et al., 2018; Veilleux et al., 2015). Longitudinal studies that track fish populations over multiple generations could provide insights into whether certain species can acclimate to altered environmental conditions, helping scientists anticipate which populations or physiotypes are most likely to persist and what shifts we might observe, for instance in geographic distribution.

These physiological stressors are intensified in many areas due to the degradation of habitat complexity—particularly in coral reefs, kelp forests, and seagrass beds—by removing critical structural elements that many fishes rely on for energy conservation (Di Santo and Goerig, 2025). Fishes often exploit currents and physical structures within their environments to reduce the energetic costs of movement, even positioning themselves behind objects to 'draft' and take advantage of reduced water flow. Such behaviors (Liao, 2007; Liao et al., 2003) demonstrate how fish can minimize energy expenditure by using structural features for flow refuging. Additionally, species have been known to 'surf' upwelling zones, maintaining position with minimal exertion as they leverage the flow dynamics in these habitats (Papastamatiou et al., 2021). However, as ocean acidification and warming continue to degrade foundational species like coral and kelp, thus reducing the landscapes that were originally highly complex 3D environments into 2D flatlands, the natural energy-saving opportunities they provide diminish, forcing fish to expend more energy on basic locomotion (Di Santo and Goerig, 2025). Future biomechanics research could investigate how fishes adjust their locomotor strategies in response to degraded, uniform environments and explore the limits of their behavioral plasticity to help offset the energetic costs of navigating these altered landscapes. Such studies are essential to identify the species most affected by habitat loss and to inform habitat restoration projects that aim to rebuild structural complexity.

Emerging technologies in biomechanics, including high-resolution 3D kinematics, bio-logging, and artificial intelligence (AI), provide invaluable tools for studying fish responses to environmental stressors in unprecedented detail. Machine learning tools for tracking videos, including DeepLabCut (Lauer et al., 2022), SLEAP (Pereira et al., 2022) and TRex (Walter and Couzin, 2021), are decreasing a key bottleneck in behavioral research. By facilitating automated tracking of many points on individual fishes or groups of fishes, they are enabling scientists to capture fine-scale changes in movement in response to subtle shifts in water chemistry, temperature gradients, or oxygen availability, offering novel insights into behavioral and physiological responses across longer video sequences. They also are enabling high-resolution 3D kinematics, allowing researchers to process many videos for "high-throughput biomechanics" (e.g., Tidswell et al., 2024). Bio-logging devices capable of monitoring metabolic rates, heart rates, and kinematic patterns over extended periods allow researchers to study how fishes adjust locomotor strategies in natural settings compared to controlled lab environments. For instance, White and Lauder (2024) used multiple data loggers to quantify time synchronization and drift in animal locomotion studies, highlighting the importance of precise temporal alignment in multi-sensor data collection. Furthermore, AI-driven simulations enable complex, multi-variable modeling that reveals how different environmental stressors interact over time, helping to identify vulnerable species and life stages. By combining empirical

observations with predictive AI models, biomechanics research can shift toward a proactive approach that anticipates how fish populations might shift, adjust, or decline under various climate and altered flow scenarios, offering essential insights for management practices.

The future of biomechanics research in the context of climate change will also rely on interdisciplinary collaboration to develop effective conservation strategies. Biomechanists, ecologists, conservation scientists, and climate modelers may work together to build integrated models that consider the multiple factors impacting fish populations. For example, biomechanics insights on fish energy expenditure and locomotor efficiency under stressors can be incorporated into ecological models to simulate population-level responses to habitat loss and environmental change. Such collaborations could help refine marine protected areas by identifying critical habitats that support energy-efficient behaviors in fish (e.g., Hernández et al., 2019) and guiding restoration initiatives aimed at preserving structural complexity (Di Santo and Goerig, 2025).

Adaptive conservation strategies informed by integrative studies can enhance habitat restoration efforts and shape policies that strengthen species resilience. For instance, in regions with frequent upwelling, habitat restoration could prioritize maintaining or increasing structural complexity to maximize energy-saving opportunities for local fish populations (Castro-Santos et al., 2022; Di Santo and Goerig, 2025; Lacey et al., 2012; Silva et al., 2018). Policies aimed at reducing nutrient runoff and improving water quality could also help mitigate hypoxia in coastal zones, supporting the energy demands of migratory and high-performance species (Pörtner, 2010). Predictive models that combine biomechanics, physiology, and ecological data can guide these conservation efforts, allowing management strategies to be tailored to the specific needs and vulnerabilities of fish populations facing climate-driven stressors. By aligning biomechanical insights with ecological data, scientists can provide actionable information that supports marine management efforts and helps to safeguard fish populations' adaptive potential, fostering resilience within marine ecosystems under unprecedented environmental pressures.

References

Afroz, F., Lang, A., Habegger, M.L., Motta, P., Hueter, R., 2016. Experimental study of laminar and turbulent boundary layer separation control of shark skin. Bioinspir. Biomim. 12, 016009. https://doi.org/10.1088/1748-3190/12/1/016009

Aiello, B.R., Hardy, A.R., Westneat, M.W., Hale, M.E., 2018. Fins as mechanosensors for movement and touch-related behaviors. Integr. Comp. Biol. 58, 844–859. https://doi.org/10.1093/icb/icy065

Aiello, B.R., Olsen, A.M., Mathis, C.E., Westneat, M.W., Hale, M.E., 2020. Pectoral fin kinematics and motor patterns are shaped by fin ray mechanosensation during steady swimming in *Scarus quoyi*. J. Exp. Biol. 223, jeb211466. https://doi.org/10.1242/jeb.211466

Aiello, B.R., Stewart, T.A., Hale, M.E., 2016. Mechanosensation in an adipose fin. Proc. R. Soc. B Biol. Sci. 283, 20152794. https://doi.org/10.1098/rspb.2015.2794

Aiello, B.R., Westneat, M.W., Hale, M.E., 2017. Mechanosensation is evolutionarily tuned to locomotor mechanics. Proc. Natl. Acad. Sci., 201616839. https://doi.org/10.1073/pnas.1616839114

Akanyeti, O., Putney, J., Yanagitsuru, Y.R., Lauder, G.V., Stewart, W.J., Liao, J.C., 2017. Accelerating fishes increase propulsive efficiency by modulating vortex ring geometry. Proc. Natl. Acad. Sci. 114, 13828–13833. https://doi.org/10.1073/pnas.1705968115

Akanyeti, O., Santo, V.D., Goerig, E., Wainwright, D.K., Liao, J.C., Castro-Santos, T., et al., 2022. Fish-inspired segment models for undulatory steady swimming. Bioinspir. Biomim. 17, 046007. https://doi.org/10.1088/1748-3190/ac6bd6

Akbarzadeh, A.M., Borazjani, I., 2019. Reducing flow separation of an inclined plate via travelling waves. J. Fluid Mech. 880, 831–863. https://doi.org/10.1017/jfm.2019.705

Alben, S., Madden, P.G., Lauder, G.V., 2006. The mechanics of active fin-shape control in ray-finned fishes. J. R. Soc. Interface 4, 243. https://doi.org/10.1098/rsif.2006.0181

Alexander, R.M., 1990. Size, speed and buoyancy adaptations in aquatic animals. Am. Zool. 30, 189–196. https://doi.org/10.1093/icb/30.1.189

Alexander, R.M., 1983. The history of fish mechanics. In: Webb, P.W., Weihs, D. (Eds.), Fish Biomechanics, Fish Physiology. Praeger Publishers, pp. 1–35.

Alexander, R.M., 1982. Buoyancy. Locomotion of Animals. Springer, pp. 39–53.

Alexander, R.M., 1969. The orientation of muscle fibres in the myomeres of fishes. J. Mar. Biol. Assoc. UK. 49, 263–290.

Aleyev, Y.G., 1977. Nekton. Junk. The Hague.

Allan, B.J., Miller, G.M., McCormick, M.I., Domenici, P., Munday, P.L., 2014. Parental effects improve escape performance of juvenile reef fish in a high-CO_2 world. Proc. R. Soc. B Biol. Sci. 281, 20132179.

Anastasiadis, A., Paez, L., Melo, K., Tytell, E.D., Ijspeert, A.J., Mulleners, K., 2023. Identification of the trade-off between speed and efficiency in undulatory swimming using a bio-inspired robot. Sci. Rep. 13, 15032. https://doi.org/10.1038/s41598-023-41074-9

Anastasiadis, A., Rossi, A., Paez, L., Melo, K., Tytell, E.D., Ijspeert, A.J., et al., 2024. Eel-like robot swims more efficiently with increasing joint amplitudes compared to constant joint amplitudes. Phys. Rev. Fluids 9, 110509. https://doi.org/10.1103/PhysRevFluids.9.110509

Anderson, E.J., McGillis, W.R., Grosenbaugh, M.A., 2001. The boundary layer of swimming fish. J. Exp. Biol. 204, 81–102.

Archer, S.D., Johnston, I.A., 1989. Kinematics of labriform and subcarangiform swimming in the antarctic fish *Notothenia neglecta*. J. Exp. Biol. 143, 195–210. https://doi.org/10.1242/jeb.143.1.195

Aristotle, 1937. Movement of Animals. Heinemann, London.

Aristotle, 1937. Progression of Animals. Heinemann, London.

Aristotle, 1910. History of animals. Historia Animalium. Clarendon, Oxford.

Arita, G.S., 1971. A re-examination of the functional morphology of the soft-rays in teleosts. Copeia 1971, 691–697. https://doi.org/10.2307/1442639

Ashley-Ross, M.A., 2002. Mechanical properties of the dorsal fin muscle of seahorse (*Hippocampus*) and pipefish (*Syngnathus*). J. Exp. Zool. 293, 561–577. https://doi.org/10.1002/jez.10183

Bainbridge, R., 1963. Caudal fin and body movement in the propulsion of some fish. J. Exp. Biol. 40, 23–56. https://doi.org/10.1242/jeb.40.1.23

Bainbridge, R., 1958. The speed of swimming of fish as related to size and to the frequency and amplitude of the tail beat. J. Exp. Biol. 35, 109–133. https://doi.org/10.1242/jeb.35.1.109

Bale, R., Hao, M., Bhalla, A.P.S., Patankar, N.A., 2014. Energy efficiency and allometry of movement of swimming and flying animals. Proc. Natl. Acad. Sci. 111, 7517–7521.

Bale, R., Neveln, I.D., Bhalla, A.P.S., MacIver, M.A., Patankar, N.A., 2015. Convergent evolution of mechanically optimal locomotion in aquatic invertebrates and vertebrates. PLOS Biol. 13, e1002123.

Bandyopadhyay, P.R., 2002. Maneuvering hydrodynamics of fish and small underwater vehicles. Integr. Comp. Biol. 42, 102–117. https://doi.org/10.1093/icb/42.1.102

Barenblatt, G.I., 2003. Scaling. Cambridge University Press, Cambridge.

Becerra, J., Montes, G.S., Bexiga, S.R.R., Junqueira, L.C.U., 1983. Structure of the tail fin in teleosts. Cell Tissue Res. 230, 127–137. https://doi.org/10.1007/BF00216033

Benfield, M.C., Cook, S., Sharuga, S., Valentine, M.M., 2013. Five in situ observations of live oarfish *Regalecus glesne* (Regalecidae) by remotely operated vehicles in the oceanic waters of the northern Gulf of Mexico. J. Fish. Biol. 83, 28–38. https://doi.org/10.1111/jfb.12144

Berio, F., Moreord, C., Di Santo, V., 2023. Ontogenetic plasticity in shoaling behavior in a forage fish under warming. Integr. Comp. Biol. 63, 730–741.

Blake, R.W., 2004. Fish functional design and swimming performance. J. Fish. Biol. 65, 1193–1222. https://doi.org/10.1111/j.0022-1112.2004.00568.x

Blake, R.W., 1983a. Swimming in the electric eels and knifefishes. Can. J. Zool. 61, 1432–1441. https://doi.org/10.1139/z83-192

Blake, R.W., 1983b. Median and paired fin propulsion. Fish Biomechanics. Praeger Publishers, New York, pp. 214–247.

Blake, R.W., 1983c. Fish locomotion. CUP Archive.

Blake, R.W., 1981. Influence of pectoral fin shape on thrust and drag in labriform locomotion. J. Zool. 194, 53–66.

Blake, R.W., Li, J., Chan, K.H.S., 2009. Swimming in four goldfish *Carassius auratus* morphotypes: understanding functional design and performance employing artificially selected forms. J. Fish. Biol. 75, 591–617. https://doi.org/10.1111/j.1095-8649.2009.02309.x

Blight, A.R., 1977. The muscular control of vertebrate swimming movements. Biol. Rev. 52, 181–218.

Bone, Q., Roberts, B.L., 1969. The density of elasmobranchs. J. Mar. Biol. Assoc. UK. 49, 913–937. https://doi.org/10.1017/S0025315400038017

Borelli, G., 1680. De motu animalium pars I. Bernabo, Rome.

Breder, C.M., 1926. The locomotion of fishes. Zoologica 4, 159–297.

Breder, C.M., Jr, Edgerton, H.E., 1942. An analysis of the locomotion of the seahorse, *Hippocampus*, by means of high speed cinematography. Ann. N. Y. Acad. Sci. 43, 145–172. https://doi.org/10.1111/j.1749-6632.1942.tb47947.x

Brett, J.R., 1967. Swimming performance of sockeye salmon (*Oncorhynchus nerka*) in relation to fatigue time and temperature. J. Fish. Res. Board. Can. 24, 1731–1741. https://doi.org/10.1139/f67-142

Brett, J.R., 1962. Some considerations in the study of respiratory metabolism in fish, particularly salmon. J. Fish. Board. Can. 19, 1025–1038.

Buckland-Nicks, J., Reimchen, T.E., 2022. Innervation and structure of the adipose fin of a lanternfish. J. Fish. Biol. 101, 1210–1216. https://doi.org/10.1111/jfb.15192

Buckland-Nicks, J.A., 2016. New details of the neural architecture of the salmonid adipose fin. J. Fish. Biol. 89, 1991–2003. https://doi.org/10.1111/jfb.13098

Buckland-Nicks, J.A., Gillis, M., Reimchen, T.E., 2011. Neural network detected in a presumed vestigial trait: ultrastructure of the salmonid adipose fin. Proc. R. Soc. B Biol. Sci. 279, 553–563. https://doi.org/10.1098/rspb.2011.1009

Castro-Santos, T., Goerig, E., He, P., Lauder, G.V., 2022. Applied aspects of locomotion and biomechanics. In: Cooke, S.J., Fangue, N.A., Farrell, A.P., Brauner, C.J., Eliason, E.J. (Eds.), Fish Physiology, Conservation Physiology for the Anthropocene – A Systems Approach. Academic Press, pp. 91–140. https://doi.org/10.1016/bs.fp.2022.04.003

Chadwell, B.A., Ashley-Ross, M.A., 2012. Musculoskeletal morphology and regionalization within the dorsal and anal fins of bluegill sunfish (*Lepomis macrochirus*). J. Morphol. 273, 405–422. https://doi.org/10.1002/jmor.11031

Chang, M., Zhang, J., Miao, D., 2006. A lamprey from the Cretaceous Jehol biota of China. Nature 441, 972–974. https://doi.org/10.1038/nature04730

Checkley, D.M., Dickson, A.G., Takahashi, M., Radich, J.A., Eisenkolb, N., Asch, R., 2009. Elevated CO_2 enhances otolith growth in young fish. Science 324, 1683. https://doi.org/10.1126/science.1169806

China, V., Holzman, R., 2014. Hydrodynamic starvation in first-feeding larval fishes. Proc. Natl. Acad. Sci. 111, 8083–8088. https://doi.org/10.1073/pnas.1323205111

Chung, W.-S., Marshall, N.J., Watson, S.-A., Munday, P.L., Nilsson, G.E., 2014. Ocean acidification slows retinal function in a damselfish through interference with GABAA receptors. J. Exp. Biol. 217, 323–326. https://doi.org/10.1242/jeb.092478

Claireaux, C., Chabot, D., 2016. Responses by fishes to environmental hypoxia: integration through Fry's concept of aerobic metabolic scope. J. Fish. Biol. 88, 232–251.

Clark, A., Amarnadh, V., 2025. Biomechanics of fish tissues. In: Lauder, G.V., Higham, T.E. (Eds.), Fish Biomechanics, Fish Physiology. Elselvier Academic Press.

Clark, T.D., Sandblom, E., Jutfelt, F., 2013. Aerobic scope measurements of fishes in an era of climate change: respirometry, relevance and recommendations. J. Exp. Biol. 216, 2771–2782. https://doi.org/10.1242/jeb.084251

Coffey, D.M., Royer, M.A., Meyer, C.G., Holland, K.N., 2020. Diel patterns in swimming behavior of a vertically migrating deepwater shark, the bluntnose sixgill (*Hexanchus griseus*). PLoS One 15, e0228253. https://doi.org/10.1371/journal.pone.0228253

Combes, S.A., Daniel, T.L., 2001. Shape, flapping and flexion: wing and fin design for forward flight. J. Exp. Biol. 204, 2073–2085. https://doi.org/10.1242/jeb.204.12.2073

Compagno, L.J.V., 1999. Systematics and body form. In: Hamlett, W.C. (Ed.), Sharks, Skates, and Rays: The Biology of Elasmobranch Fishes. John Hopkins University Press, Baltimore, MD, pp. 1–42.

Coughlin, D.J., 2002. Aerobic muscle function during steady swimming in fish. Fish. Fish. 3, 63–78. https://doi.org/10.1046/j.1467-2979.2002.00069.x

Coughlin, D.J., Morris, C., Postupaka, D., Gee, P., Reynolds, Z., Wood, B., 2024. Field kinematics of intermittent swimming in bluegill sunfish (*Lepomis macrochirus*)—pelagic locomotion and littoral maneuverability. J. Plankton Res., fbae048. https://doi.org/10.1093/plankt/fbae048

Coughlin, D.J., Rome, L.C., 1999. Muscle activity in steady swimming scup, *Stenotomus chrysops*, varies with fiber type and body position. Biol. Bull. 196, 145–152. https://doi.org/10.2307/1542560

Coughlin, D.J., Rome, L.C., 1996. The roles of pink and red muscle in powering steady swimming in scup, *Stenotomus chrysops*. Am. Zool. 36, 666–677. https://doi.org/10.1093/icb/36.6.666

Dabiri, J.O., Bose, S., Gemmell, B.J., Colin, S.P., Costello, J.H., 2014. An algorithm to estimate unsteady and quasi-steady pressure fields from velocity field measurements. J. Exp. Biol. 217, 331–336.

Dabiri, J.O., Colin, S.P., Gemmell, B.J., Lucas, K.N., Leftwich, M.C., Costello, J.H., 2020. Jellyfish and fish solve the challenges of turning dynamics similarly to achieve high maneuverability. Fluids 5, 106. https://doi.org/10.3390/fluids5030106

Danos, N., Lauder, G.V., 2012. Challenging zebrafish escape responses by increasing water viscosity. J. Exp. Biol. 215, 1854–1862. https://doi.org/10.1242/jeb.068957

Denny, M.W., 1993. Air and Water: The Biology and Physics of Life's Media. Princeton University Press, Princeton, N.J.

Dewar, H., Graham, J., 1994. Studies of tropical tuna swimming performance in a large water tunnel - energetics. J. Exp. Biol. 192, 13–31. https://doi.org/10.1242/jeb.192.1.13

Di Santo, V., 2024. Sharks at risk from climate-driven coastal upwelling. Nat. Clim. Change. https://doi.org/10.1038/s41558-024-01975-7

Di Santo, V., 2022. EcoPhysioMechanics: integrating energetics and biomechanics to understand fish locomotion under climate change. Integr. Comp. Biol. 62, 711–720. https://doi.org/10.1093/icb/icac095

Di Santo, V., 2019. Ocean acidification and warming affect skeletal mineralization in a marine fish. Proc. R. Soc. B Biol. Sci. 286, 20182187. https://doi.org/10.1098/rspb.2018.2187

Di Santo, V., 2016. Intraspecific variation in physiological performance of a benthic elasmobranch challenged by ocean acidification and warming. J. Exp. Biol. 219, 1725–1733. https://doi.org/10.1242/jeb.139204

Di Santo, V., Blevins, E.L., Lauder, G.V., 2017a. Batoid locomotion: effects of speed on pectoral fin deformation in the little skate, *Leucoraja erinacea*. J. Exp. Biol. 220, 705–712. https://doi.org/10.1242/jeb.148767

Di Santo, V., Goerig, E., 2025. Swimming smarter, not harder: fishes exploit habitat heterogeneity to increase locomotor performance. J. Exp. Biol. 228, JEB247918. https://doi.org/10.1242/jeb.247918

Di Santo, V., Goerig, E., Wainwright, D.K., Akanyeti, O., Liao, J.C., Castro-Santos, T., et al., 2021. Convergence of undulatory swimming kinematics across a diversity of fishes. Proc. Natl. Acad. Sci. 118. https://doi.org/10.1073/pnas.2113206118

Di Santo, V., Kenaley, C.P., 2016. Skating by: low energetic costs of swimming in a batoid fish. J. Exp. Biol. 219, 1804–1807. https://doi.org/10.1242/jeb.136358

Di Santo, V., Kenaley, C.P., Lauder, G.V., 2017b. High postural costs and anaerobic metabolism during swimming support the hypothesis of a U-shaped metabolism–speed curve in fishes. Proc. Natl. Acad. Sci. 114, 13048–13053. https://doi.org/10.1073/pnas.1715141114

Di Santo, V., Qi, X., Berio, F., Albi, A., Akanyeti, O., 2025. Inherent instability leads to high costs of hovering in near-neutrally buoyant fishes. Proc. Natl. Acad. Sci. 122, e2420015122.

Di Santo, V., Tran, A.H., Svendsen, J.C., 2016. Progressive hypoxia decouples activity and aerobic performance of skate embryos. Conserv. Physiol. 4, cov067. https://doi.org/10.1093/conphys/cov067

Domel, A.G., Saadat, M., Weaver, J.C., Haj-Hariri, H., Bertoldi, K., Lauder, G.V., 2018. Shark skin-inspired designs that improve aerodynamic performance. J. R. Soc. Interface 15, 20170828. https://doi.org/10.1098/rsif.2017.0828

Domenici, P., Hale, M.E., 2019. Escape responses of fish: a review of the diversity in motor control, kinematics and behaviour. J. Exp. Biol. 222, jeb166009. https://doi.org/10.1242/jeb.166009

Donatelli, C.M., Summers, A.P., Tytell, E.D., 2017. Long-axis twisting during locomotion of elongate fishes. J. Exp. Biol. 220, 3632–3640. https://doi.org/10.1242/jeb.156497

Donelson, J.M., Munday, P.L., McCormick, M.I., Pitcher, C.R., 2012. Rapid transgenerational acclimation of a tropical reef fish to climate change. Nat. Clim. Change 2, 30–32. https://doi.org/10.1038/nclimate1323

Downie, A.T., Illing, B., Faria, A.M., Rummer, J.L., 2020. Swimming performance of marine fish larvae: review of a universal trait under ecological and environmental pressure. Rev. Fish Biol. Fish. 30, 93–108. https://doi.org/10.1007/s11160-019-09592-w

Downs, A.M., Kolpas, A., Block, B.A., Fish, F.E., 2023. Multiple behaviors for turning performance of Pacific bluefin tuna (*Thunnus orientalis*). J. Exp. Biol. 226, jeb244144. https://doi.org/10.1242/jeb.244144

Drucker, E.G., Jensen, J.S., 1996. Pectoral fin locomotion in the striped surfperch: I. Kinematic effects of swimming speed and body size. J. Exp. Biol. 199, 2235–2242. https://doi.org/10.1242/jeb.199.10.2235

Drucker, E.G., Lauder, G.V., 2005. Locomotor function of the dorsal fin in rainbow trout: kinematic patterns and hydrodynamic forces. J. Exp. Biol. 208, 4479–4494. https://doi.org/10.1242/jeb.01922

Drucker, E.G., Lauder, G.V., 2002. Wake dynamics and locomotor function in fishes: interpreting evolutionary patterns in pectoral fin design. Integr. Comp. Biol. 42, 997–1008. https://doi.org/10.1093/icb/42.5.997

Drucker, E.G., Lauder, G.V., 2001. Wake dynamics and fluid forces of turning maneuvers in sunfish. J. Exp. Biol. 204, 431–442. https://doi.org/10.1242/jeb.204.3.431

Drucker, E.G., Lauder, G.V., 2000. A hydrodynamic analysis of fish swimming speed: wake structure and locomotor force in slow and fast labriform swimmers. J. Exp. Biol. 203, 2379–2393. https://doi.org/10.1242/jeb.203.16.2379

Drucker, E.G., Lauder, G.V., 1999. Locomotor forces on a swimming fish: three-dimensional vortex wake dynamics quantified using digital particle image velocimetry. J. Exp. Biol. 202, 2393–2412. https://doi.org/10.1242/jeb.202.18.2393

Drucker, E.G., Summers, A.P., 2008. A historical perspective on the study of animal locomotion with fins and limbs. Fins Into Limbs. University of Chicago Press, pp. 39–48.

Drucker, E.G., Walker, J.A., Westneat, M.W., 2006. Mechanics of pectoral fin swimming in fishes. In: Fish Biomechanics, Fish Physiology. Academic Press, pp. 369–423. https://doi.org/10.1016/S1546-5098(05)23010-8

Eaton Jr, T.H., 1945. Skeletal supports of the median fins of fishes. J. Morphol. 76, 193–212. https://doi.org/10.1002/jmor.1050760305

Eloy, C., 2012. Optimal Strouhal number for swimming animals. J. Fluids Struct. 30, 205–218. https://doi.org/10.1016/j.jfluidstructs.2012.02.008

Faber, T.E., 1995. Fluid Dynamics for Physicists. Cambridge University Press, Cambridge.

Fath, M.A., Nguyen, S., Donahue, J., McMenamin, S., Tytell, E.D., 2023. Static stability and swim bladder volume in the bluegill sunfish *Lepomis macrochirus*. Integr. Org. Biol. 5, obad005. https://doi.org/10.1093/iob/obad005

Ferrón, H.G., Martínez-Pérez, C., Botella, H., 2017. Ecomorphological inferences in early vertebrates: reconstructing *Dunkleosteus terrelli* (Arthrodira, Placodermi) caudal fin from palaeoecological data. PeerJ. 5, e4081. https://doi.org/10.7717/peerj.4081

Ferry, L.A., Lauder, G.V., 1996. Heterocercal tail function in leopard sharks: a three-dimensional kinematic analysis of two models. J. Exp. Biol. 199, 2253–2268. https://doi.org/10.1242/jeb.199.10.2253

Fish, F.E., 1999. Performance constraints on the maneuverability of flexible and rigid biological systems. In: International Symposium on Unmanned Untethered Submersible Technology. University of New Hampshire.

Fish, F.E., Dong, H., Zhu, J.J., Bart-Smith, H., 2017. Kinematics and hydrodynamics of mobuliform swimming: oscillatory winged propulsion by large pelagic batoids. Mar. Technol. Soc. J. 51, 35–47. https://doi.org/10.4031/MTSJ.51.5.5

Fish, F.E., Hoffman, J.L., 2015. Stability design and response to waves by batoids. Integr. Comp. Biol. 55, 648–661. https://doi.org/10.1093/icb/icv059

Fish, F.E., Kolpas, A., Crossett, A., Dudas, M.A., Moored, K.W., Bart-Smith, H., 2018. Kinematics of swimming of the manta ray: three-dimensional analysis of open-water maneuverability. J. Exp. Biol. 221, jeb166041. https://doi.org/10.1242/jeb.166041

Fish, F.E., Lauder, G.V., 2017. Control surfaces of aquatic vertebrates: active and passive design and function. J. Exp. Biol. 220, 4351–4363. https://doi.org/10.1242/jeb.149617

Fish, F.E., Lauder, G.V., 2006. Passive and active flow control by swimming fishes and mammals. Annu. Rev. Fluid Mech. 38, 193–224.

Fish, F.E., Schreiber, C.M., Moored, K.W., Liu, G., Haibo, D., Bart-Smith, H., 2016. Hydrodynamic performance of aquatic flapping: efficiency of underwater flight in the manta. Aerospace 3, 20. https://doi.org/10.3390/aerospace3030020

Flammang, B.E., Alben, S., Madden, P.G.A., Lauder, G.V., 2013. Functional morphology of the fin rays of teleost fishes. J. Morphol. 274, 1044–1059. https://doi.org/10.1002/jmor.20161

Flammang, B.E., Lauder, G.V., 2013. Pectoral fins aid in navigation of a complex environment by bluegill sunfish under sensory deprivation conditions. J. Exp. Biol. 216, 3084–3089. https://doi.org/10.1242/jeb.080077

Flammang, B.E., Lauder, G.V., 2009. Caudal fin shape modulation and control during acceleration, braking and backing maneuvers in bluegill sunfish, *Lepomis macrochirus*. J. Exp. Biol. 212, 277–286.

Flammang, B.E., Lauder, G.V., 2008. Speed-dependent intrinsic caudal fin muscle recruitment during steady swimming in bluegill sunfish, *Lepomis macrochirus*. J. Exp. Biol. 211, 587–598. https://doi.org/10.1242/jeb.012096

Flammang, B.E., Lauder, G.V., Troolin, D.R., Strand, T.E., 2011. Volumetric imaging of fish locomotion. Biol. Lett. 7, 695–698. https://doi.org/10.1098/rsbl.2011.0282

Fleuren, M., van Leeuwen, J.L., Quicazan-Rubio, E.M., Pieters, R.P.M., Pollux, B.J.A., Voesenek, C.J., 2018. Three-dimensional analysis of the fast-start escape response of the least killifish, *Heterandria formosa*. J. Exp. Biol. 221, jeb168609. https://doi.org/10.1242/jeb.168609

Foster, K.L., Higham, T.E., 2010. How to build a pectoral fin: functional morphology and steady swimming kinematics of the spotted ratfish (*Hydrolagus colliei*). Can. J. Zool. 88, 774–780. https://doi.org/10.1139/Z10-043

François-Franck, C.A., 1906. Analyse graphique des mouvements respiratoires des poissons téléostéens. Hebd. Séances Mém. Soc. Biol. 799, 802.

Fraser, T.W.K., Hansen, T., Fleming, M.S., Fjelldal, P.G., 2015. The prevalence of vertebral deformities is increased with higher egg incubation temperatures and triploidy in Atlantic salmon *Salmo salar* L. J. Fish. Dis. 38, 75–89. https://doi.org/10.1111/jfd.12206

Gazzola, M., Argentina, M., Mahadevan, L., 2014. Scaling macroscopic aquatic locomotion. Nat. Phys. 10, 758–761.

Gemballa, S., Vogel, F., 2002. Spatial arrangement of white muscle fibers and myoseptal tendons in fishes. Comp. Biochem. 133, 1013–1037. https://doi.org/10.1016/S1095-6433(02)00186-1

Gemmell, B.J., Colin, S.P., Costello, J.H., Dabiri, J.O., 2015. Suction-based propulsion as a basis for efficient animal swimming. Nat. Commun. 6, 8790. https://doi.org/10.1038/ncomms9790

George, A.B., Westneat, M.W., 2019. Functional morphology of endurance swimming performance and gait transition strategies in balistoid fishes. J. Exp. Biol. 222, jeb194704. https://doi.org/10.1242/jeb.194704

Gerstner, C.L., 1999. Maneuverability of four species of coral-reef fish that differ in body and pectoral-fin morphology. Can. J. Zool. 77, 1102–1110. https://doi.org/10.1139/z99-086

Giammona, F.F., 2021. Form and function of the caudal fin throughout the phylogeny of fishes. Integr. Comp. Biol. 61, 550–572. https://doi.org/10.1093/icb/icab127

Gibb, A.C., Jayne, B.C., Lauder, G.V., 1994. Kinematics of pectoral fin locomotion in the bluegill sunfish *Lepomis macrochirus*. J. Exp. Biol. 189, 133–161. https://doi.org/10.1242/jeb.189.1.133

Gillis, G.B., 1998. Neuromuscular control of anguilliform locomotion: patterns of red and white muscle activity during swimming in the American eel *Anguilla rostrata*. J. Exp. Biol. 201, 3245–3256.

Gleiss, A.C., Potvin, J., Goldbogen, J.A., 2017. Physical trade-offs shape the evolution of buoyancy control in sharks. Proc. R. Soc. B Biol. Sci. 284, 20171345. https://doi.org/10.1098/rspb.2017.1345

Gleiss, A.C., Schallert, R.J., Dale, J.J., Wilson, S.G., Block, B.A., 2019. Direct measurement of swimming and diving kinematics of giant Atlantic bluefin tuna (*Thunnus thynnus*). R. Soc. Open. Sci. 6, 190203. https://doi.org/10.1098/rsos.190203

Godoy-Diana, R., Thiria, B., 2018. On the diverse roles of fluid dynamic drag in animal swimming and flying. J. R. Soc. Interface 15, 20170715. https://doi.org/10.1098/rsif.2017.0715

Gray, J., 1935. Studies in animal locomotion: IV. The neuromuscular mechanism of swimming in the eel. J. Exp. Biol. 13, 170–180. https://doi.org/10.1242/jeb.13.2.170

Gray, J., 1933. Studies in animal locomotion: I. The movement of fish with special reference to the Eel. J. Exp. Biol. 10, 88–104. https://doi.org/10.1242/jeb.10.1.88

Greek-Walker, M., Pull, G.A., 1975. A survey of red and white muscle in marine fish. J. Fish. Biol. 7, 295–300. https://doi.org/10.1111/j.1095-8649.1975.tb04602.x

Hale, M.E., Galdston, S., Arnold, B.W., Song, C., 2022. The water to land transition submerged: multifunctional design of pectoral fins for use in swimming and in association with underwater substrate. Integr. Comp. Biol. 62, 908–921. https://doi.org/10.1093/icb/icac061

Hamilton, T.J., Holcombe, A., Tresguerres, M., 2014. CO_2-induced ocean acidification increases anxiety in Rockfish via alteration of GABAA receptor functioning. Proc. R. Soc. B Biol. Sci. 281, 20132509. https://doi.org/10.1098/rspb.2013.2509

Harris, J.E., 1938. The role of the fins in the equilibrium of the swimming fish: II. The role of the pelvic fins. J. Exp. Biol. 15, 32–47. https://doi.org/10.1242/jeb.15.1.32

Hawkins, O.H., Ortega-Jiménez, V.M., Sanford, C.P., 2022. Knifefish turning control and hydrodynamics during forward swimming. J. Exp. Biol. 225, jeb243498. https://doi.org/10.1242/jeb.243498

Hedrick, T.L., 2008. Software techniques for two- and three-dimensional kinematic measurements of biological and biomimetic systems. Bioinspir. Biomim. 3, 34001. https://doi.org/10.1088/1748-3182/3/3/034001

Heine, C.E., 1992. Mechanics of flapping fin locomotion in the cownose ray. Rhinoptera Bonasus (Elasmobranchii: Myliobatidae) (Ph.D.). Duke University, Durham, NC, USA.

Hernández, C.M., Witting, J., Willis, C., Thorrold, S.R., Llopiz, J.K., Rotjan, R.D., 2019. Evidence and patterns of tuna spawning inside a large no-take marine protected area. Sci. Rep. 9, 10772. https://doi.org/10.1038/s41598-019-47161-0

Holzman, R., China, V., Yaniv, S., Zilka, M., 2015. Hydrodynamic constraints of suction feeding in low Reynolds numbers, and the critical period of larval fishes. Integr. Comp. Biol. 55, 48–61. https://doi.org/10.1093/icb/icv030

Hoover, A., Tytell, E., 2020. Decoding the relationships between body shape, tail beat frequency, and stability for swimming fish. Fluids 5, 215. https://doi.org/10.3390/fluids5040215

Hove, J.R., O'Bryan, L.M., Gordon, M.S., Webb, P.W., Weihs, D., 2001. Boxfishes (Teleostei: Ostraciidae) as a model system for fishes swimming with many fins: kinematics. J. Exp. Biol. 204, 1459–1471. https://doi.org/10.1242/jeb.204.8.1459

Howe, S.P., Astley, H.C., 2020. The control of routine fish maneuvers: connecting midline kinematics to turn outcomes. J. Exp. Zool. Part. Ecol. Integr. Physiol. 333, 579–594. https://doi.org/10.1002/jez.2398

Hunter, J.R., Zweifel, J.R., 1971. Swimming speed, tail beat frequency, tail beat amplitude and size in jack mackerel, *Trachurus symmetricus*, and other fishes. Fish. Bull. 69, 253–266.

Jagnandan, K., Sanford, C.P., 2013. Kinematics of ribbon-fin locomotion in the bowfin, *Amia calva*. J. Exp. Zool. Part. Ecol. Genet. Physiol. 319, 569–583. https://doi.org/10.1002/jez.1819

Jayne, B.C., Lauder, G.V., 1995a. Red muscle motor patterns during steady swimming in largemouth bass: effects of speed and correlations with axial kinematics. J. Exp. Biol. 198, 1575–1587.

Jayne, B.C., Lauder, G.V., 1995b. Speed effects on midline kinematics during steady undulatory swimming of largemouth bass, *Micropterus salmoides*. J. Exp. Biol. 198, 585–602. https://doi.org/10.1242/jeb.198.2.585

Jayne, B.C., Lauder, G.V., 1995c. Are muscle fibers within fish myotomes activated synchronously? Patterns of recruitment within deep myomeric musculature during swimming in largemouth bass. J. Exp. Biol. 198, 805–815.

Jayne, B.C., Lauder, G.V., 1994. How swimming fish use slow and fast muscle fibers: implications for models of vertebrate muscle recruitment. J. Comp. Physiol. A 175, 123–131.

Jayne, B.C., Lozada, A.F., Lauder, G.V., 1996. Function of the dorsal fin in bluegill sunfish: motor patterns during four distinct locomotor behaviors. J. Morphol. 228, 307–326. https://doi.org/10.1002/(SICI)1097-4687(199606)228:3<307::AID-JMOR3>3.0.CO;2-Z

Jimenez, Y.E., Brainerd, E.L., 2021. Motor control in the epaxial musculature of bluegill sunfish in feeding and locomotion. J. Exp. Biol. 224, jeb242903. https://doi.org/10.1242/jeb.242903

Jimenez, Y.E., Camp, A.L., 2023. Beam theory predicts muscle deformation and vertebral curvature during feeding in rainbow trout (Oncorhynchus mykiss). J. Exp. Biol. 226, jeb245788. https://doi.org/10.1242/jeb.245788

Jimenez, Y.E., Marsh, R.L., Brainerd, E.L., 2021. A biomechanical paradox in fish: swimming and suction feeding produce orthogonal strain gradients in the axial musculature. Sci. Rep. 11, 10334. https://doi.org/10.1038/s41598-021-88828-x

Kells, V., Rocha, L.A., Allen, L.G., 2016. A Field Guide to Coastal Fishes. Johns Hopkins University Press, Baltimore, MD.

Kemp, N.E., 1977. Banding pattern and fibrillogenesis of ceratotrichia in shark fins. J. Morphol. 154, 187–203. https://doi.org/10.1002/jmor.1051540202

Klausewitz, W., 1964. Der lokomotionsmodus der flugelrochen (Myliobatoidei). Zool. Anz. 173, 111–120.

Korsmeyer, K.E., Steffensen, J.F., Herskin, J., 2002. Energetics of median and paired fin swimming, body and caudal fin swimming, and gait transition in parrotfish (*Scarus schlegeli*) and triggerfish (*Rhinecanthus aculeatus*). J. Exp. Biol. 205, 1253–1263. https://doi.org/10.1242/jeb.205.9.1253

Kwan, G.T., Tresguerres, M., 2022. Elucidating the acid-base mechanisms underlying otolith overgrowth in fish exposed to ocean acidification. Sci. Total. Environ. 823, 153690.

Lacey, R.J., Neary, V.S., Liao, J.C., Enders, E.C., Tritico, H.M., 2012. The IPOS framework: linking fish swimming performance in altered flows from laboratory experiments to rivers. River Res. Appl. 28, 429–443.

Lamb, A., Edgell, P., 2010. Coastal Fishes of the Pacific Northwest, 2nd ed. Harbour Publishing, Maderia Park.

Lang, A., Motta, P., Habegger, M.L., Hueter, R., Afroz, F., 2011. Shark skin separation control mechanisms. Mar. Technol. Soc. J. 45, 208–215. https://doi.org/10.4031/MTSJ.45.4.12

Larsson, M., 2012. Why do fish school? Curr. Zool 58, 116–128. https://doi.org/10.1093/czoolo/58.1.116

Lauder, G., Tytell, E., 2006. Hydrodynamics of undulatory propulsion. Fish. Physiol. Fish Biomechanics 23, 425–468. https://doi.org/10.1016/S1546-5098(05)23011-X

Lauder, G.V., 2022. Robotics as a comparative method in ecology and evolutionary biology. Integr. Comp. Biol. 62, 721–734. https://doi.org/10.1093/icb/icac016

Lauder, G.V., 2000. Function of the caudal fin during locomotion in fishes: kinematics, flow visualization, and evolutionary patterns. Am. Zool 40, 101–122. https://doi.org/10.1093/icb/40.1.101

Lauder, G.V., 1989. Caudal fin locomotion in ray-finned fishes: historical and functional analyses. Am. Zool 29, 85–102.

Lauder, G.V., Di Santo, V., 2015. Swimming mechanics and energetics of elasmobranch fishes. In: Shadwick, R.E., Farrell, A.P., Brauner, C.J. (Eds.), Fish Physiology, Physiology of Elasmobranch Fishes: Structure and Interaction with Environment. Academic Press, pp. 219–253. https://doi.org/10.1016/B978-0-12-801289-5.00006-7

Lauder, G.V., Drucker, E.G., 2004. Morphology and experimental hydrodynamics of fish fin control surfaces. IEEE J. Ocean. Eng. 29, 556–571. https://doi.org/10.1109/JOE.2004.833219

Lauder, G.V., Madden, P.G.A., 2007. Fish locomotion: kinematics and hydrodynamics of flexible foil-like fins. Exp. Fluids 43, 641–653. https://doi.org/10.1007/s00348-007-0357-4

Lauder, G.V., Madden, P.G.A., Mittal, R., Dong, H., Bozkurttas, M., 2006. Locomotion with flexible propulsors: I. Experimental analysis of pectoral fin swimming in sunfish. Bioinspir. Biomim. 1, S25–S34.

Lauer, J., Zhou, M., Ye, S., Menegas, W., Schneider, S., Nath, T., et al., 2022. Multi-animal pose estimation, identification and tracking with DeepLabCut. Nat. Methods 19, 496–504. https://doi.org/10.1038/s41592-022-01443-0

Li, F., Hu, T., Wang, G., Shen, L., 2005. Locomotion of *Gymnarchus niloticus*: experiment and kinematics. J. Bionic Eng. 2, 115–121. https://doi.org/10.1007/BF03399488

Li, G., Liu, H., Müller, U.K., Voesenek, C.J., van Leeuwen, J.L., 2021. Fishes regulate tail-beat kinematics to minimize speed-specific cost of transport. Proc. R. Soc. B Biol. Sci. 288, 20211601. https://doi.org/10.1098/rspb.2021.1601

Li, X., 2021. Hydrodynamic analysis for the morphing median fins of tuna during yaw motions. Appl. Bionics Biomech. 2021, 6630839. https://doi.org/10.1155/2021/6630839

Liao, J., Lauder, G.V., 2000. Function of the heterocercal tail in white sturgeon: flow visualization during steady swimming and vertical maneuvering. J. Exp. Biol. 203, 3585–3594. https://doi.org/10.1242/jeb.203.23.3585

Liao, J.C., 2007. A review of fish swimming mechanics and behaviour in altered flows. Philos. Trans. R. Soc. B 362, 1973–1993.

Liao, J.V., Beal, D.N., Lauder, G.V., Triantafyllou, M.S., 2003. Fish exploiting vortices decrease muscle activity. Sci 302, 1566–1569.

Lighthill, M.J., 1970. Large-amplitude elongated-body theory of fish locomotion. Proc. R. Soc. Lond. B. 179, 125–138.

Lighthill, M.J., 1969. Hydromechanics of aquatic animal propulsion. Annu. Rev. Fluid Mech. 1, 413–446. https://doi.org/10.1146/annurev.fl.01.010169.002213

Lighthill, M.J., 1960. Note on the swimming of slender fish. J. Fluid Mech. 9, 305–317. https://doi.org/10.1017/S0022112060001110

Lim, J., Winegard, T., 2015. Diverse anguilliform swimming kinematics in Pacific hagfish (*Eptatretus stoutii*) and Atlantic hagfish (*Myxine glutinosa*). Can. J. Zool 213–223.

Lin, L.-Y., Hung, G.-Y., Yeh, Y.-H., Chen, S.-W., Horng, J.-L., 2019. Acidified water impairs the lateral line system of zebrafish embryos. Aquat. Toxicol. 217, 105351.

Long Jr., J.H., 1998. Muscles, elastic energy, and the dynamics of body stiffness in swimming eels. Am. Zool 38, 771–792. https://doi.org/10.1093/icb/38.4.771

Long Jr, J.H., Nipper, K.S., 1996. The importance of body stiffness in undulatory propulsion. Am. Zool. 36, 678–694. https://doi.org/10.1093/icb/36.6.678

Lowenstein, O., 1956. Pressure receptors in the fins of the dogfish *Scylliorhinus canicula*. J. Exp. Biol. 33, 417–421. https://doi.org/10.1242/jeb.33.2.417

Lu, X.-Y., Yin, X.-Z., 2005. Propulsive performance of a fish-like travelling wavy wall. Acta Mech. 175, 197–215. https://doi.org/10.1007/s00707-004-0117-y

Lubitz, N., Daly, R., Smoothey, A.F., Vianello, P., Roberts, M.J., Schoeman, D.S., et al., 2024. Climate change-driven cooling can kill marine megafauna at their distributional limits. Nat. Clim. Change 14, 526–535. https://doi.org/10.1038/s41558-024-01966-8

Lucas, K.N., Dabiri, J.O., Lauder, G.V., 2017. A pressure-based force and torque prediction technique for the study of fish-like swimming. PLoS One 12, e0189225.

Lucas, K.N., Lauder, G.V., Tytell, E.D., 2020. Airfoil-like mechanics generate thrust on the anterior body of swimming fishes. Proc. Natl. Acad. Sci. USA 117, 10585–10592. https://doi.org/10.1073/pnas.1919055117

Maia, A., Lauder, G.V., Wilga, C.D., 2017. Hydrodynamic function of dorsal fins in spiny dogfish and bamboo sharks during steady swimming. J. Exp. Biol. 220, 3967–3975. https://doi.org/10.1242/jeb.152215

Maia, A., Wilga, C.A., 2016. Dorsal fin function in spiny dogfish during steady swimming. J. Zool 298, 139–149. https://doi.org/10.1111/jzo.12300

Maia, A., Wilga, C.A., 2013. Function of dorsal fins in bamboo shark during steady swimming. Zoology 116, 224–231.

Mandic, M., Regan, M.D., 2018. Can variation among hypoxic environments explain why different fish species use different hypoxic survival strategies? J. Exp. Biol. 221, jeb161349. https://doi.org/10.1242/jeb.161349

Marey, E.-J., 1894. Movement. Heinemann, London.

Marey, E.-J., 1890. La locomotion aquatique étudiée par la chronophotographie. C. R. Aad. Sci. 111, 213–216.

Marketaki, S.Z., Berio, F., Di Santo, V., 2025. Compensatory sensory mechanisms in naïve blind cavefish navigating novel environments after lateral line ablation. Comp. Biochem. 305, 111863. https://doi.org/10.1016/j.cbpa.2025.111863

Mathis, A., Mamidanna, P., Cury, K.M., Abe, T., Murthy, V.N., Mathis, M.W., et al., 2018. DeepLabCut: markerless pose estimation of user-defined body parts with deep learning. Nat. Neurosci. 21, 1281–1289. https://doi.org/10.1038/s41593-018-0209-y

Mathis, M.W., Mathis, A., 2020. Deep learning tools for the measurement of animal behavior in neuroscience. Curr. Opin. Neurobiol., Neurobiol. Behav. 60, 1–11. https://doi.org/10.1016/j.conb.2019.10.008

Mayerl, C.J., Dial, T.R., Mainwaring, M.C., Heers, A.M., German, R.Z., 2023. Birth and the pathway to adulthood: integration across development, environment, and evolution. Integr. Comp. Biol. 63, 548–556.

McBryan, T.L., Anttila, K., Healy, T.M., Schulte, P.M., 2013. Responses to temperature and hypoxia as interacting stressors in fish: implications for adaptation to environmental change. Integr. Comp. Biol. 53, 648–659.

McGlinchey, S.M., Saporetti, K.A., Forry, J.A., Pohronezny, J.A., Coughlin, D.J., 2001. Red muscle function during steady swimming in brook trout, Salvelinus fontinalis. Comp. Biochem. 129, 727–738. https://doi.org/10.1016/S1095-6433(01)00334-8

McHenry, M.J., Hedrick, T.L., 2023. The science and technology of kinematic measurements in a century of Journal of Experimental Biology. J. Exp. Biol. 226, jeb245147. https://doi.org/10.1242/jeb.245147

McHenry, M.J., Jed, J., 2003. The ontogenetic scaling of hydrodynamics and swimming performance in jellyfish (*Aurelia aurita*). J. Exp. Biol. 206, 4125–4137.

McHenry, M.J., Peterson, A., 2025. Sensing and control of locomotion in fishes. In: Lauder, G.V., Higham, T.E. (Eds.), Fish Biomechanics, Fish Physiology. Elselvier Academic Press.

McMillen, T., Williams, T.L., Holmes, P.J., 2008. Nonlinear muscles, passive viscoelasticity and body taper conspire to create neuromechanical phase lags in anguilliform swimmers. PLoS Comput. Biol. 4, e1000157.

Mehner, T., 2012. Habitat-specific normal and reverse diel vertical migration in the plankton-feeding basking shark. Fresh. Biol.

Moored, K.W., Dewey, P.A., Smits, A.J., Haj-Hariri, H., 2012. Hydrodynamic wake resonance as an underlying principle of efficient unsteady propulsion. J. Fluid Mech. 708, 329–348. https://doi.org/10.1017/jfm.2012.313

Müller, U.K., Smit, J., Stamhuis, E.J., Videler, J.J., 2001. How the body contributes to the wake in undulatory fish swimming: flow fields of a swimming eel (*Anguilla anguilla*). J. Exp. Biol. 204, 2751–2762. https://doi.org/10.1242/jeb.204.16.2751

Müller, U.K., Stamhuis, E.J., Videler, J.J., 2000. Hydrodynamics of unsteady fish swimming and the effects of body size: comparing the flow fields of fish larvae and adults. J. Exp. Biol. 203, 193–206. https://doi.org/10.1242/jeb.203.2.193

Müller, U.K., van den Boogaart, J.G.M., van Leeuwen, J.L., 2008. Flow patterns of larval fish: undulatory swimming in the intermediate flow regime. J. Exp. Biol. 211, 196–205. https://doi.org/10.1242/jeb.005629

Müller, U.K., Van Den Heuvel, B.L.E., Stamhuis, E.J., Videler, J.J., 1997. Fish foot prints: morphology and energetics of the wake behind a continuously swimming mullet (*Chelon labrosus risso*). J. Exp. Biol. 200, 2893–2906. https://doi.org/10.1242/jeb.200.22.2893

Müller, U.K., Videler, J.J., 1996. Inertia as a 'safe harbour': do fish larvae increase length growth to escape viscous drag? Rev. Fish Biol. Fish. 6, 353–360. https://doi.org/10.1007/BF00122586

Munday, P.L., Dixson, D.L., Donelson, J.M., Jones, G.P., Pratchett, M.S., Devitsina, G.V., et al., 2009. Ocean acidification impairs olfactory discrimination and homing ability of a marine fish. Proc. Natl. Acad. Sci. 106, 1848–1852. https://doi.org/10.1073/pnas.0809996106

Mussi, M., Summers, A.P., Domenici, P., 2002. Gait transition speed, pectoral fin-beat frequency and amplitude in *Cymatogaster aggregata, Embiotoca lateralis* and *Damalichthys vacca*. J. Fish. Biol. 61, 1282–1293. https://doi.org/10.1111/j.1095-8649.2002.tb02471.x

Nangia, N., Bale, R., Chen, N., Hanna, Y., Patankar, N.A., 2017. Optimal specific wavelength for maximum thrust production in undulatory propulsion. PLoS ONE 12, 1–23. https://doi.org/10.1371/journal.pone.0179727

Nauen, J.C., Lauder, G.V., 2002. Hydrodynamics of caudal fin locomotion by chub mackerel, Scomber japonicus (Scombridae). J. Exp. Biol. 205, 1709–1724. https://doi.org/10.1242/jeb.205.12.1709

Neilson, J.D., Perry, R.I., 1990. Diel vertical migrations of marine fishes: an obligate or facultative process? In: Blaxter, J.H.S., Southward, A.J. (Eds.), Advances in Marine Biology. Academic Press, pp. 115–168. https://doi.org/10.1016/S0065-2881(08)60200-X

Nelson, J.S., Grande, T.C., Wilson, M.V.H., 2016. Fishes of the World. John Wiley & Sons.

Nilsson, G.E., Dixson, D.L., Domenici, P., McCormick, M.I., Sørensen, C., Watson, S.-A., et al., 2012. Near-future carbon dioxide levels alter fish behaviour by interfering with neurotransmitter function. Nat. Clim. Change 2, 201–204. https://doi.org/10.1038/nclimate1352

Nowroozi, B.N., Strother, J.A., Horton, J.M., Summers, A.P., Brainerd, E.L., 2009. Whole-body lift and ground effect during pectoral fin locomotion in the northern spearnose poacher (*Agonopsis vulsa*). Zoology 112, 393–402. https://doi.org/10.1016/j.zool.2008.10.005

Oeffner, J., Lauder, G.V., 2012. The hydrodynamic function of shark skin and two biomimetic applications. J. Exp. Biol. 215, 785–795. https://doi.org/10.1242/jeb.063040

Ottervall, C.D., 2025. Examining Behavioral Alterations in Zebrafish (Danio rerio) Larvae in the Context of Anthropogenic Climate Change (MS). University of Miami, Coral Gables, FL.

Oudheusden, B.W. van, 2013. PIV-based pressure measurement. Meas. Sci. Technol. 24, 032001. https://doi.org/10.1088/0957-0233/24/3/032001

Papastamatiou, Y.P., Iosilevskii, G., Di Santo, V., Huveneers, C., Hattab, T., Planes, S., et al., 2021. Sharks surf the slope: current updrafts reduce energy expenditure for aggregating marine predators. J. Anim. Ecol. 90, 2302–2314. https://doi.org/10.1111/1365-2656.13536

Parson, J.M., Fish, F.E., Nicastro, A.J., 2011. Turning performance of batoids: limitations of a rigid body. J. Exp. Mar. Biol. Ecol. 402, 12–18. https://doi.org/10.1016/j.jembe.2011.03.010

Pavlov, V., Rosental, B., Hansen, N.F., Beers, J.M., Parish, G., Rowbotham, I., et al., 2017. Hydraulic control of tuna fins: a role for the lymphatic system in vertebrate locomotion. Science. https://doi.org/10.1126/science.aak9607

Pereira, T.D., Tabris, N., Matsliah, A., Turner, D.M., Li, J., Ravindranath, S., et al., 2022. SLEAP: a deep learning system for multi-animal pose tracking. Nat. Methods 19, 486–495. https://doi.org/10.1038/s41592-022-01426-1

Pettigrew, J.B., 1874. Animal locomotion, or walking, swimming, and flying. Edinb. Med. J. 19, 860–864.

Pimentel, M.S., Faleiro, F., Marques, T., Bispo, R., Dionísio, G., Faria, A.M., et al., 2016. Foraging behaviour, swimming performance and malformations of early stages of commercially important fishes under ocean acidification and warming. Clim. Change 137, 495–509. https://doi.org/10.1007/s10584-016-1682-5

Piñeirua, M., Godoy-Diana, R., Thiria, B., 2015. Resistive thrust production can be as crucial as added mass mechanisms for inertial undulatory swimmers. Phys. Rev. E 92, 21001.

Porter, M.E., Roque, C.M., Long, J.H., 2009. Turning maneuvers in sharks: predicting body curvature from axial morphology. J. Morphol. 270, 954–965. https://doi.org/10.1002/jmor.10732

Pörtner, H.-O., 2010. Oxygen- and capacity-limitation of thermal tolerance: a matrix for integrating climate-related stressor effects in marine ecosystems. J. Exp. Biol. 213, 881–893. https://doi.org/10.1242/jeb.037523

Pörtner, H.O., Knust, R., 2007. Climate change affects marine fishes through the oxygen limitation of thermal tolerance. Science 315, 95–97. https://doi.org/10.1126/science.1135471

Priede, I.G., Holliday, F., 1980. The use of a new tilting tunnel respirometer to investigate some aspects of metabolism and swimming activity of the plaice (Pleuronectes platessa L.). J. Exp. Biol. 85, 295–309.

Reimchen, T.E., Temple, N.F., 2004. Hydrodynamic and phylogenetic aspects of the adipose fin in fishes. Can. J. Zool 82, 910–916. https://doi.org/10.1139/z04-069

Revzen, S., Guckenheimer, J.M., 2008. Estimating the phase of synchronized oscillators. Phys. Rev. E 78, 51907–51912.

Ridge, R.M.A.P., 1977. Physiological responses of stretch receptors in the pectoral fin of the ray *Raja clavata*. J. Mar. Biol. Assoc. UK. 57, 535–541. https://doi.org/10.1017/S0025315400021901

Roche, D., Tytell, E.D., Domenici, P., 2023. Kinematics and behaviour in fish escape responses: guidelines for conducting, analysing, and reporting experiments. J. Exp. Biol. 226, jeb245686. https://doi.org/10.1242/jeb.245686

Rohr, J.J., Fish, F.E., 2004. Strouhal numbers and optimization of swimming by odontocete cetaceans. J. Exp. Biol. 207, 1633–1642. https://doi.org/10.1242/jeb.00948

Romer, A.S., Parsons, T.S., 1986. The vertebrate body. CBS International, 6th ed. Saunders College.

Rondelet, G., 1554. Liber de piscibus marinus, in quibis verae piscium effigies expressae sunt. Bonhomme, Lyons.

Rosenberger, L.J., 2001. Pectoral fin locomotion in batoid fishes: undulation versus oscillation. J. Exp. Biol. 204, 379–394. https://doi.org/10.1242/jeb.204.2.379

Rosenberger, L.J., Westneat, M.W., 1999. Functional morphology of undulatory pectoral fin locomotion in the stingray *Taeniura lymma* (Chondrichthyes: dasyatidae). J. Exp. Biol. 202, 3523–3539. https://doi.org/10.1242/jeb.202.24.3523

Ruiz-Torres, R., Curet, O.M., Lauder, G.V., Maciver, M.A., 2013. Kinematics of the ribbon fin in hovering and swimming of the electric ghost knifefish. J. Exp. Biol. 216, 823–834. https://doi.org/10.1242/jeb.076471

Ryu, T., Veilleux, H.D., Donelson, J.M., Munday, P.L., Ravasi, T., 2018. The epigenetic landscape of transgenerational acclimation to ocean warming. Nat. Clim. Change 8, 504–509. https://doi.org/10.1038/s41558-018-0159-0

Saadat, M., Fish, F.E., Domel, A.G., Di Santo, V., Lauder, G.V., Haj-Hariri, H., 2017. On the rules for aquatic locomotion. Phys. Rev. Fluids 2, 083102.

Sánchez-Rodríguez, J., Raufaste, C., Argentina, M., 2023. Scaling the tail beat frequency and swimming speed in underwater undulatory swimming. Nat. Commun. 14, 5569. https://doi.org/10.1038/s41467-023-41368-6

Sassi, A., Annabi, A., Kessabi, K., Kerkeni, A., Saïd, K., Messaoudi, I., 2010. Influence of high temperature on cadmium-induced skeletal deformities in juvenile mosquitofish (Gambusia affinis). Fish. Physiol. Biochem. 36, 403–409. https://doi.org/10.1007/s10695-009-9307-9

Schaefer, J.T., Summers, A.P., 2005. Batoid wing skeletal structure: novel morphologies, mechanical implications, and phylogenetic patterns. J. Morphol. 264, 298–313. https://doi.org/10.1002/jmor.10331

Schmidt-Nielsen, K., 1984. Scaling: Why is Animal Size So Important? Cambridge University Press.

Schmidt-Nielsen, K., 1970. Energy metabolism, body size, and problems of scaling. Presented at the American Physiological Society. Federation Proceedings, Davis, CA, USA, pp. 1524–1532.

Schultz, W.W., Webb, P.W., 2002. Power requirements of swimming: do new methods resolve old questions? Integr. Comp. Biol. 42, 1018–1025.

Schwalbe, M.A.B., Boden, A.L., Wise, T.N., Tytell, E.D., 2019. Red muscle activity in bluegill sunfish *Lepomis macrochirus* during forward accelerations. Sci. Rep. 9, 8088. https://doi.org/10.1038/s41598-019-44409-7

Sefati, S., Neveln, I.D., Roth, E., Mitchell, T.R.T., Snyder, J.B., MacIver, M.A., et al., 2013. Mutually opposing forces during locomotion can eliminate the tradeoff between maneuverability and stability. Proc. Natl. Acad. Sci. USA 110, 18798–18803.

Sepulveda, C., Dickson, K., Graham, J., 2003. Swimming performance studies on the eastern Pacific bonito Sarda chiliensis, a close relative of the tunas (family Scombridae) I. Energetics. J. Exp. Biol. 206, 2739–2748.

Sfakiotakis, M., Lane, D.M., Davies, J.B.C., 1999. Review of fish swimming modes for aquatic locomotion. IEEE J. Ocean. Eng. 24, 237–252. https://doi.org/10.1109/48.757275

Shadwick, R.E., 2024. Fish tendons: structure and function. In: Alderman, S.L., Gillis, T.E. (Eds.), Encycl. Fish. Physiol, (Second. ed.).,. Academic Press, Oxford, pp. 460–467. https://doi.org/10.1016/B978-0-323-90801-6.00034-3

Shadwick, R.E., Gemballa, S., 2006. Structure, kinematics, and muscle dynamics in undulatory swimming. In: Shadwick, R.E., Lauder, G.V. (Eds.), Fish Biomechanics. Elsevier Academic Press, San Diego, pp. 241–280.

Shadwick, R.E., Goldbogen, J.A., 2012. Muscle function and swimming in sharks. J. Fish. Biol. 80, 1904–1939. https://doi.org/10.1111/j.1095-8649.2012.03266.x

Silva, A.T., Lucas, M.C., Castro-Santos, T., Katopodis, C., Baumgartner, L.J., Thiem, J.D., et al., 2018. The future of fish passage science, engineering, and practice. Fish. Fish. 19, 340–362. https://doi.org/10.1111/faf.12258

Sims, D.W., Southall, E.J., Tarling, G.A., Metcalfe, J.D., 2005. Diel patterns in swimming behavior of a vertically migrating deepwater shark, the bluntnose sixgill (*Hexanchus griseus*). J. Ani. Ecol. 74, 755–761.

Siomava, N., Diogo, R., 2018. Comparative anatomy of zebrafish paired and median fin muscles: basis for functional, developmental, and macroevolutionary studies. J. Anat. 232, 186–199. https://doi.org/10.1111/joa.12728

Smits, A.J., 2000. A Physical Introduction to Fluid Mechanics. John Wiley and Sons, New York.

Snyder, J.B., Nelson, M., Burdick, J.W., MacIver, M.A., 2007. Omnidirectional sensory and motor volumes in electric fish. PLoS Biol. 5, e301.

Standen, E.M., 2010. Muscle activity and hydrodynamic function of pelvic fins in trout (*Oncorhynchus mykiss*). J. Exp. Biol. 213, 831–841. https://doi.org/10.1242/jeb.033084

Standen, E.M., 2008. Pelvic fin locomotor function in fishes: three-dimensional kinematics in rainbow trout (*Oncorhynchus mykiss*). J. Exp. Biol. 211, 2931–2942. https://doi.org/10.1242/jeb.018572

Standen, E.M., Lauder, G.V., 2007. Hydrodynamic function of dorsal and anal fins in brook trout (*Salvelinus fontinalis*). J. Exp. Biol. 210, 325–339. https://doi.org/10.1242/jeb.02661

Standen, E.M., Lauder, G.V., 2005. Dorsal and anal fin function in bluegill sunfish *Lepomis macrochirus*: three-dimensional kinematics during propulsion and maneuvering. J. Exp. Biol. 208, 2753–2763. https://doi.org/10.1242/jeb.01706

Steen, J.B., 1970. The swim bladder as a hydrostatic organ. In: Hoar, W.S., Randall, D.J. (Eds.), Fish Physiology, The Nervous System, Circulation, and Respiration. Academic Press, pp. 413–443. https://doi.org/10.1016/S1546-5098(08)60135-1

Steffensen, J.F., 1989. Some errors in respirometry of aquatic breathers: how to avoid and correct for them. Fish. Physiol. Biochem. 6, 49–59.

Stin, V., Godoy-Diana, R., Bonnet, X., Herrel, A., 2024. Form and function of anguilliform swimming. Biol. Rev. https://doi.org/10.1111/brv.13116

Summers, A.P., Long, J.H., 2006. Skin and bones, sinew and gristle: The mechanical behavior of fish skeletal tissues.

Svendsen, J.C., Steffensen, J.F., Aarestrup, K., Frisk, M., Etzerodt, A., Jyde, M., 2012. Excess posthypoxic oxygen consumption in rainbow trout (*Oncorhynchus mykiss*): recovery in normoxia and hypoxia. Can. J. Zool. 90, 1–11. https://doi.org/10.1139/z11-095

Svendsen, J.C., Tudorache, C., Jordan, A.D., Steffensen, J.F., Aarestrup, K., Domenici, P., 2010. Partition of aerobic and anaerobic swimming costs related to gait transitions in a labriform swimmer. J. Exp. Biol. 213, 2177–2183. https://doi.org/10.1242/jeb.041368

Syme, D.A., 2006. Functional properties of skeletal muscle. Fish Physiology. Fish Biomchanics. Academic Press, pp. 179–240.

Tack, N.B., Du Clos, K.T., Gemmell, B.J., 2024. Fish can use coordinated fin motions to recapture their own vortex wake energy. R. Soc. Open. Sci. 11, 231265. https://doi.org/10.1098/rsos.231265

Tack, N.B., Du Clos, K.T., Gemmell, B.J., 2021. Anguilliform locomotion across a natural range of swimming speeds. Fluids 6, 127. https://doi.org/10.3390/fluids6030127

Takle, H., Baeverfjord, G., Lunde, M., Kolstad, K., Andersen, Ø., 2005. The effect of heat and cold exposure on *HSP70* expression and development of deformities during embryogenesis of Atlantic salmon (*Salmo salar*). Aquaculture 249, 515–524. https://doi.org/10.1016/j.aquaculture.2005.04.043

Taylor, G.I., 1952. Analysis of the swimming of long and narrow animals. Proc. R. Soc. Math. Phys. Eng. Sci. 214, 158–183.

Taylor, G.K., Nudds, R.L., Thomas, A.L.R., 2003. Flying and swimming animals cruise at a Strouhal number tuned for high power efficiency. Nature 425, 707–711. https://doi.org/10.1038/nature02000

Temple, N.F., Reimchen, T.E., 2008. Adipose fin condition and flow regime in catfish. Can. J. Zool 86, 1079–1082. https://doi.org/10.1139/Z08-086

Thandiackal, R., Lauder, G.V., 2020. How zebrafish turn: analysis of pressure force dynamics and mechanical work. J. Exp. Biol. 223. https://doi.org/10.1242/jeb.223230

Tidswell, B.K., Veliko-Shapko, A., Tytell, E.D., 2024. The role of vision and lateral line sensing for schooling in giant danios (*Devario aequipinnatus*). J. Exp. Biol. https://doi.org/10.1242/jeb.246887. jeb.246887.

Todgham, A.E., Stillman, J.H., 2013. Physiological responses to shifts in multiple environmental stressors: relevance in a changing world. Integr. Comp. Biol. 53, 539–544. https://doi.org/10.1093/icb/ict086

Triantafyllou, G.S., Triantafyllou, M.S., Grosenbaugh, M.A., 1993. Optimal thrust development in oscillating foils with application to fish propulsion. J. Fluids Struct. 7, 205–224. https://doi.org/10.1006/jfls.1993.1012

Triantafyllou, M.S., Triantafyllou, G.S., Gopalkrishnan, R., 1991. Wake mechanics for thrust generation in oscillating foils. Phys. Fluids Fluid Dyn. 3, 2835.

Triantafyllou, M.S., Triantafyllou, G.S., Yue, D.K.P., 2000. Hydrodynamics of fishlike swimming. Annu. Rev. Fluid Mech. 32, 33–53. https://doi.org/10.1146/annurev.fluid.32.1.33

Tytell, E., Hawkins, O., & Di Santo, V. (2025). fishmechr: Code for biomechanical analysis of swimming fish (v1.0.0). Zenodo. https://doi.org/10.5281/zenodo.14797994,.

Tytell, E.D., 2007. Do trout swim better than eels? Challenges for estimating performance based on the wake of self-propelled bodies. Exp. Fluids 43, 701–712. https://doi.org/10.1007/s00348-007-0343-x

Tytell, E.D., 2006. Median fin function in bluegill sunfish *Lepomis macrochirus*: streamwise vortex structure during steady swimming. J. Exp. Biol. 209, 1516–1534. https://doi.org/10.1242/jeb.02154

Tytell, E.D., 2004. Kinematics and hydrodynamics of linear acceleration in eels, *Anguilla rostrata*. Proc. R. Soc. Lond. B 271, 2535–2541. https://doi.org/10.1098/rspb.2004.2901

Tytell, E.D., Borazjani, I., Sotiropoulos, F., Baker, T.V., Anderson, E.J., Lauder, G.V., 2010. Disentangling the functional roles of morphology and motion in the swimming of fish. Integr. Comp. Biol. 50, 1140–1154. https://doi.org/10.1093/icb/icq057

Tytell, E.D., Lauder, G.V., 2004. The hydrodynamics of eel swimming: I. Wake structure. J. Exp. Biol. 207, 1825–1841. https://doi.org/10.1242/jeb.00968

Tytell, E.D., Standen, E.M., Lauder, G.V., 2008. Escaping flatland: three-dimensional kinematics and hydrodynamics of median fins in fishes. J. Exp. Biol. 211, 187–195. https://doi.org/10.1242/jeb.008128

van Ginneken, V., Antonissen, E., Müller, U.K., Booms, R., Eding, E., Verreth, J., et al., 2005. Eel migration to the Sargasso: remarkably high swimming efficiency and low energy costs. J. Exp. Biol. 208, 1329–1335.

van Leeuwen, J.L., 1999. A mechanical analysis of myomere shape in fish. J. Exp. Biol. 202, 3405–3414. https://doi.org/10.1242/jeb.202.23.3405

van Weerden, J.F., Reid, D.A., Hemelrijk, C.K., 2014. A meta-analysis of steady undulatory swimming. Fish. Fish. 15, 97–409.

Vandenberg, M.L., Hawkins, O.H., Chier, E., Kahane-Rapport, S.R., Summers, A.P., Donatelli, C.M., 2024. How rugose can you go? Spiny Agonidae armour decreases boundary layer separation. Biol. J. Linn. Soc. 143, blae075. https://doi.org/10.1093/biolinnean/blae075

Veilleux, H.D., Ryu, T., Donelson, J.M., van Herwerden, L., Seridi, L., Ghosheh, Y., et al., 2015. Molecular processes of transgenerational acclimation to a warming ocean. Nat. Clim. Change 5, 1074–1078. https://doi.org/10.1038/nclimate2724

Videler, J.J., 1993. Fish Swimming. Chapman and Hall, London.

Vilmar, M., Di Santo, V., 2022. Swimming performance of sharks and rays under climate change. Rev. Fish. Biol. Fish. 32, 765–781. https://doi.org/10.1007/s11160-022-09706-x

Vogel, S., 1994. Life in Moving Fluids, 2nd ed. Princeton University Press, Princeton, NJ.

Wainwright, S., 1983. To bend a fish. In: Weihs, D., Webb, P.W. (Eds.), Fish Biomechanics, Fish Physiology. Praeger Publishers, New York, pp. 68–91.

Wakeling, J.M., 2006. Fast start mechanics. In: Fish Biomechanics, Fish Physiology. Elselvier Academic Press, pp. 333–363.

Wakeling, J.M., Johnston, I.A., 1999. White muscle strain in the common carp and red to white muscle gearing ratios in fish. J. Exp. Biol. 202, 521–528.

Walker, J.A., 2004. Kinematics and performance of maneuvering control surfaces in teleost fishes. IEEE J. Ocean. Eng. 29, 572–584. https://doi.org/10.1109/JOE.2004.833217

Walker, J.A., 2000. Does a rigid body limit maneuverability? J. Exp. Biol. 203, 3391–3396. https://doi.org/10.1242/jeb.203.22.3391

Walker, J.A., Westneat, M.W., 2002. Performance limits of labriform propulsion and correlates with fin shape and motion. J. Exp. Biol. 205, 177–187. https://doi.org/10.1242/jeb.205.2.177

Walter, T., Couzin, I.D., 2021. TRex, a fast multi-animal tracking system with markerless identification, and 2D estimation of posture and visual fields. eLife 10, e64000. https://doi.org/10.7554/eLife.64000

Wang, X., Song, L., Chen, Y., Ran, H., Song, J., 2017. Impact of ocean acidification on the early development and escape behavior of marine medaka (Oryzias melastigma). Mar. Environ. Res. 131, 10–18. https://doi.org/10.1016/j.marenvres.2017.09.001

Wang, Z., Li, E., Xie, H., Huang, Y., Qiao, J., Yang, Q., 2022. Research on hydrodynamic performance of underwater flexible follow-up flaps based on two-way fluid-structure coupling.

In: OCEANS2022, Hampton Roads. Presented at the OCEANS 2022, Hampton Roads, IEEE, Hampton Roads, VA, USA, pp. 1–6. https://doi.org/10.1109/OCEANS47191.2022.9977116

Wardle, C.S., Videler, J.J., Altringham, J.D., 1995. Tuning in to fish swimming waves: body form, swimming mode and muscle function. J. Exp. Biol. 198, 1629–1636.

Webb, P.W., 2024. Maneuverability. In: Alderman, S.L., Gillis, T.E. (Eds.), Encyclopedia of Fish Physiology, Second ed. Academic Press, Oxford, pp. 607–613. https://doi.org/10.1016/B978-0-323-90801-6.00026-4

Webb, P.W., 2006. Stability and maneuverability. Fish Physiology, Fish Biomechanics. Academic Press, pp. 281–332. https://doi.org/10.1016/S1546-5098(05)23008-X

Webb, P.W., 2002. Control of posture, depth, and swimming trajectories of fishes. Integr. Comp. Biol. 42, 94–101.

Webb, P.W., 1991. Composition and mechanics of routine swimming of rainbow trout, *Oncorhynchus mykiss*. Can. J. Fish. Aquat. Sci. 48, 583–590.

Webb, P.W., 1984. Form and function in fish swimming. Sci. Am. 251, 72–83.

Webb, P.W., 1975. Hydrodynamics and energetics of fish propulsion. Bull. Fish. Res. Board. Can. 158.

Webb, P.W., 1973. Kinematics of pectoral fin propulsion in cymatogaster aggregata. J. Exp. Biol. 59, 697–710. https://doi.org/10.1242/jeb.59.3.697

Webb, P.W., Keyes, R.S., 1982. Swimming kinematics of sharks. Fish. Bull 80, 803–812.

Webb, P.W., Kostecki, P.T., Stevens, E.D., 1984. The effect of size and swimming speed on locomotor kinematics of rainbow trout. J. Exp. Biol. 109, 77–95. https://doi.org/10.1242/jeb.109.1.77

Webb, P.W., Weihs, D., 2015. Stability versus maneuvering: challenges for stability during swimming by fishes. Integr. Comp. Biol. 55, 753–764. https://doi.org/10.1093/icb/icv053

Webb, P.W., Weihs, D., 1994. Hydrostatic stability of fish with swim bladders: not all fish are unstable. Can. J. Zool. 72, 1149–1154. https://doi.org/10.1139/z94-153

Webb, P.W., Weihs, D., 1986. Functional locomotor morphology of early life history stages of fishes. Trans. Am. Fish. Soc. 115, 115–127. https://doi.org/10.1577/1548-8659(1986)115<115:FLMOEL>2.0.CO;2

Weber, J.-M., 1991. Effect of endurance swimming on the lactate kinetics of rainbow trout. J. Exp. Biol. 158, 463–476. https://doi.org/10.1242/jeb.158.1.463

Weihs, D., 1993. Stability of aquatic animal locomotion. Cont. Math. 141, 443–461.

Weihs, D., Webb, P.W., 1983. Optimization of locomotion. In: Weihs, D., Webb, P.W. (Eds.), Fish Biomechanics, Fish Physiology. Praeger Publishers, New York, pp. 339–371.

Westneat, M., Wainwright, S., 2001. Mechanical design for swimming: muscle, tendon, and bone. Fish. Physiol. 19, 271–311. https://doi.org/10.1016/S1546-5098(01)19008-4

Westneat, M.W., Hoese, W., Pell, C.A., Wainwright, S.A., 1993. The horizontal septum: mechanisms of force transfer in locomotion of scombrid fishes (Scombridae, Perciformes). J. Morphol. 217, 183–204. https://doi.org/10.1002/jmor.1052170207

Westneat, M.W., Walker, J.A., 1997. Motor patterns of labriform locomotion: kinematic and electromyographic analysis of pectoral fin swimming in the labrid fish gomphosus varius. J. Exp. Biol. 200, 1881–1893. https://doi.org/10.1242/jeb.200.13.1881

White, C.F., Lauder, G.V., 2024. Studying animal locomotion with multiple data loggers: quantifying time drift between tags. Anim. Biotelemetry 12, 5. https://doi.org/10.1186/s40317-024-00363-4

White, C.R., Kearney, M.R., 2014. Metabolic scaling in animals: methods, empirical results, and theoretical explanations. Compr. Physiol. 4, 231–256.

Wilga, C.D., Lauder, G.V., 2002. Function of the heterocercal tail in sharks: quantitative wake dynamics during steady horizontal swimming and vertical maneuvering. J. Exp. Biol. 205, 2365–2374. https://doi.org/10.1242/jeb.205.16.2365

Wilga, C.D., Lauder, G.V., 2000. Three-dimensional kinematics and wake structure of the pectoral fins during locomotion in leopard sharks *Triakis semifasciata*. J. Exp. Biol. 203, 2261–2278. https://doi.org/10.1242/jeb.203.15.2261

Wilga, C.D., Lauder, G.V., 1999. Locomotion in sturgeon: function of the pectoral fins. J. Exp. Biol. 202, 2413–2432. https://doi.org/10.1242/jeb.202.18.2413

Williams, R.I.V., Hale, M.E., 2015. Fin ray sensation participates in the generation of normal fin movement in the hovering behavior of the bluegill sunfish (Lepomis macrochirus). J. Exp. Biol. 218, 3435–3447. https://doi.org/10.1242/jeb.123638

Williams, R., IV, Neubarth, N., Hale, M.E., 2013. The function of fin rays as proprioceptive sensors in fish. Nat. Commun. 4, 1729. https://doi.org/10.1038/ncomms2751

Williams, T.L., Grillner, S., Smoljaninov, V.V., Wallén, P., Kashin, S., Rossignol, S., 1989. Locomotion in lamprey and trout: the relative timing of activation and movement. J. Exp. Biol. 143, 559–566.

Winterbottom, R., 1973. A descriptive synonymy of the striated muscles of the Teleostei. Proc. Acad. Nat. Sci. Phila. 125, 225–317.

Wise, T.N., Schwalbe, M.A.B., Tytell, E.D., 2018. Hydrodynamics of linear acceleration in bluegill sunfish *Lepomis macrochirus*. J. Exp. Biol. 221. https://doi.org/10.1242/jeb.190892. jeb.190892.

Wright, B., 2000. Form and function in aquatic flapping propulsion: morphology, kinematics, hydrodynamics, and performance of the triggerfishes (Tetraodontiforms: Balistidae) (Ph.D.). Organismal Biology and Anatomy. University of Chicago.

Wu, T.Y.-T., 1971a. Hydromechanics of swimming of fishes and cetaceans. In: Yih, C.-S. (Ed.), Advances in Applied Mechanics. Elsevier, pp. 1–63. https://doi.org/10.1016/S0065-2156(08)70340-5

Wu, T.Y.-T., 1971b. Hydromechanics of swimming propulsion. Part 1. Swimming of a two-dimensional flexible plate at variable forward speeds in an inviscid fluid. J. Fluid Mech. 46, 337–355. https://doi.org/10.1017/S0022112071000570

Wu, T.Y.-T., 1971c. Hydromechanics of swimming propulsion. Part 2. Some optimum shape problems. J. Fluid Mech. 46, 521–544. https://doi.org/10.1017/S0022112071000685

Wu, T.Y.-T., 1971d. Hydromechanics of swimming propulsion. Part 3. Swimming and optimum movements of a slender fish with side fins. J. Fluid Mech. 46, 545–568. https://doi.org/10.1017/S0022112071000697

Yanase, K., Saarenrinne, P., 2015. Unsteady turbulent boundary layers in swimming rainbow trout. J. Exp. Biol. 218, 1373–1385. https://doi.org/10.1242/jeb.108043

Yavno, S., Holzman, R., 2018. Do viscous forces affect survival of marine fish larvae? Revisiting the 'safe harbour' hypothesis. Rev. Fish. Biol. Fish. 28, 201–212. https://doi.org/10.1007/s11160-017-9503-0

Youngerman, E.D., Flammang, B.E., Lauder, G.V., 2014. Locomotion of free-swimming ghost knifefish: anal fin kinematics during four behaviors. Zoology 117, 337–348. https://doi.org/10.1016/j.zool.2014.04.004

Ytteborg, E., Torgersen, J., Baeverfjord, G., Takle, H., 2010. Morphological and molecular characterization of developing vertebral fusions using a teleost model. BMC Physiol. 10, 13. https://doi.org/10.1186/1472-6793-10-13

Yu, C.-L., Hsu, Y.-H., Yang, J.-T., 2013. The dependence of propulsive performance on the slip number in an undulatory swimming fish. Ocean. Eng. 70, 51–60. https://doi.org/10.1016/j.oceaneng.2013.05.030

Yu, C.-L., Ting, S.-C., Hsu, Y.-H., Yeh, M.-K., Yang, J.-T., 2012. Mechanical capability and timing of a fish to maneuver from a steady straight-line swimming state. Mech. Res. Commun. 39, 59–64. https://doi.org/10.1016/j.mechrescom.2011.11.009

Zhang, Y., Lauder, G.V., 2024. Energy conservation by collective movement in schooling fish. eLife 12, RP90352. https://doi.org/10.7554/eLife.90352